Structural and Functional Microbial Ecology of Denitrifying Bacteria Using Different Organic Carbon Sources

Huijie Lu

Submitted in partial fulfillment of the
requirements for the degree of
Doctor of Philosophy
in the Graduate School of Arts and Sciences

COLUMBIA UNIVERSITY
2011

ABSTRACT

Structural and Functional Microbial Ecology of Denitrifying Bacteria Using Different Organic Carbon Sources

Huijie Lu

This dissertation research represents one of the first attempts to investigate the structural and functional microbial ecology of methanol, ethanol and glycerol fostered denitrification. The overarching goal of this research was to elucidate the link between the structure and function of denitrifying microbial populations grown on different carbon sources. Specific objectives were to:

1) diagnose bacteria specifically assimilating methanol and ethanol and determine denitrification kinetics induced by the two carbon sources;

2) investigate factors leading to nitrous oxide (N_2O) and nitric oxide (NO) emissions from methanol and ethanol feeding denitrification reactors;

3) characterize glycerol assimilating populations that perform suspended- and biofilm-growth denitrification;

4) examine the potential of using alcohol dehydrogenase gene as a biomarker for methanol and glycerol induced denitrification activity;

5) evaluate the impact of different carbon sources (methanol and ethanol) on the transcript and proteome of a model facultative methylotroph, *Methyloversatilis universalis* FAM5.

First, the technique of DNA stable isotope probing and quantitative polymerase chain reaction were adapted to diagnose and track methylotrophic denitrifying bacteria in activated sludge. Methanol assimilating populations in the methanol fed denitrifying

sequencing batch reactor (SBR) were *Methyloversatilis* spp. and *Hyphomicrobium* spp. related species. Upon switching to ethanol, only *Methyloversatilis* spp. was sustained pointing to their metabolic versatility at least with respect to carbon assimilation. This study represents one of the first investigations of the existence and utilization of facultative methylotrophy in activated sludge.

Second, the potential of N_2O and NO emitted from methanol and ethanol fed denitrifying SBRs was studied during different transient shocks, including organic carbon limitation, nitrite inhibition and oxygen inhibition. Organic carbon limitation and exposure to nitrite did not result in statistically significant emissions over the control. However, statistically higher N_2O emissions were observed during exposure to oxygen on the ethanol fed biomass and coincided with sustained denitrification activity in the presence of oxygen. Therefore, the results suggest that the dosage of ethanol to anoxic zones needs to be strictly controlled to minimize N_2O emissions in the downstream aerobic zones.

Third, the structure-function analysis of denitrification was extended to glycerol (the main component of biodiesel waste and a potential replacement for methanol) in both suspended and biofilm phases of a hybrid integrated fixed-film bioreactor. During long-term operation on glycerol, the biofilm community had a higher phylogenetic diversity (dominated by *Comamonas* spp., *Bradyrhizobium* spp., and *Tessaracoccus* spp.), and lower denitrification kinetics than the suspended community (dominated by *Comamonas* spp. and *Diaphorobacter* spp.). Distinct identities of glycerol assimilating populations due to the different substrate availability in the suspended and biofilm phases were shown for the first time.

Fourth, carbon source-specific biomarkers of denitrification activity based on gene expression were developed. Based on short-term batch denitrification activity assays as well as long-term bioreactor operation, the applicability of alcohol dehydrogenase gene expression as quantitative descriptors of denitrification activity on methanol and glycerol in mixed cultures was demonstrated.

Finally, *Methyloversatilis universalis* was selected as model organism to study the effects of varying electron donors (from methanol to ethanol) on its gene and protein expression profiles. Genes encoding essential enzymes that involve carbon oxidation, C1 assimilation and central metabolism were found to be differentially expressed during growth on methanol and ethanol. Several physiological and metabolic responses by *M. universalis* pointed to a well-defined strategy to overcome carbon limitation for surviving in engineered or natural denitrifying environments.

In sum, the structural and functional ecology and the metabolism of heterotrophic denitrification on methanol, ethanol and glycerol as applicable to engineered denitrifying bioreactors was investigated in detail. From an engineering perspective, the knowledge gained can help to guide the selection and application of potential organic carbon sources for denitrification in biological nitrogen removal systems. It is expected that such judicious selection can also eventually result in better design, operation and control of engineered nitrogen removal processes and thus help attain ever more stringent nitrogen standards.

Table of Contents

LIST OF FIGURES

LIST OF TABLES

LIST OF ABBREVIATIONS AND SYMBOLS

16S ribosomal RNA	16S rRNA
Alcohol dehydrogenase	ADH
Anaerobic oxidation of ammonium	ANAMMOX
Biological nitrogen removal	BNR
Chemical oxygen demand	COD
Denaturing gradient gel electrophoresis	DGGE
Dissolved oxygen	DO
Fluorescent *in situ* hybridization	FISH
Gas chromatography	GC
Hydraulic retention time	HRT
Integrated fixed-film activated sludge	IFAS
Nitrate reductase	NAR
Nitrite reductase	NIR
Nitric oxide reductase	NOR
Nitrous oxide reductase	N_2OR
Oxidation reduction potential	ORP
Polyhydroxy β-butyrate	PHB
Polymerase chain reaction	PCR
Quantitative polymerase chain reaction	qPCR
Reverse transcription quantitative polymerase chain reaction	RT-qPCR
Ribulose monophosphate	RuMP
Sequencing batch reactor	SBR
Solid retention time	SRT
Specific denitrification rate	sDNR
Stable isotope probing	SIP
Terminal restriction fragment length polymorphism	T-RFLP
Growth yield	Y
Specific growth rate	μ

Half-saturation coefficient	Ks
Inhibition constant	Ki
Substrate concentration	S
Biomass concentration	X
Substrate utilization rate	q
Temperature coefficient	θ

ACKNOWLEDGEMENTS

First of all, I owe my advisor, Prof. Kartik Chandran my deepest gratitude and respect. I feel honored and very fortunate to be his student. Without his input, I would not have been able to complete a dissertation of this quality and depth. I received insightful academic guidance from him during the past four years, and learnt much from his endless passion and rigorous attitude towards research. I really appreciate his patience and understanding when I face difficulties in my research and personal life.

I am very thankful for the support and advice from all the members of my dissertation committee: Dr. Nickolas Themelis, Dr. William Becker, Dr. Patricia Culligan, Dr. David Stensel and Dr. Marina Kalyuzhanaya. Each of them brought a unique set of experiences and ideas, and my dissertation has greatly benefited from this synergy.

I would like to acknowledge the National Fish and Wildlife Foundation, the Water Environment Research Foundation Nutrient Challenge Program and the National Science Foundation for funding the projects that form my dissertation research.

I am equally grateful for the help and friendship of my colleagues at Columbia University: Dr. Wendell O. Khunjar, Dr. Hongkeun Park, Dr. Ran Yu, Dr. Joon Ho Ahn, Dr. Sungpyo Kim, Dr. Daqian Jiang, Vladimir Baytshtok, Farhan Nuruzzaman, Aleeza Gordon, Janani Ravindhar, Edris Taher and Suneethi Sundar. I thank all my friends in the United States and China. Their continued friendship and love have made my life full of happiness.

Last but not least, thank you my dear parents and grandparents for raising me, loving me and teaching me the wisdom of life. Despite our distance, your support has allowed me to face all challenges bravely and never give up my dreams.

CHAPTER 1

INTRODUCTION

1.1 Biological denitrification

Heterotrophic denitrification is the dissimilatory reduction of ionic nitrogen oxides such as nitrate (NO_3^-) and nitrite (NO_2^-) to gaseous oxides such as nitric oxide (NO) and nitrous oxide (N_2O) and eventually to dinitrogen (N_2) gas under anoxic conditions using organic electron donors and assimilative carbon sources [1]. The nitrogen oxides act as terminal electron acceptors in the absence of oxygen. Various organic carbons, such as methanol, acetate, or glucose can serve as electron donors and carbon sources for growth. The overall reaction when using methanol as carbon source for denitrification is shown below (cell growth is not taken into account):

$$5CH_3OH + 6NO_3^- \rightarrow 3N_2 + 5CO_2 + 7H_2O + 6OH^-$$

Over the last century, extensive research has been conducted on denitrification [1, 2]. Interest in denitrification exists for several reasons. First, denitrification constitutes one of the main branches of the global nitrogen cycle catalyzed by bacteria (Figure 1-1). Nitrogen in the atmosphere is introduced into the biosphere by biological or chemical N_2 fixation, and removed from there by denitrification. Second, denitrification is one of the two main reactions involved in achieving engineered biological nitrogen removal (BNR) in wastewater treatment utilities. Third, biological denitrification is an important source of nitrous oxide (N_2O), which has a greenhouse gas effect approximately 300 times more potent than carbon dioxide [3].

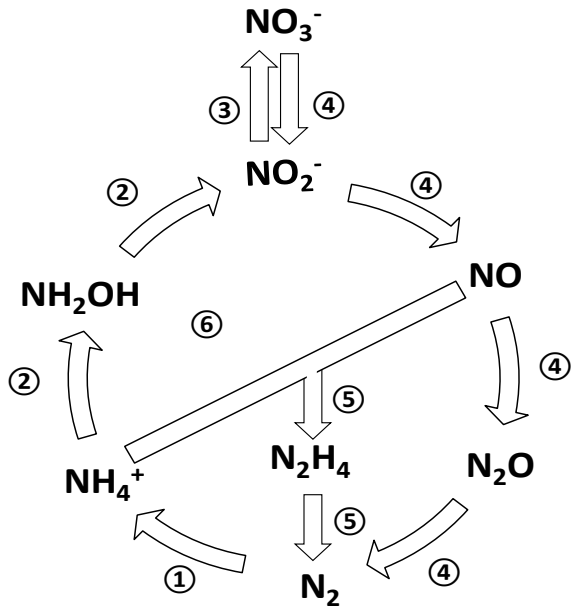

Figure 1-1. Microbial nitrogen cycle. 1-Dinitrogen fixation; 2-Aerobic oxidation of ammonia to nitrite; 3-Aerobic oxidation of nitrite to nitrate; 4-Classic denitrification; 5-Anaerobic oxidation of ammonium (ANAMMOX); 6-Dissimilatory nitrite reduction to ammonium (Ammonification) (Adapted from [4])

Table 1-I. Genera of denitrifying bacteria detected in activated sludge [5]

Achromobacter	*Escherichia*	*Neisseria*
Acinetobacter	*Flavobacterium*	*Paracoccus*
Agrobacterium	*Gluconobacer*	*Propionibacterium*
Alcaligens	*Holobacterium*	*Pseudomonas*
Bacillus	*Hyphomicrobium*	*Rhizobium*
Chromobacterium	*Kingella*	*Rhodopseudomonas*
Corynebacterium	*Methanonas*	*Spirillum*
Denitrobacillus	*Moraxella*	*Thiobacillus*
Enterobacter	*Xanthomonas*	

Unlike nitrifying bacteria, which are phylogenetically closely related [6], denitrifying bacteria are distributed in a large variety of physiological and taxonomic groups belonging to various subclasses of the *Proteobacteria* (Table 1-I). Additionally, the prospect of new classes of denitrifying bacteria which could be present and active in activated sludge needs to be considered. Although autotrophic bacteria can also perform

denitrification, the focus of this work is on chemorganoheterotrophic denitrifying bacteria. Notwithstanding the discovery and application of novel chemolithoautotrophic denitrification processes such as anaerobic ammonia oxidation, chemoorganoheterotrophic denitrification remains widely practiced for engineered biological nitrogen removal (BNR).

1.2 Molecular basis and biochemistry of chemoorganoheterotrophic denitrification

Bacterial nitrate reduction is performed for three cellular purposes: respiration (the generation of metabolic energy by using nitrate as a terminal electron acceptor), dissimilation (the dissipation of excess reducing power for redox balancing) and assimilation (the utilization of nitrate as a nitrogen source for growth) (Table 1-II) [7]. Chemoorganoheterotrophic denitrification (the respiratory branch) generates metabolic energy and is catalyzed by four types of N reductases in sequence: nitrate reductase (*nar*), nitrite reductase (*nir*), nitric oxide reductase (*nor*) and nitrous oxide reductase (*nos*) [1].

The membrane-bound nitrate reductase is a complex, three-subunit quinol dehydrogenase. It contains a 140-kDa bis-MGD catalytic large or α subunit, NarG; a 60-kDa electron transfer subunit, NarH (also called small or β subunit), which binds four FeS clusters; and an integral membrane Cytochrome *b* or γ subunit, NarI. The NarI function is ascribed to quinol oxidation and electron transport to NarH [2]. Potent inhibitors to the activity of *nar* include, but not limited to: pentachlorophenol, azide, chlorate, cyanide, and thiocyanate [8, 9].

Table 1-II. Prokaryotic nitrate reduction, adapted from [2, 7]

		Assimilatory	Respiratory		Dissimilatory
Nitrate reductase	Reaction	$NO_3^- \rightarrow NO_2^-$	$NO_3^- \rightarrow NO_2^-$		$NO_3^- \rightarrow NO_2^-$
	Location	Cytoplasm	Membrane		Periplasm
	Structural genes	*nasCA, narB*	*narGHI*		*napAB*
	Function	Biosynthesis of N compounds	Nitrate respiration and denitrification		reducing power dissipation and denitrification
			Type I	**Type II**	
Nitrite reductase	Reaction	$NO_2^- \rightarrow NH_4^+$	$NO_2^- \rightarrow NO$	$NO_2^- \rightarrow NH_4^+$	$NO_2^- \rightarrow NH_4^+$
	Location	Cytoplasm	Periplasm	Periplasm	Cytoplasm
	Structural genes	*nasB, nirA*	*nirS, nirK*	*nrfA*	*nirBD*
	Function	Biosynthesis of N compounds	PMF denitrification	PMF ammonification	reducing power dissipation and nitrite detoxification
Nitric oxide reductase	Reaction	N/A	$NO \rightarrow N_2O$	N/A	N/A
	Location		Periplasm		
	Structural genes		*norB*		
	Function		Nitric oxide respiration		
Nitrous oxide reductase	Reaction	N/A	$N_2O \rightarrow N_2$	N/A	N/A
	Location		Periplasm		
	Structural genes		*nosZ*		
	Function		Nitrous oxide respiration		

Two different respiratory enzymes that can reduce nitrite to nitric oxide in the periplasm of denitrifying bacteria were found in bacteria: the NirS-encoded cytochrome cd1 nitrite reductase and the NirK-encoded copper nitrite reductase. These two types of nitrite reductases are structurally different but functionally equivalent. NirS has been found mostly in denitrifiers, and NirK is present in more taxonomically unrelated bacteria (not necessarily performing complete denitrification) [10]. However, all denitrifying bacteria could possess only one of the two nitrite reductases [11]. Two well-characterized nitric oxide reductases include membrane-bound dimer (encoded by cNorB) and the single component reductase with an N-terminal extension coding for quinol as electron donor (encoded by qNorB). Both cNorB and qNorB have been detected in denitrifying bacteria [12-14]. The conversion of N_2O to N_2 is catalyzed by Cu-containing nitrous oxide reductase (N_2OR), which is a functional homodimer comprising monomers with a molecular mass of 65 kDa. N_2OR is encoded by *nosZ*, which is largely unique to denitrifying bacteria. N_2OR exists in several forms, each distinguished by its redox and spectroscopic properties and enzymatic activity [2].

Not all bacteria are capable of complete denitrification, and in fact, many denitrifying bacteria can reduce nitrate only to nitrite due to the lack of nitrite reductase enzymes [15, 16]. Such bacteria are not termed denitrifiers *sensu stricto*, since they cannot produce gaseous products by nitrate reduction. In the marine and sediments, nitrate reduction to nitrite or ammonia is of the comparable magnitude as complete denitrification [17, 18].

1.3 Denitrification in engineered biological wastewater treatment plants

It has been widely noticed that discharge of excess nutrients (mainly nitrogen and phosphorus) due to the rapid industrialization and urbanization can lead to severe eutrophication and ground water pollution in terrestrial and oceanic ecosystems [19]. As a result, the processes of nitrification and denitrification have been employed in concert to meet increasingly stringent effluent wastewater limits for effluent total nitrogen (3 mg total N/L or less). However, given that most domestic wastewater streams may not contain adequate organic carbon and electron donor concentrations to achieve this limit, addition of external organic carbon sources to enhance denitrification rates becomes necessary [20].

Carbon sources can be supplemented to pre- and post-anoxic zones of many activated sludge BNR configurations. The pre-denitrification system has two reactors in series, the first one anoxic and the second aerobic with high recirculation ratios. Biodegradable organic materials in the influent can help to reduce the demand for carbon augmentation in the anoxic zone, but the main disadvantage associated with this configuration is the incomplete nitrate removal - nitrate generated in the downstream aerobic zone is discharged directly. In contrast, post-denitrification can achieve much higher nitrate removal with external carbon sources added into the secondary anoxic zone, and may lead to considerably lower reactor volume. Barnard [21] combined the pre- and post-denitrification into the four-stage Bardenpho process (Figure 1-2). In this process, the pre-anoxic zone uses organics in the influent to remove a large part of nitrate (recirculated from the following aerobic zone). The remaining nitrate is reduced in the secondary anoxic zone where supplemental carbon sources are added. Re-aeration in the

fourth reactor removes N_2 formed in the post-denitrification reactor and improves biomass settling.

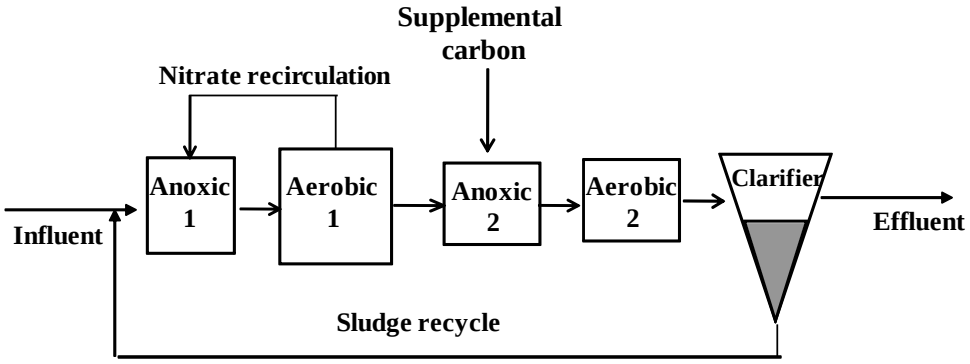

Figure 1-2: Addition of external carbon sources to the post anoxic zone of the four stage Bardenpho process (adapted from [22])

Several organic carbon sources have historically been used to augment the rate of the denitrification process, including methanol, ethanol, acetate, molasses, and brewery wastes (summarized in the following section) [23]. Of these external electron donors, methanol is one of the most widely used owing to its low cost and low sludge production rate (low growth yield) [24]. However, the price of methanol experienced significant variability from 2007-2010 (Figure 1-3). In addition, as a highly flammable liquid with a low flash point of 49^{o}C [25], handling concerns of methanol must be considered into design and operation to meet National Fire Protection Association (NFPA) and other code requirements. Consequently, other easy-to-obtain and relatively inexpensive carbon sources, such as biodiesel waste (glycerine-g-phase) could be suitable replacements for methanol.

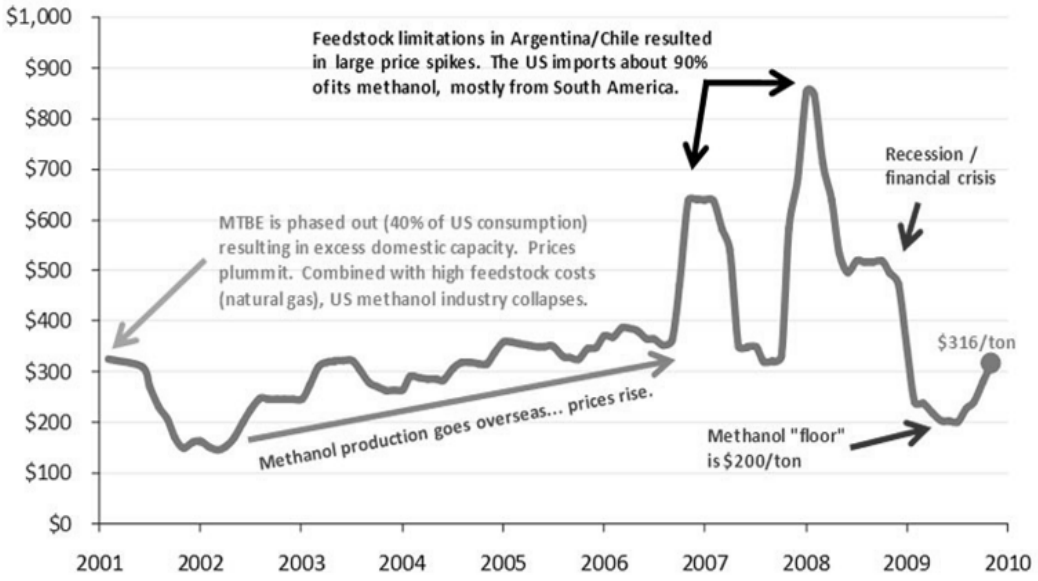

Figure 1-3: Historic contract price of methanol at U.S. Gulf Coast spot market ($/ton)[1].

1.4 Stochiometry and biokinetics

The reaction stoichiometry for the electron donor (e.g. methanol), electron acceptor (nitrate) and cell synthesis (ammonium as nitrogen source) is shown below [26]:

$$Ra: \frac{1}{5}NO_3^- + \frac{6}{5}H^+ + e^- \rightarrow \frac{1}{10}N_2 + \frac{3}{5}H_2O$$

$$Rd: \frac{1}{6}CH_3OH + \frac{1}{26}H_2O \rightarrow \frac{1}{6}CO_2 + H^+ + e^-$$

$$Rc: \frac{1}{5}CO_2 + \frac{1}{20}HCO_3^- + \frac{1}{20}NH_4^+ + H^+ + e^- \rightarrow \frac{1}{20}C_5H_7NO_2 + \frac{9}{20}H_2O$$

When denitrifiers use organic carbons as electron donors for synthesis, a portion of the electrons (fe) is transferred to electron acceptor in order to provide energy for converting the other portion of electrons (fs) to cells (Figure 1-4) [26]. Therefore, the overall reaction that includes energy generation and biosynthesis can be written as:

[1] Source: Gas Technologies LLC.

$$R = f_e Ra + f_s Rc - Rd \qquad \text{(Equation 1-1)}$$

where f_s can be expressed in mass units and are called observed yield (Y_{obs})

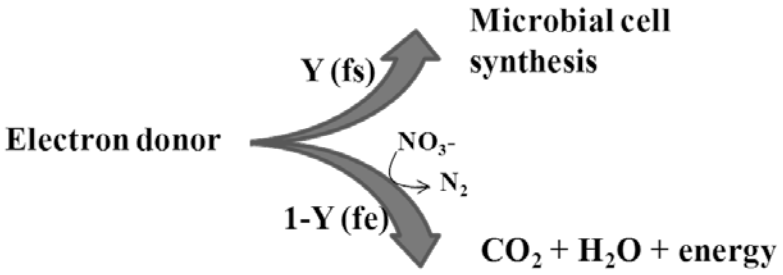

Figure 1-4: Utilization of electrons for energy production and biosynthesis

The amount of nitrate that can be removed from a given wastewater is a function of organic carbon availability, and is primarily determined as the stoichiometric ratio between the electron donor and acceptor, the COD/N ratio. Many studies reported a wide range of the COD/N ratio required for satisfactory denitrification between 3 and 7 g COD/g N [27-29]. However, this ratio largely depends on the nature of the influent (concentrations of biodegradable COD and nitrogen species) and the microbial ecology of the denitrification process itself. For instance, if the influent wastewater COD/N ratio is not sufficient, external carbon source is required for achieving complete nitrate reduction to N_2. Further, denitrifying bacteria with a higher growth yield coefficient require a higher dosage of external electron donors (Eqn. 1-2) [22].

$$\text{Carbon dose} = \frac{2.86}{1-Y} \times (NO_{3\ in}^{-} - NO_{3\ eff}^{-}) \qquad \text{(Equation 1-2)}$$

where ($NO_3^-{}_{in}$ -$NO_3^-{}_{eff}$) is the degree of denitrification required (mg N/d, calculated by multiplying the difference between the influent and effluent concentrations of nitrate (mg N/L) by the flow rate (L/d)); Y is the anoxic growth yield of denitrifying bacteria on

specific carbon sources (mg biomass COD produced/ mg COD removed, typical values are listed in Table 1-III); carbon dose is in mg COD/d.

On the other hand, the kinetics of denitrification directly influence anoxic reactor zone sizing in BNR reactors. Microbial kinetics is generally described by the Monod model (Eqn. 1-3 and Figure 1-5). Biokinetic parameters that are essential to full-scale denitrification process design and operation, such as maximum specific growth rate (μ_{max}) and half-saturation coefficients (Ks) can be obtained by non-linear regressions of Eqn. 1-4, 5, 6.

$$\mu = \frac{\mu_{\max} S_{COD}}{1 + k_{s,COD} S_{COD}} \qquad \text{(Equation 1-3)}$$

$$\frac{dX_H}{dt} = \mu X_H = \frac{\mu_{\max} S_{COD}}{1 + k_{s,COD} S_{COD}} X_H \qquad \text{(Equation 1-4)}$$

$$\frac{dS_{NO}}{dt} = -\frac{1 - Y_H}{2.86 Y_H} \frac{dX_H}{dt} \qquad \text{(Equation 1-5)}$$

$$\frac{dS_{COD}}{dt} = -\frac{1}{Y_H} \frac{dX_H}{dt} \qquad \text{(Equation 1-6)}$$

where, μ is the specific growth rate (t^{-1}); μ_{max} is the maximum specific growth rate (t^{-1}); $K_{S,COD}$ is the half saturation coefficient of organic carbon (ML^{-3}); Y_H is the growth yield of heterotrophs (mg COD biomass formed/mg COD removed); X_H is the biomass concentration (ML^{-3}); and S is the substrate concentration (ML^{-3}, S_{COD}: organic carbon; S_{NO}: nitrate)

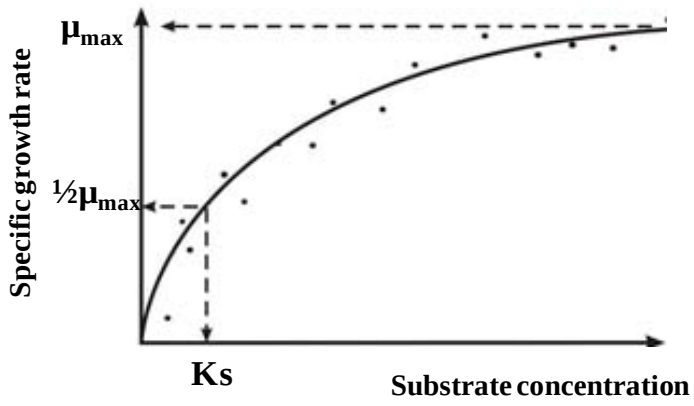

Figure 1-5: Monod model that defines the relation between the growth rate (μ) and the concentration of the limiting nutrient (S) [30].

Using methanol as the carbon source, values for μ_{max} range from 0.2-2.0 d^{-1} according to [31]. μ_{max} is also a function of temperature, as reported by [32]. The specific substrate utilization rate (*q*) is related to μ by the growth yield, Y (Eqn. 1-7). The specific denitrification rate (sDNR) is a direct measure of denitrification activity (Eqn. 1-8) and can be obtained by extant denitrification batch assays (described in more details in the Materials and Methods section of Chapter 2).

$$q = \frac{\mu}{Y} \qquad \text{(Equation 1-7)}$$

$$\frac{dS_{NO}}{dt} = sDNR \times X_H \qquad \text{(Equation 1-8)}$$

A double-substrate Monod model can be used to describe the impacts of both carbon and nitrate concentrations on the specific denitrification rate (Eqn. 1-9). However, the half saturation coefficient of nitrate ($K_{S,NO}$) was found < 1 mg/N and has little influence on the measured sDNR values [33, 34].

$$sDNR = sDNR_{max} \times \frac{S_{COD}}{K_{S,COD} + S_{COD}} \times \frac{S_{NO}}{K_{S,NO} + S_{NO}} \qquad \text{(Equation 1-9)}$$

For treatment processes with single anoxic zone, the denitrifying reactor can be sized based on the sDNR values, concentration of VSS in the mixed liquor and the degree of denitrification required (Eqn. 1-10).

$$V_{ANX} = \frac{S_{NO,in} - S_{NO,eff}}{sDNR \cdot X_{VSS}} \qquad \text{(Equation 1-10)}$$

where V_{ANX} is the calculated volume of the anoxic zone (L); ($S_{NO,in}$ - $S_{NO,eff}$) is the degree of denitrification required (mg N/d); sDNR is the specific denitrification rate (mg N/ mg VSS/ d); X_{VSS} is the concentration of volatile suspended solids in the anoxic zone (mg VSS/L).

1.5 Factors controlling denitrification

Temperature

In a fashion similar to other heterotrophs, the kinetics of denitrifying bacteria is affected by temperature based on the Arrhenius equation:

$$k = Ae^{-Ea/RT} \qquad \text{(Equation 1-11)}$$

$$k_1 = k_2\theta^{T_1 - T_2} \qquad \text{(Equation 1-12)}$$

where k is the specific denitrification rate at temperature T (mg NO_3-N/mg VSS/d); A is the prefactor; Ea is the activation energy in J/mol; R is the ideal gas constant (8.314 J/mol/K), T is the absolute temperature and θ is the temperature coefficient (dimensionless).

Denitrification rate is therefore a bell-shaped curve, and the maximum value is obtained at the optimal temperature (ranging from 20-60 ºC, [1, 35]), and then declines rapidly above this temperature. Various θ values have been reported based on a number of site-specific studies, yielding a range from 1.03 through 1.20 [35].

pH

Alkalinity is produced during denitrification, and 3.57 g alkalinity (as $CaCO_3$) is generated per g of NO_3-N reduced to N_2. Denitrification may occur at a pH up to 11 in wastes, but the optimum pH for denitrification was found in the range of 7-9 [1, 36]. Denitrification activity with denitrification rates falling off sharply outside this region, which may be attributed to the inhibitory effects of H^+ or OH^- on N reductases, such as N_2OR [37].

Oxygen

Oxygen inhibits denitrification by providing a better electron acceptor for denitrifying species to generate energy. The Gibbs standard free energy of water-oxygen is -78.73 KJ/e- eq and that for nitrogen-nitrate is -72.20 KJ/e- eq [26]. The threshold oxygen inhibition concentration is around 0.2 mg O_2/L [1]. In practice, the oxidation reduction potential (ORP), which is a measure of the activity or strength of oxidizers and reducers in relation to their concentration in wastewater, has been used to indicate the aerobic, anoxic and anaerobic conditions. The ORP generally shows a strong response to DO especially at low oxygen concentrations, and is a better monitoring and controlling parameter under anoxic and anaerobic conditions than using DO concentrations. In general, ORP values lower than -200 mV indicates anaerobic conditions; between - 200 and + 200 mV are for anoxic conditions; and higher than + 200 mV are for aerobic conditions.

Denitrification rates decrease with the increased DO concentrations [38], as a result of the inhibition effects of oxygen on the activity of nearly all N reductases [2, 39]. Oxygen has an immediate and reversible inhibitory effect on nitrate respiration, with the

maximal inhibition reached at as low as 0.2% oxygen saturation [40]. Nitrite reductase appeared to be less sensitive to O_2 than nitrate reductase, with a threshold inhibitory concentration of 2.5 mg O_2/L [41]. With the presence of oxygen, NO reductase was constitutively synthesized at low levels [42]. N_2OR is the most sensitive enzyme to oxygen compared to the other upstream reductases, resulting in significant accumulation of N_2O at relatively low DO concentrations [1, 41].

The inhibition of oxygen to denitrification is reversible, and the response time of the enzymatic system to electron acceptor switch is generally in the magnitude of minutes [43]. An expended Monod expression of denitrification kinetics, including the non-competitive inhibition term for oxygen is shown in Eqn. 1-13.

$$\frac{dS_{NO}}{dt} = \left(\frac{1-Y}{2.86Y}\right)\mu_{\max}\left(\frac{S_{COD}}{K_{S,COD}+S_{COD}}\right)\left(\frac{S_{NO}}{K_{S,NO}+S_{NO}}\right)\left(\frac{K_{I,O}}{K_{I,O}+S_O}\right)\eta X_{bH} \quad \text{(Equation 1-13)}$$

where, S_S, S_{NO} and S_O are the concentrations of organic carbon source, nitrate-N and oxygen (in COD mg/L, mg N/L and mg O_2/L, respectively); $K_{S,\,COD}$ and $K_{S,\,NO}$ are the half saturation coefficients of organic carbon source (mg COD/L) and nitrate (mg N/L), respectively; $K_{I,O}$ is the inhibition coefficient of oxygen on nitrate reduction, which was found to be around 0.1 mg O_2/ L using both mixed and pure cultures [22, 43]; η is the correlation factor for growth under anoxic conditions (dimensionless, with the typical value of 0.8) .

Nitrogen species

Nitrite inhibition of bacteria growth has long been known for both pure and mixed cultures [44, 45]. The two possible mechanisms for nitrite mediated inhibition of nitrate reduction include: 1) the competition for NADH between nitrate and nitrite reductase;

and 2) the internal accumulation of toxic nitrite resulted from high rate of nitrate reduction [46]. Several studies have indicated that instead of nitrite, the inhibition is actually caused by the undissociated nitrous acid (HNO_2) [44, 45]. The threshold inhibitory concentration of HNO_2 varied upon the culture condition, pH and carbon availability [45, 47, 48].

Similar to nitrite, nitric oxide (NO) is able to inhibit nitrite reductase as well as the nitrous oxide reductase [49], and therefore is kept in cells at very low concentrations [50-52]. No inhibition effects have been reported for nitrous oxide on any of the denitrification steps so far.

1.6 Effects of different carbon sources

Denitrification stoichiometry and kinetics

Soluble and readily degradable substrates support the highest rates of denitrification. Although methanol is reported as the most widely used exogenous carbon source, it is not as efficient as other carbon substrates, e.g., ethanol and acetate on the kinetic basis [53]. Denitrifying bacteria enriched by ethanol and acetate also grow at higher yields. One explanation is that these C2 compounds can easily be converted into Acetyl Co-A by bacterial cells, before entering the TCA cycle for central metabolism [54]. On the other hand, energy is lost during C1 assimilation in heterotrophic methylotrophs [55, 56]. The stoichiometric and kinetic coefficients of denitrification with various carbon sources have been extensively measured mainly via empirical full-scale implementations [57, 58], and results are summarized in Table 1-III.

Table 1-III: Representative stoichiometric and kinetic parameters for denitrifying biomass grown on different carbon sources

Carbon source	COD/N	Y (gVSS/gCOD)	μ_{max} (d^{-1})	sDNR (mgN/gVSS·h)	Reference
Methanol	4.1-4.5	0.23-0.25	0.77-2	32-91	[59]
	4.7		0.4-1.0	6.07	[60]
		0.4		3.2	[61]
Ethanol		0.42		9.6	[61]
		0.22		27	[58]
	5.877	0.36			[62]
Acetate		0.65		12	[61]
	3.5		1.2-3.5		[60]
		0.3		3.6	[63]
Glucose				2.7	[58]
		0.38			[64]
Biodiesel	4.8			1.8	[65]

Structure of denitrifying communities

Since methanol is the most economical carbon source in supporting wastewater denitrification, methylotrophic denitrifiers have been widely studied [66-69]. Methanol denitrification selects special groups of bacteria [59, 70], which use serine or ribulose monophosphate (RuMP) pathways for assimilating the important intermediate, formaldehyde. Methylotrophic denitrifiers can be divided into three subgroups: obligate, restricted facultative and typical facultative methylotrophs [71]. The obligate methylotroph can only use C1 compounds, and examples are *Hyphomicrobium methylooorum* KM146 and *Methylococcus capsulatus* [71]. The restricted methylotroph can grow on a limited range of complex organic compounds, for example *Methylophilus*

glucosoxydans and *Methylophilus rhizosphaerae* [71]. Typical facultative methylotrophs, such as *Methylobacterium extorquens* AM1, can grow on a wide range of poly-carbon compounds [72, 73].

Adaptation of denitrifying communities to the change of external carbon sources may involve both enrichment of new populations and the regulation of enzyme expression in existing populations. Methanol addition often requires an adaptation period of up to several months before the denitrification rates significantly increase [84]. This may be attributed to the necessary population shifts in the microbial community [70] to enrich methylotrophs. In contrast, activated sludge responds immediately to acetate and ethanol [85-87], as these two carbons select *Azoarcus, Dechloromonas, Thauera*, and *Acidovorax*-like denitrifiers, which have broad substrate specificities [78, 86]. Denitrifying species identified in activated sludge processes with different carbon sources are summarized in Table 1-IV.

Table 1-IV. Denitrifying populations grown on different types of carbon sources

Carbon source	Dominant functional groups	Techniques	References
Methanol	*Methylophilales,Methyloversatilis Hyphomicrobium, Paracoccus*	Culture isolation, Stable isotope probing (SIP), 16S rRNA gene sequencing, Fluorescence *in situ* hybridization (FISH)	[70, 74-77]
Ethanol	*Methyloversatilis, Azoarcus Dechloromonas, Pseudomonas Hydrogenophaga*	SIP, 16S rRNA sequencing	[77, 78]
Acetate	*Comamonas, Acidovorax, Thauera, Dechloromonas, Paracoccus, Rhodobacter*	SIP, 16S rRNA gene sequencing, FISH	[79, 80]
Glycerol	*Comamonas, Bradyrhizobium, Diaphorobacter, Tessaracoccus*	SIP	[81]
Glucose	*Arthrobacter, Phenylobacterium, Pseudomonas, Proteobacterium*	Denaturing gradient gel electrophoresis (DGGE)	[82]
landfill leachate	*Thauera, Acidovorax, Alcaligenes*	16S rRNA gene sequencing	[83]

1.7 Molecular techniques to study the structure and function of denitrifying communities

A variety of molecular methods have been applied to investigate denitrifying communities in the natural environments or wastewater treatment facilities [70, 88-91]. These culture-independent approaches aim at characterizing the microbial community diversity and structure, quantifying the abundance of denitrifiers or ecologically important genes, such as *narG*, *nirK* and *nirS*. Alternative molecular techniques for examining denitrifying community structure and function are presented in Figure 1-6.

Typical molecular microbial ecology analysis starts from the extraction of nucleic acid (either DNA or RNA) or protein from mixed-culture samples such as activated sludge. For DNA samples, quantitative real time polymerase chain reaction (qPCR) assay combines the traditional end-point PCR with fluorescent detection, thus enabling the simultaneous amplification and quantification of a given targeted gene sequence. For RNA samples, reverse transcription of RNA to complimentary DNA (cDNA) is required before quantifying the mRNA transcripts of targeted functional genes via qPCR (RT-qPCR). Oligonucleotide primers are designed to specifically target the genes of interest based on known sequence alignments. Although qPCR could detect and quantify activated sludge samples in both a sensitive and a specific manner, the major problem associated with this technique is the prerequisite of sequence data.

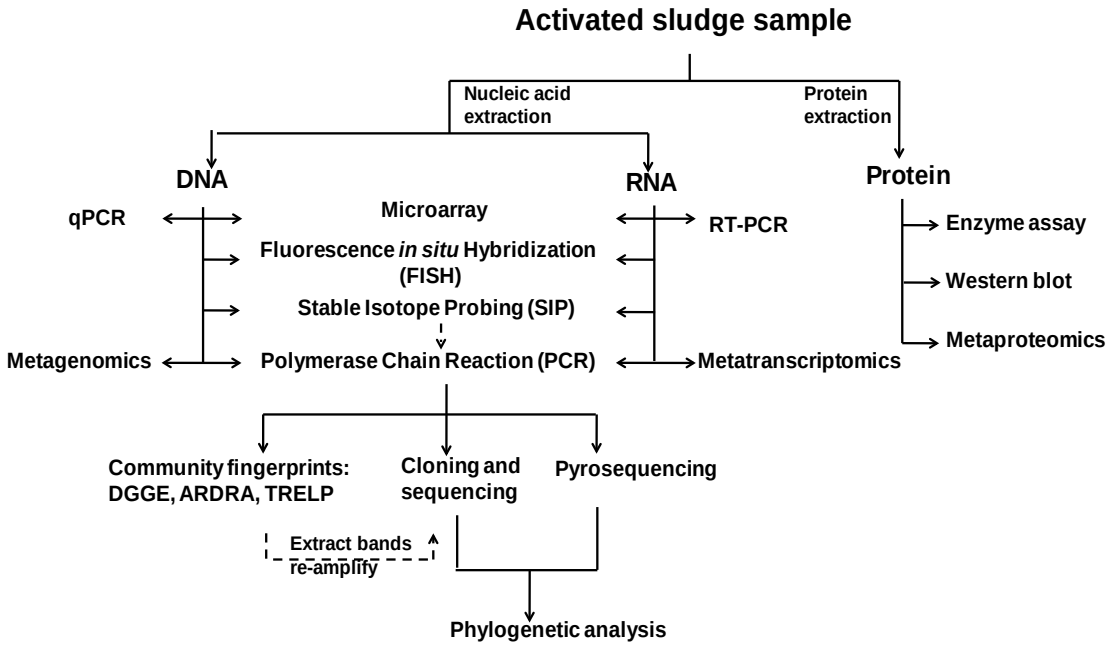

Figure 1-6: Molecular approaches for studying denitrifying community structure and function.

In order to investigate the denitrifying community diversity and composition, a number of different DNA fingerprinting techniques could be applied following the end-point PCR amplification. Terminal restriction fragment length polymorphism (T-RFLP) cut the gene fragments of 16S rRNA PCR products by restriction enzymes. Gene variants are subsequently separated via gel electrophoresis, and the relative abundances of the dominant variants (representing the dominant denitrifiers) are obtained. One of the disadvantages of T-RFLP is that this technique provides little information of specific species of the community. Another widely used fingerprinting tool is the denaturing gradient gel electrophoresis (DGGE). Denatured DNA fragments are separated based on their sequence diversity and GC content using gel electrophoresis, and each band represents a unique sequence variant or an operational taxonomic unit. The bands could be extracted and subject to phylogenetic analysis later on. Therefore, compared to T-

RFLP, DGGE is less quantitative but could yield more information about specific species identity via sequencing. Another technique that provides more detailed description of community structure is cloning and sequencing (PCR-based assays). A common strategy is to construct a library of gene sequences from PCR-amplified gene fragments. By collecting a large number of clones, the community diversity and composition can be measured.

Stable isotope probing (SIP) [92] can be used to directly link distinct taxa within a mixed microbial community to specific metabolic properties using labeled substrates, such as ^{13}C or ^{15}N for carbon and nitrogen utilization in microbial communities. The identification of active microorganisms is achieved by recovering and analyzing the isotope-enriched cellular components (DNA or RNA). SIP-based investigations are subject to the uncertainties posed by secondary utilization of labeled substrate, which could be minimized by shortening the incubation time [93]. ^{13}C based DNA SIP is discussed in more details in Chapter 2.

Any technique that uses PCR is subject to biases during the amplification process [94], and approaches that avoid PCR amplification have also been developed. The application of fluorescent *in situ* hybridization (FISH) technique enables the direct visual resolution of microbial cells, including those that are non-culturable, and is useful to determine the abundance of respective populations in microbial community samples. Microarray technology is based on the ability of complementary sequences of nucleic acids to hybridize or bind to one another. Applications of microarray technology include the detection of denitrifying bacteria and comparative functional gene expression [95, 96]. The high cost and the common occurrence of artifacts associated with image and data

analysis are main disadvantages of using microarray. Figure 1-7 summarizes the degrees of information that some of the above techniques can provide to study the structure and function of microbial communities.

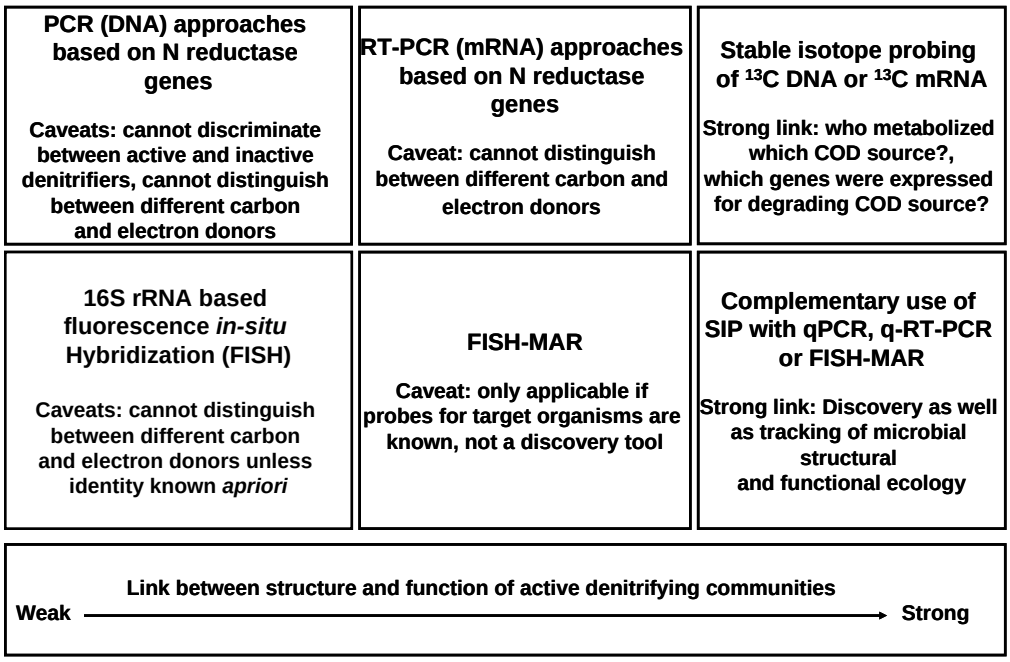

Figure 1-7: Varying degrees of information obtained on denitrification structure and f unction from different molecular techniques (after [97])

Molecular techniques have advanced at an especially fast pace in the recent past. Some of the more recent developments include: the high-throughput metagenomics, metatranscriptomics and metaproteomics. Metagenomics refers to culture-independent studies of the collective set of genomes of mixed microbial communities, and can be performed using newly developed pyrosequencing [98]. This faster and cheaper sequencing technique, although can only read short sequences (100-250 bases), is reliable and accurate enough for microbial community analysis [99]. In addition, the direct sequencing of transcripts (RNA-Seq) does not depend on genome annotation for prior probe selection and avoids biases introduced during hybridization of microarrays.

Therefore, RNA-Seq provides a far more precise transcriptome profiling of microbial communities [100]. The metaproteome represents the overall protein expression profile in a community, going beyond potential gene expression as determined by targeting mRNA. In proteomic analysis, both gel-based (one dimensional or two dimensional) and non-gel based liquid chromatography can be used to separate peptides, which are then identified by mass spectrometry. In recent studies, metaproteomics have been applied to quantitative protein detection in activated sludge systems [101, 102].

As presented in the different chapters of this dissertation, the microbial structure and function of denitrification using different organic electron donors in suspended and biofilm communities has been elucidated using ^{13}C-DNA SIP. Based on the rapid emergence of more high-throughput molecular techniques, the combination of meta-genomics, transcriptomics and proteomics with ^{13}C SIP offers exciting new prospects to extend this work even further.

1.8 Research hypothesis and objectives

The overall hypothesis of the study was that microbial community structure and function of denitrifying bacteria will vary upon the carbon sources added. Five specific objectives were used to test this principal hypothesis:

1) Characterize the molecular microbial ecology and biokinetics of methanol and ethanol assimilating denitrifying bacteria in a sequencing batch reactor (SBR);
2) Evaluate N_2O and NO emissions from denitrification SBRs using methanol and ethanol in response to three stressors: transient organic carbon limitation, high nitrite spike and oxygen inhibition;

3) Diagnose and quantify glycerol assimilating denitrifying bacteria in both the suspended and biofilm phases of a sequencing batch integrated fixed-film activated sludge reactor (SB-IFAS);
4) Examine the applicability of using the mRNA concentrations of alcohol dehydrogenase genes (*mdh2*, *mxaF* and *dhaD*) as biomarkers for carbon specific denitrification activities;
5) Compare the global proteome and functional gene expression of *Methyloversatilis universalis* FAM5, a model denitrifying bacterium, under anoxic growth on methanol and ethanol as carbon sources

This dissertation consists of eight chapters. Chapter 1 presents an introduction to denitrification.

Chapter 2 identifies the methanol assimilating populations in a denitrifying sequencing batch reactor (SBR), using stable isotope probing (SIP) of ^{13}C DNA and quantifies the dominant methylotrophic denitrifiers upon carbon switch from methanol to ethanol.

Chapter 3 characterizes the emissions of nitric oxide and nitrous oxide from two identical SBRs fed with methanol and ethanol separately, under steady-state, carbon limitation, nitrite pulse and different levels of oxygen inhibition conditions.

Chapter 4 distinguishes the glycerol assimilating denitrifying bacteria in the suspended and biolfilm phases of a sequencing batch integrated fixed-film activated sludge reactor operated with glycerol as electron donor, and also quantitatively tracks

dominated glycerol assimilating species and the denitrification kinetics in the two phases over one year operation.

Chapter 5 explores the potential of using alcohol dehydrogenase gene mRNA concentration as a biomarker for denitrification activity using methanol and glycerol as carbon sources.

Chapter 6 compares the global proteome and functional gene expression of *Methyloversatilis universalis* FAM5 grown with methanol and ethanol as electron donors under anoxic conditions.

In Chapter 7, implications and suggestions to wastewater engineering, as well as future research directions are discussed. In addition to the full chapters, supplementary information to Chapter 2-6 and the details of molecular techniques applied in the whole dissertation research are presented in Appendices AI and AII.

CHAPTER 2

IMPACT OF VARYING ELECTRON DONORS ON THE MOLECULAR MICROBIAL ECOLOGY AND BIOKINETICS OF METHYLOTROPHIC DENITRIFYING BACTERIA

This chapter has been published as:

Baytshtok V, Lu H, Park H, Kim S, Yu R, Chandran K*. 2009. Impact of varying electron donors on the molecular microbial ecology and biokinetics of methylotrophic denitrifying bacteria. *Biotechnology and Bioengineering* 102(6):1527-36. [2]

[2] The first two authors contributed equally to the work.

2.1 Introduction

Denitrification is the dissimilatory biochemical reduction of ionic nitrogen oxides such as nitrate-nitrogen (NO_3^--N) and nitrite-nitrogen (NO_2^--N) to gaseous oxides such as nitric oxide (NO) and nitrous oxide (N_2O) and eventually to dinitrogen (N_2) gas or under extremely anaerobic conditions to ammonium-nitrogen (NH_4^+-N) [1]. Although recently developed autotrophic processes for engineered biological nitrogen removal (BNR), such as anaerobic ammonia oxidation, (ANAMMOX) [103], completely autotrophic nitrogen removal over nitrite (CANON) [104], oxygen limited autotrophic nitrification and denitrification [105, 106] are novel and cost effective alternates to conventional nitrification and denitrification, such processes are most suited for high nitrogen containing streams such as anaerobic digestion reject water. While there is significant interest and ongoing research in understanding the constituent metabolic pathways of some of these more novel processes (with the genome of the first ANAMMOX enrichment sequenced recently [107], autotrophic aerobic nitrification followed by heterotrophic denitrification is still by far the most prevalent strategy followed by wastewater treatment plants to achieve BNR.

Wastewater utilities typically practice addition of external organic electron donors to enhance the rates of denitrification [22]. Of these external electron donors, methanol is one of the most widely used, mainly owing to its lower cost than alternates such as acetate and ethanol [108]. Despite extensive research and practical implementation of denitrification, a mechanistic understanding of ‘active’ denitrifying microbial fractions in activated sludge fed with different carbon and electron sources is lacking. Consequently, full-scale implementation of heterotrophic denitrification is

still guided by a somewhat empirical understanding of its microbial ecology and biokinetics, which in turn limites efforts to optimize denitrification reactor design, monitoring and modeling. Although biokinetic parameters for methylotrophic denitrification in activated sludge have been extensively reported [24, 109-115], the actual abundance and diversity of organisms in activated sludge that actually metabolize methanol and alternate carbon and electron sources has only recently been identified [70, 79, 80, 116]. The reason for such sparse data on the identity of bacterial populations denitrifying using specific electron donors is that unlike nitrifying bacteria, which are phylogenetically closely related [6], denitifying bacteria are distributed widely across taxonomic groups [2]. Thus, methods that directly inspect the uptake and metabolism of these electron donors during denitrification are needed.

With increasing methanol prices, it is conceivable that wastewater utilities may adopt alternates, which though expensive can foster significantly higher denitrification rates (for e.g., ethanol). Therefore, from an engineering perspective, it is also essential to determine the impact of changing between external carbon sources for denitrification on the constituent microbial ecology of activated sludge. The ability to link changes in the microbial ecology with resulting reactor performance and biokinetics could lead to better understanding of the ‘black-box’ of heterotrophic denitrification in activated sludge and result in better reactor operation, monitoring and control.

Given the limited diversity of methylotrophic organisms recognized to date and their specific nutritional requirement for methanol and other single-carbon

compounds as energy sources [117], we hypothesized that switching the carbon source from methanol to ethanol in a denitrifying reactor would result in the washout of methylotrophic organisms and the subsequent enrichment of a more diverse non-methylotrophic ethanol degrading population.

The specific objectives of this study were to:

(1) *Determine the microbial ecology of a denitrifying SBR fed with methanol followed by ethanol, using SIP and 16S ribosomal RNA gene sequence enabled phylogenetic interpretation of* ^{13}C *labeled DNA*

(2) *Quantitatively track the performance, biokinetics and microbial ecology of the SBR upon switching the electron donor in the influent stream from methanol to ethanol*

2.2 Materials and Methods

A methylotrophic enrichment consortium was cultivated in a SBR (V = 9.2 L, hydraulic retention time, HRT = 1d, solids retention time, SRT = 10d) operated at 21^{o}C. Each SBR cycle was six hours long with 1 h anoxic feed and react, 3.5 h anoxic react, 0.5 h aerobic mixing (to strip out dinitrogen gas and improve settling), 0.75 h settle and 0.25 h decant periods. SBR cycles were automatically controlled via a digital controller (Chrontrol Corp, San Diego, CA). The seed biomass for the SBR was kindly provided by the New York City Department of Environmental Protection and obtained from a pilot-scale BNR reactor treating domestic wastewater fed with methanol. The SBR was operated for 225 days with methanol and 260 days on ethanol using nitrate as the terminal electron acceptor (Table 2-I). In addition to the

organic electron donor and acceptor, the SBR feed medium contained (per liter), 0.2 g of MgSO4•7H_2O, 0.02 g of $CaCl_2$•2H_2O, 0.087 g of K_2HPO_4, 1 mL of trace elements solution (10 mg of Na_2MoO_4•2H_2O, 172 mg of $MnCl_2$•4H_2O, 10 mg of $ZnSO_4$•7H_2O, 0.4 mg of $CoCl_2$•6H_2O in a total volume made up to 100 mL with distilled water).

Table 2-I. Operating conditions of the denitrifying SBR

	Phase 1 **Methanol + Nitrate**	**Phase 2** **Ethanol + Nitrate**
Influent COD (mg COD/L)	500	500
Influent Nitrate (mg-N/L)	100	100
Period of operation (days)	225	260
% nitrogen removal	92.5 ± 11.6	98.5 ± 2.5
SRT	10 ± 0.0	10.3 ± 3.7

2.2.1 Microbial ecology of denitrification on methanol and ethanol via SIP

The overall schematic of the SIP enabled identification and quantitative tracking of denitrifying microorganisms using different COD sources is summarized in Figure 2-1. SIP was used to determine the ecological diversity of the SBR microbial community capable of utilizing methanol or ethanol for denitrification, as described previously [118]. For SIP experiments, 2 L biomass was withdrawn from the SBR just prior to the start of the 'settle' phase and washed by centrifugation at 1000*g for 20 min at room temperature and resuspending in COD and nitrogen free medium. SIP experiments were initiated by spiking the biomass with 250 mg COD/L of ^{13}C methanol (day 124 of operation) or ^{13}C ethanol (day 485 of operation) and 100 mg NO_3^--N/L to identify the dominant microbial communities assimilating these organic carbon sources. Samples for phylogenetic characterization of the specific communities metabolizing ^{13}C methanol or ^{13}C ethanol via SIP were obtained just at

the point of nitrate depletion during the SIP batch assay. It was independently determined for methanol that collecting samples at the point of nitrate depletion resulted in good discrimination of ^{12}C and ^{13}C DNA with longer incubations resulting in increased secondary ^{13}C uptake (data not shown). An unspiked sample was also obtained just before the ^{13}C spike (t=0) to characterize the 'overall' community in the reactor. Genomic DNA was extracted (DNeasy Blood & Tissue Kit, Qiagen, Valencia, CA) and subjected to isopcynic density gradient ultracentrifugation (55,000 RPM, T=20^{o} C, 22 h). Sixteen density-gradient fractions per sample were collected and quantified by real-time PCR (qPCR) using eubacterial primers [119] at conditions described previously [120] (BioRad *iQ*5, Hercules, CA). Out of the sixteen DNA fractions (Figure 2-2**)**, the fraction containing the highest ^{13}C concentration of DNA (for *e.g.*, at t=22.4 h, corresponding to a density of 1.753 g/mL) and the fraction containing the highest ^{12}C concentration of DNA (for *e.g.*, at t=0 h corresponding to a density of 1.7142 g/ml) were amplified against eubacterial 16S rRNA primers 11f [121] and 1492r [122]. Amplicons were cloned (TOPO TA Cloning® for Sequencing, Invitrogen, Carlsbad, CA) and plasmid inserts were sequenced (Molecular Cloning Laboratories, San Francisco, CA). Sequences were aligned, edited manually, and screened for chimera (CHIMERA_CHECK, (http://rdp8.cme.msu.edu/html/)). The closest matching sequences were obtained from GenBank (http://www.ncbi.nlm.nih.gov). ClustalX (InforMax, Inc., North Bethesda, MD) software was used to establish and bootstrap phylogenetic trees. The Neighbour Joining [123] method [124] was used for tree construction and positions with gaps were excluded and multiple substitutions were corrected. The tree was subjected to

1,000 bootstrap trials. The rooted bootstrapped tree was rendered using TreeView® software (http://taxonomy.zoology.gla.ac.uk/rod/rod.html) with *Methanosarcina thermophila* as the outgroup.

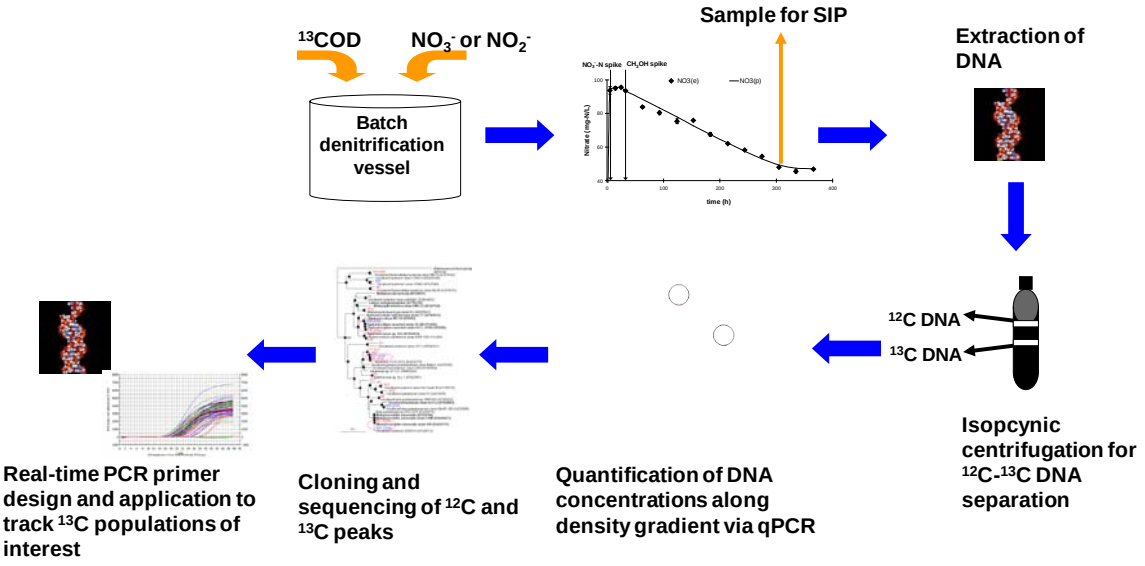

Figure 2-1: Schematic of SIP enabled identification and quantitative tracking of denitrify ing bacteria using different carbon sources

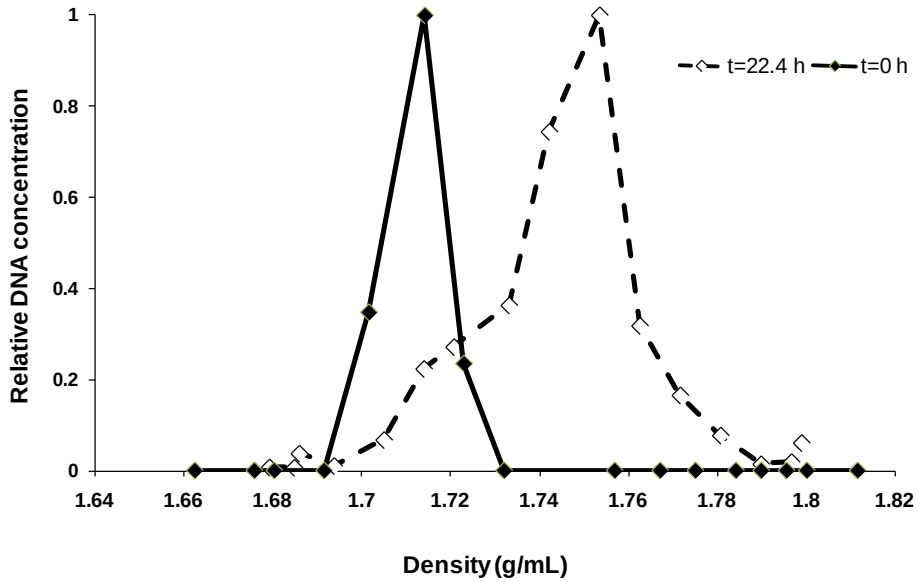

Figure 2-2: SIP profiles of methylotrophic biomass samples before and after ^{13}C methanol spike. Continuous line and shaded symbols were obtained at t=0; dashed line and open symbols were obtained at t=22.4h after the spike. DNA concentrations have been normalized to the maximum concentration for each respective profile.

2.2.2 Development of quantitative PCR assays for tracking methylotrophic biomass concentrations

Based on the identification of *Hyphomicrobium* spp. and *Methyloversatilis* spp. related bacteria as the dominant methylotrophic populations during phase 1 of this study (Figure 2-3), qPCR assays were designed, experimentally optimized and applied for determining their abundance over the three phases of reactor operation. qPCR primer sets were designed using PrimerQuest® software package (Integrated DNA Technologies, Coralville, IA) specifically targeting clones related to *Hyphomicrobium* spp. (Hzf- ACAATGGGCAGCAACACAGC and Hzr-ATTCACCGCGCCATGCTGAT) and *Methyloversatilis* spp. (Muf-AAGGCCTACCAAGGCAACGA and Mur-ACCGTTTCGTTCCTGCCGAA). Experimental optimization of qPCR assays was performed using genomic DNA from monocultures of *Hyphomicrobium zavarzinii* strain ZV620 (ATCC 27495) and *Methyloversatilis universalis 500* (ATCC BAA-1314) as standards. Monocultures of *H. Zavarzinii* ZV 620 and *M. Universalis* 500 were grown at 37^{o}C in nutrient broth to stationary phase as per ATCC instructions. Genomic DNA was extracted and purified from the cultures (DNeasy, Qiagen, Valencia, CA) and serially diluted to prepare standard curves for qPCR.

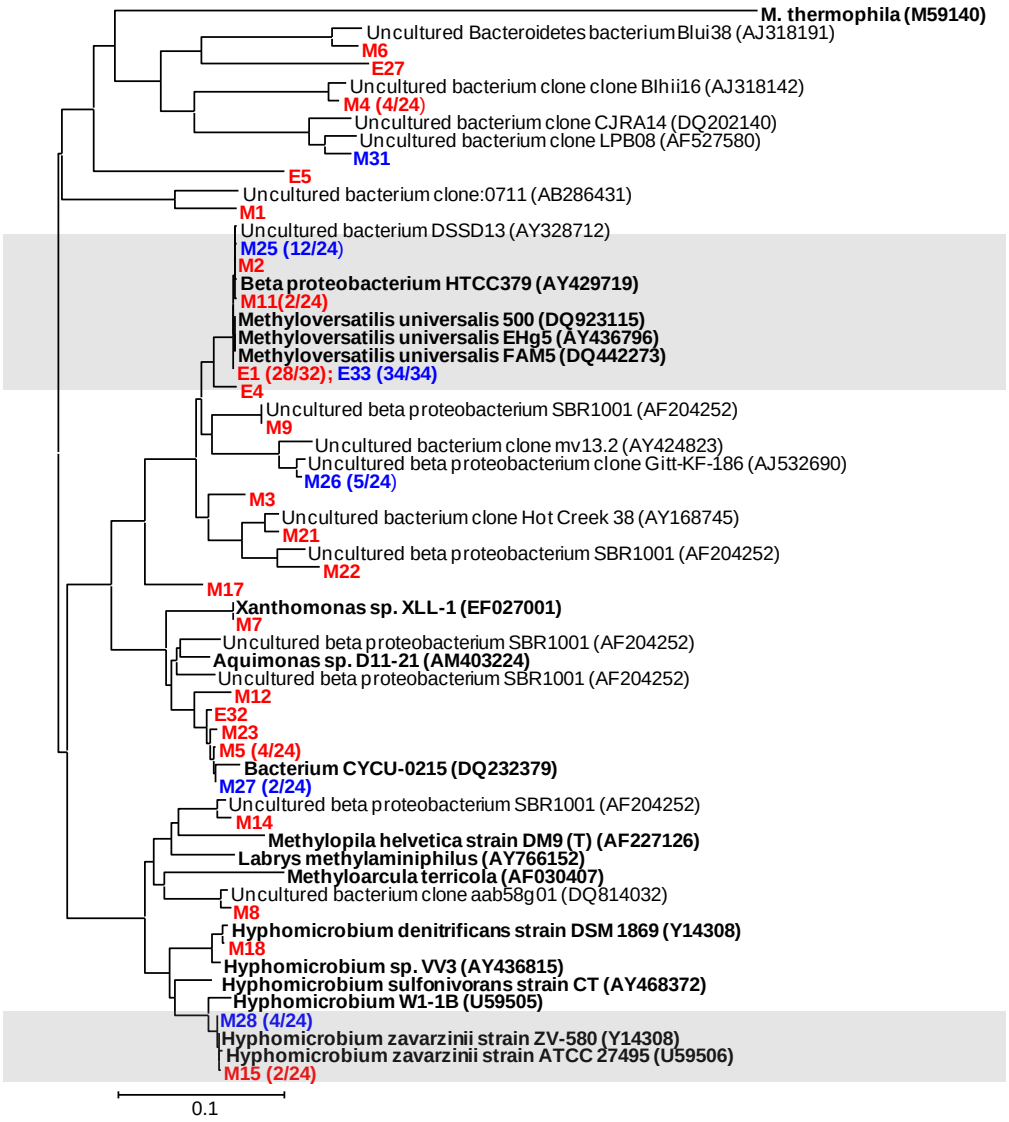

Figure 2-3: Phylogenetic tree depicting dominant OVERALL populations (RED) and populations assimilating either 13C methanol in phase 1 (denoted by "M", BLUE) or 13C ethanol in phase 2 (denoted by "E", BLUE) of SBR operation. Numbers in parentheses represent fraction of clones most closely associated with a given phylogenetic lineage. Shaded rectangles indicate 16S rRNA gene sequences with >97% similarity.

2.2.3 Performance and biokinetics of the denitrifying SBR

Denitrifying SBR performance was determined via influent and effluent nitrite (diazotization), nitrate (ion-selective electrode, Accumet®) and influent total and effluent soluble COD measurements, all according to standard methods [125]. Denitrification biokinetics were determined via 'extant' batch assays (similar to [126],

Figure S-3 in the Supplementary Information) using nitrite or nitrate as electron acceptors. For sDNR assays, biomass was withdrawn and processed identical to that for the SIP assays, but instead spiked with nitrate or nitrite and regular (^{12}C) methanol. Initial COD:N ratios were 2.5:1 and 1.5:1 for nitrate and nitrite extant batch kinetic assays respectively, thereby rendering organic carbon as the limiting nutrient, based on stoichiometric COD:N requirements of 5:1 and 3:1 for nitrate and nitrite, respectively [22]. Specific denitrification rates (sDNR) were computed by linear regression of the nitrate or nitrite depletion profiles normalized to total COD (tCOD) of the SBR mixed liquor.

2.3 Results

2.3.1 Microbial ecology of denitrification using methanol and ethanol

Based on 16S rRNA gene clone libraries, the organisms that assimilated ^{13}C methanol most rapidly during phase 1 (methanol feed) were a subset of the overall SBR biomass, and were most closely related to *Hyphomicrobium zavarainii* ZV 620 *and Methyloversatilis universalis* strain 500 (Figure 2-3)**.** The remaining SBR populations did not assimilate ^{13}C methanol rapidly enough during the period of the ^{13}C spike or were potentially sustained on endogenous bacterial metabolites during long-term SBR operation.

The diversity of the ethanol-fed biomass was significantly lower than that of the methanol fed-biomass, and most of the ^{12}C and ^{13}C clones in phase 2 were closely clustered with known bacteria related to *Methyloversatilis* spp. (Figure 2-3). These results suggest that the methylotrophic bacteria enriched in the SBR on methanol during phase 1 were indeed mainly sustained by assimilating ethanol during phase 2

and not on secondary metabolites or endogenous biomass products. Significantly, the long-term addition of ethanol to the SBR during phase 2 (260 days) did not result in the enrichment of a necessarily more diverse non-methylotrophic community as initially hypothesized.

Based on the newly developed and optimized qPCR assays, *Methyloversatilis* spp. were in general more abundant than *Hyphomicrobium* spp. during phase 1 of SBR operation (Figure 2-4). The change in organic electron donor from methanol to ethanol resulted in a significant decline in the concentrations of *Hyphomicrobium* spp. but not in the concentrations of *Methyloversatilis* spp. (Figure 2-4). Thus, both qualitative clone library analysis and quantitative PCR were consistent in pointing to the overall preponderance of *Methyloversatilis* spp. over *Hyphomicrobium* spp. during phase 2 (ethanol feed) as a result of changing the electron donor from methanol to ethanol (Figure 2-3 and Figure 2-4).

The applicability of the primer set targeting *Methyloversatilis* spp. that was designed based on the SIP results during phase 1 in targeting the additional *Methyloversatilis* spp. clones obtained in phase 2 (Figure 2-3) was evaluated and confirmed based on a BLASTn search (http://www.ncbi.nlm.nih.gov/blast/). Thus, the *Methyloversatilis* spp. concentraitons obtained by qPCR indeed included the entire *Methyloversatilis* spp. populations inferred from both clone libraries (phase 1 and 2). It is to be expected that the ^{13}C ethanol clone library (based on 34 clones) did not reveal *Hyphomicrobium* spp., since by the end of phase 2, their concentrations were three orders of magnitude lower than *Methyloversatilis* spp. On the other hand, the

detection of both populations by qPCR was in keeping with a broader operational linear range of qPCR assays from $10^4 – 10^{10}$ copies/mL.

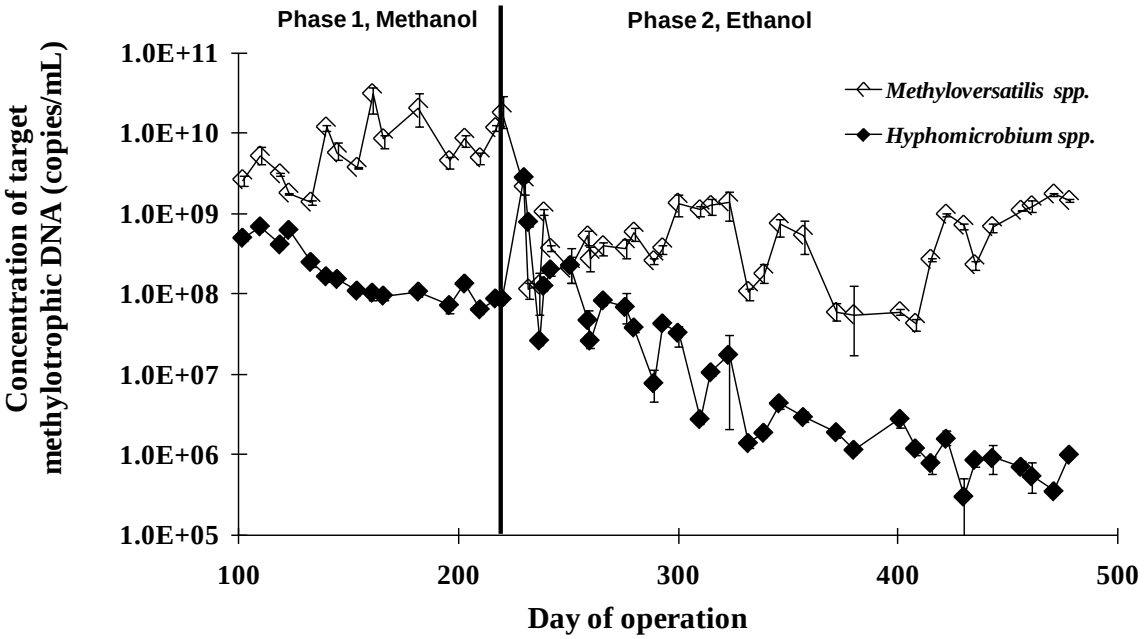

Figure 2-4: Relative abundance of *Hyphomicrobium* spp. related and *Methyloversatilis* spp. related methylotrophic bacteria in the SBR obtained via duplicate qPCR measurements during phase 1 (methanol feed) and phase 2 (ethanol feed) of denitrifying SBR operation

2.3.2 Performance and biokinetics of the SBR

Near complete steady-state nitrate and nitrite removal was obtained during the entire period of SBR operation (Table 2-I and Figure S-2 in the Supplementary Information). During phase 2, the switch in the electron-donor from methanol to ethanol resulted in a significant decrease in sDNR for methanol spiked biomass for both nitrate (p=9.5e-12, <0.050) and nitrite (p=2.76e-10, <0.050) as electron acceptor. sDNR values with nitrite as the terminal electron acceptor were in general higher than those with nitrate (Figure 2-5) and were in congruence with the lack of nitrite accumulation during the entire period of SBR operation (Figure S-2 in the SI). During

phase 2, sDNR values from ethanol spiked biomass were also higher than for methanol spiked biomass for both electron acceptors (data not shown).

Thus, based on the retention of *Methyloversatilis* spp., which could actively assimilate both methanol and ethanol and sustained SBR denitrification performance during phase 2, our initial hypothesis that the switch from methanol to ethanol would cause the less diverse methylotrophic community to be supplanted by a more diverse and distinct ethanol degrading community was comprehensively rejected.

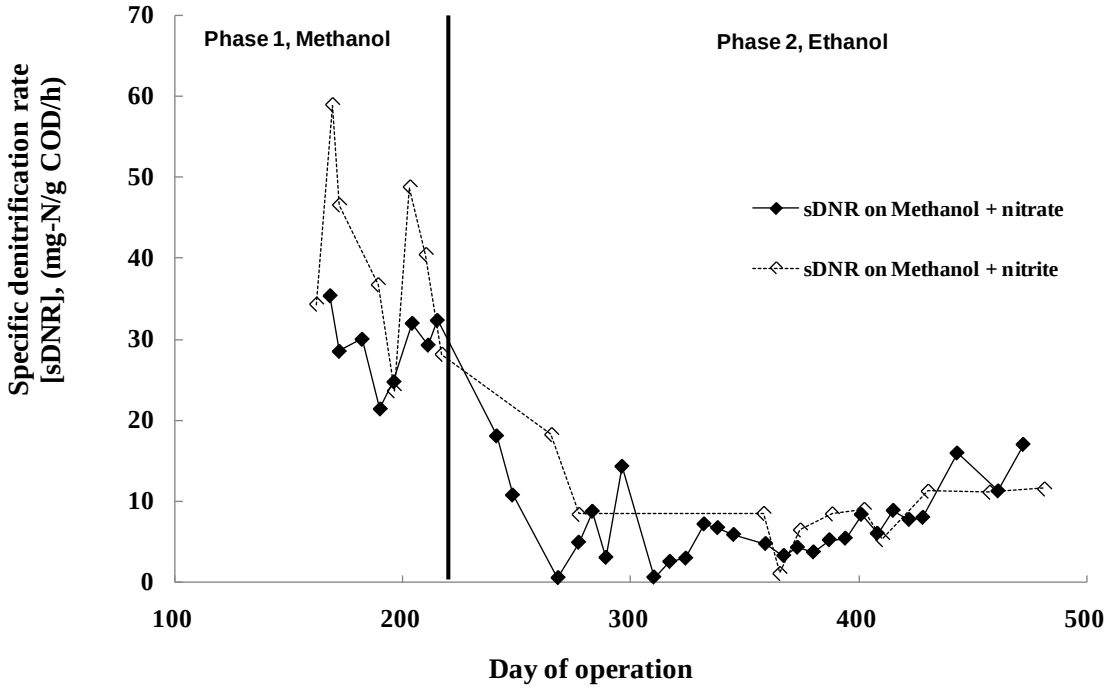

Figure 2-5: Time profiles of batch nitrate (continuous line and closed symbols) and nitrite (dashed line and open symbols) sDNR during phase 1 (methanol feed) and phase 2 (ethanol feed) of denitrifying SBR operation

2.4 Discussion

2.4.1 The microbial ecology of methylotrophic denitrification

Notwithstanding the preferred and widespread use of methanol, ethanol, acetate and now glycerol or sludge fermentate as external carbon sources for

enhanced denitrification in BNR facilities, very little is still known about the microbial structure-function link of denitrification relating to these carbon sources. *Hyphomicrobium* spp. have been long speculated to be the dominant microbial group engaged in methylotrophic denitrification based on isolation techniques [1, 66, 127-129] or direct molecular inspection techniques [130-132]. However, several recent studies have implicated a considerably higher diversity of methylotrophic denitrification in activated sludge [70, 79, 133]. According to two recent SIP based studies, *Hyphomicrobium* spp. were not the dominant active methylotrophic populations in methanol fed denitrifying reactors [70, 79]. Instead, the reactors were mostly comprised of obligately methylotrophic *Methylobacillus* and *Methylophilus* belonging to the order *Methylophilales* of the *Betaproteobacteria* [70] or a co-culture of *Hyphomicrobium* spp. and *Methylophilaceae* [79]. In another study, *Hyphomicrobium* spp. constituted just 2% of the total population of a methanol-fed denitrifying filter [133].

Despite the implication of bacteria other than *Hyphomicrobium* spp. in denitrification with methanol (which is in good agreement with the results herein), the impact of long-term changes in the type of carbon source on the ecological diversity and concentrations of these methylotrophic communities, and correlations with their metabolic capabilities has not been determined before. The short-term ability of denitrifying biomass grown on methanol to denitrify using ethanol (via sDNR assays) was indeed recently shown but not explained or attributed to the specific participant microbial communities [134].

From an engineered wastewater treatment standpoint, it is equally important to understand both the identities and metabolic capabilities of dominant methylotrophic denitrifying populations in activated sludge. Such information is critical, for instance to evaluate the feasibility of switching to a higher rate carbon source such as ethanol *in lieu* of methanol, which could be favored during lower winter temperatures at wastewater treatment plants, or due to the increasing price of methanol.

The observed trend in the dominant methylotrophic populations upon switching from methanol to ethanol in this study can be explained based on their nutritional modes. Most characterized *Hyphomicrobium* spp. are restricted facultative methylotrophs that can utilize mainly C1 compounds for growth [135]. Therefore, it is expected that the *Hyphomicrobium* spp. related organisms present in the SBR during phase 1 (methanol fed) of this study could not be sustained during phase 2 (ethanol fed). On the other hand, bacteria related to *Methyloversatilis universalis* can utilize several C1 and multicarbon compounds [136]. Therefore, the continued higher concentrations of *Methyloversatilis* spp. related organisms upon transition from methanol to ethanol feed correlated well with their broader metabolic capabilities.

Therefore, from a practical perspective, upon switching from methanol to ethanol for denitrification, it is the presence of facultative methylotrophs that can assimilate both ethanol and methanol results in sustained denitrification and not necessarily the rapid development of a more diverse ethanol degrading community.

2.4.2 The microbial ecology of ethanol based denitrification

Compared to methanol, even less is known about the molecular microbial ecology of ethanol based denitrification. The dominance of bacteria related to

Azoarcus, *Dechloromonas*, *Thauera*, and *Acidovorax* spp. in an ethanol-fed bioreactor was recently reported [78], although it was not clear which of these communities actually assimilated ethanol during denitrification (as explicitly done in this study). Another recent study reported that the diversity of an ethanol fed denitrifying community was lower than that of a methanol fed denitrifying community, based on sequence information of the nitrite reductase (*nirS* and *nirK*) genes [137]. However, again, the specificity of the overall community for methanol or ethanol degradation was not determined. Therefore, in general, a direct comparison of the microbial ecology of ethanol based denitrification with other studies was precluded by the paucity of information thereof and the fact that the ethanol degrading community in this study had been enriched on methanol *a priori*.

2.4.3 Techniques for characterizing the structure and function of methylotrophic denitrification in activated sludge

Elucidating the link between microbial community *structure* (composition and diversity) and *function* (reactions catalyzed) represents a singular challenge for microbial ecologists and engineers alike. However, since denitrification capabilities are phylogenetically and taxonomically diverse [2], it is nearly impossible to "structurally" probe for all denitrifying bacteria in communities such as activated sludge using 16S rRNA targeted methods. Some studies have favored a more "functional" elucidation of denitrification microbial ecology by targeting key nitrogen reductase enzymes in the denitrification pathway including nitrate reductase (*napA* and *narG*) [138-140], nitrite reductase (*nirS* and *nirK*) [90, 141-147], (*norB*) [148] and nitrous oxide reductase (*nosZ*) [149, 150]. However, it is not possible to

differentiate between the use of different COD sources or confirm denitrification activity by looking at the abundance of the nitrogen reductase genes alone (Figure 2-6).

An alternate technique, fluorescence *in-situ* hybridization combined with microautoradiography (FISH-MAR) relies upon the uptake of radio isotopic substrates into bacterial cells to infer phylogenetic composition [151, 152]. However, FISH-MAR is only applicable to identify organisms for which phylogenetic information is available *a priori*. If such information is not known, one cannot determine which probes to use. Therefore, FISH-MAR alone cannot be used as a discovery tool for functional elucidating microbial ecology, but just as a probing tool.

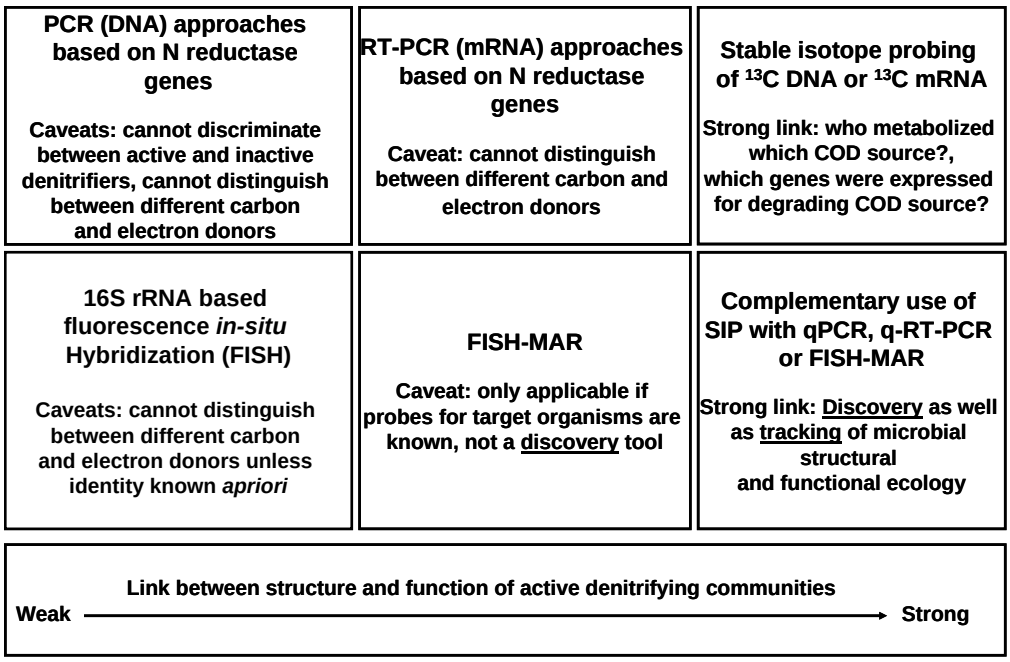

Figure 2-6: Varying degrees of information obtained on denitrification structure and function from different molecular techniques (after [97])

In contrast, SIP relies upon the incorporation of ^{13}C substrates into cellular macromolecules such as DNA, RNA, phospholipid fatty acids and proteins, which

confirms metabolism of the ^{13}C substrate [92]. When combined with DNA, RNA or phospholipid fatty acid (PLFA) based phylogenetic mapping, SIP is an effective discovery technique for linking the identity of active bacteria with their function (degradation of specific substrates) [70, 79, 80, 92, 103, 116, 153-156]. In addition to 16S rRNA genes (as followed in this study), SIP could also be combined with other biomarkers such as messenger RNA (mRNA) of genes coding for methanol anabolic and catabolic reactions including tetrahydromethanopterin-linked formaldehyde oxidation (*fae* and *fhcD*) [157, 158], methanol dehydrogenase (*mxaF*) [159] or alcohol dehydrogenase genes for both methanol and ethanol (*mdh2*) [160], which could explain the microbial pathways at work [156].

2.4.4 Significance of monitoring the concentrations and specific activities of methylotrophic bacteria in activated sludge

The utility of conducting both population and biokinetic monitoring of denitrification was amply illustrated upon switching electron donors in this study. Since, we *explicitly* measured both population abundance (by qPCR) and activity (by sDNR), we inferred that the lower (methanol + nitrate) sDNR in phase 2 was not just due to a reduction in specific activity of the methylotrophic population but also due to a reduction in the concentrations of *Hyphomicrobium* spp. in the SBR (Figure 2-4 and Figure 2-5). Additionally, the strong parallel decrease in the concentrations of *Hyphomicrobium* spp. and methanol+nitrate sDNR in phase 2 suggests that *Hyphomicrobium* spp. have higher methanol based sDNR (and correspondingly maximum specific growth rates, μ_{max}) values than *Methyloversatilis* spp. This could be one reason why previous cultivation or isolation based studies (which select for

rapidly growing organisms) routinely implicated *Hyphomicrobium* spp. as the dominant or even the sole methylotrophic bacteria in their test cultures [1, 66, 127-129]. The lower concentrations of *Hyphomicrobium* spp. during phase 1 could be due to the fact that bacteria with higher μ_{max} values are typically associated with higher half-saturation (K_S) values as well (r-strategists) [161]. R-strategists cannot scavenge low substrate concentrations (*in casu*, methanol and nitrate, reflected by near complete nitrate removal in throughout the study) and are out-competed by K-strategists, which have both lower μ_{max} and K_S values (*in casu*, *Methyloversatilis* spp.). Alternately, it may be speculated that *Hyphomicrobium* spp. have a lower biomass yield than *Methyloversatilis* spp..

2.5 Summary

In summary, this study diagnosed bacterial populations that assimilated methanol in a denitrifying sequencing batch reactor (SBR) using stable isotope probing (SIP) of ^{13}C labeled DNA, and quantitatively tracked changes in their concentrations upon changing the electron donor from methanol to ethanol in the SBR feed. Based on SIP derived ^{13}C 16S rRNA gene clone libraries, dominant SBR methylotrophic bacteria were related to *Methyloversatilis* spp. and *Hyphomicrobium* spp. These methylotrophic populations were quantified via newly developed real-time PCR assays. Upon switching the electron donor from methanol to ethanol, *Hyphomicrobium* spp. concentrations decreased significantly in accordance with their obligately methylotrophic nutritional mode. In contrast, *Methyloversatilis* spp. concentrations were relatively unchanged, in accordance with their ability to assimilate both methanol and ethanol. Direct assimilation of ethanol by

Methyloversatilis spp. but not *Hyphomicrobium* spp. was also confirmed via SIP. The reduction in methylotrophic bacterial concentration upon switching to ethanol was paralleled by a significant decrease in the methanol supported denitrification biokinetics of the SBR on nitrate. These results demonstrate that the metabolic capabilities (methanol assimilation and metabolism) and substrate specificity (obligately or facultatively methylotrophic) of two distinct methylotrophic bacterial populations contributed to their survival or washout in denitrifying bioreactors. It is expected that a change in the electron donor from methanol to ethanol will likely not result in significant disruptions to denitrification performance in BNR reactors, by virtue of the sustained presence and activity of facultatively methylotrophic bacteria therein.

2.6 Supplementary Information Available

Relative concentrations of *Methyloversatilis* spp. and *Hyphomicrobium* spp. during Phase 1 (methanol), Phase 2 (ethanol) and Phase 3 (a recovery phase operated under the same conditions as Phase 1; data collected after the manuscript was submitted); SBR reactor performance during three phases (Figure S-2); specifics of the extant denitrification batch assays (Figure S-3);

CHAPTER 3

FACTORS PROMOTING EMISSIONS OF NITROUS OXIDE AND NITRIC OXIDE FROM DENITRIFYING SEQUENCING BATCH REACTORS OPERATED WITH METHANOL AND ETHANOL AS ELECTRON DONORS

This chapter has been published as:

Lu H, Chandran K*. 2010. Factors promoting emissions of nitrous oxide and nitric oxide from denitrifying sequencing batch reactors operated with methanol and ethanol as electron donors. *Biotechnology and Bioengineering* 106 (3):390-398.

3.1 Introduction

Heterotrophic denitrification is the dissimilatory reduction of ionic nitrogen oxides such as nitrate and nitrite, to nitric oxide (NO), nitrous oxide (N_2O) and ultimately to dinitrogen gas (N_2) using organic electron donors [1]. Sequential actions of several enzymes including nitrate reductase (NaR), nitrite reductase (NiR), nitric oxide reductase (NOR) and nitrous oxide reductase (N_2OR) are involved. The greenhouse gas effect of N_2O is approximately 300 times more potent than carbon dioxide [3]. A more recent involvement of N_2O in direct depletion of the ozone layer has also been shown [162]. NO also contributes to destruction of the ozone layer and to precursors of photochemical smog [163]. As one of the two main reactions in engineered BNR systems, denitrification is implicated as a potential source of global N_2O emissions [164, 165]. Although autotrophic nitrification can itself contribute to N_2O emissions from wastewater treatment plants [166, 167], the sole focus of this work was to elucidate potential triggers of N_2O emissions from two distinctly operated heterotrophic denitrifying reactors. The mechanisms behind autotrophic N_2O and NO emissions in response to aerobic-anoxic transitions have recently been elucidated [168] and are not included herein.

Several factors have been linked to N_2O and NO generation and emission from denitrifying bioreactors including low pH [169], short solids retention time [170], organic carbon limitation [170, 171], dissolved oxygen inhibition [164, 172] and nitrite inhibition [173]. However, the impact of the specific carbon source on resulting N_2O and NO generation and emission has received limited attention. From an engineering perspective, with increasing methanol costs, wastewater utilities may

adopt alternate external carbon sources, *e.g.*, ethanol, to sustain and enhance denitrification. Although ethanol is currently more expensive than methanol, it fosters specific denitrification rates 2-3 times higher than methanol [134]. Therefore it is conceivable that ethanol might be a viable carbon source to sustain adequate denitrification kinetics and performance during low temperatures [134]. However, it is imperative to determine ethanol associated N_2O or NO emissions to ensure minimization of both aqueous and gaseous nitrogenous pollution. Such an evaluation is especially important since it has been recently shown that different organic carbon sources foster distinct microorganisms, even in mixed cultures [70, 77, 116]. Thus, it could be hypothesized that the resulting differences in microbial community structure and their tolerance or susceptibility to transient stressors could give rise to different emissions on different carbon sources.

Therefore, the overall goal of this study was to systematically evaluate N_2O and NO emissions from denitrification using two organic carbon sources, methanol and ethanol in response to three stressors, transient organic carbon limitation, exposure to high nitrite concentration spikes and a range of inhibitory oxygen concentrations. These lab-scale experiments are part of an ongoing overall multi-scale investigation on mechanisms of N_2O and NO generation and emission from wastewater treatment plants and lab-scale nitrifying and denitrifying cultures.

3.2 Materials and Methods

3.2.1 Bioreactor operation

Two denitrifying SBRs (V = 9.2 L) were inoculated with activated sludge from a step-feed BNR reactor at 26th Ward Water Pollution Control Facility in New York

City and operated with methanol and ethanol respectively, using nitrate as the terminal electron acceptor as previously described [76, 77]. The solids retention time (SRT) for both SBRs was 10 days and the hydraulic retention time (HRT) was 1 day. This conservatively high SRT was chosen to enrich for methanol and ethanol assimilating biomass in the respective SBRs and ensure complete nitrate removal, as described previously [76, 77]. Each SBR had a six-hour cycle comprising of 1 h continuously anoxic feed and react, 3.5 h anoxic react, 0.5 h aerobic mixing (to strip out dinitrogen gas and improve settling), 0.75 h settle and 0.25 h decant phases. SBR phases were automatically controlled via a digital controller (Chrontrol Corp, San Diego, CA). The influent COD and NO_3^--N concentrations for both SBRs were 500 mg chemical oxygen demand (COD)/L (methanol or ethanol) and 100 mg NO_3^--N/L, respectively. The SBR feed medium contained (per liter): 0.2 g of $MgSO_4 \cdot 7H_2O$, 0.02 g of $CaCl_2 \cdot 2H_2O$, 0.087 g of K_2HPO_4, 1 mL of trace elements solution (10 mg of $Na_2MoO_4 \cdot 2H_2O$, 172 mg of $MnCl_2 \cdot 4H_2O$, 10 mg of $ZnSO_4 \cdot 7H_2O$, 0.4 mg of $CoCl_2 \cdot 6H_2O$ in a total volume made up to 100 mL with distilled water). The pH of the SBRs was automatically controlled in the range of 7.3 ± 0.2 using concentrated hydrochloric acid during undisturbed operation, but not during gas measurements, during which, the pH ranged from about 7.3 to 8.1.

Characterization of ultimate-state and transient state operations

Aqueous and gaseous nitrogen species were measured during individual SBR cycles, corresponding to ultimate-state or transient operations with carbon limitation, nitrite and oxygen inhibition. Each transient condition was imposed at least three

times independently upon each of the two SBRs to obtain a measure of biological reproducibility. The transients were specifically imposed as follows:

(1) *Carbon limitation.* Methanol or ethanol along with nitrate was provided during the first 0.5h of anoxic feeding phase, followed by 1 h of carbon limitation (but not nitrate limitation) and finally followed by 0.5 h of carbon feeding (without nitrate). In this manner, temporary carbon limitation followed by recovery to non-limiting conditions was imposed. However, the overall carbon and nitrate mass fed during a given SBR cycle during transient limitation and ultimate-state were identical.

(2) *Nitrite inhibition.* 10 ml of stock sodium nitrite solution (46 g NO_2^--N/L) was spiked into the SBR during the middle of the feeding phase to achieve a peak NO_2^--N concentration of 50 mg-N/L. Methanol or ethanol and nitrate were fed to the SBR as during ultimate state.

(3) *Dissolved oxygen inhibition.* Oxygen inhibition in the SBR was achieved by continuously pumping air (0.5 L/min for DO = 2.5 ± 0.5 mg/L; 1 L/min for DO = 5.1 ± 1.2 mg/L) or pure oxygen (0.5L/min for DO = 9.0 ± 1.1mg/L) to maintain the desired DO concentration during the entire SBR cycle. Methanol or ethanol and nitrate were fed to the SBR as during ultimate state.

3.2.2 Headspace N_2O and NO measurements

Headspace gas collection was performed in accordance with a newly developed USEPA reviewed protocol for measuring N_2O and NO fluxes from open surface wastewater treatment plants [174]. Gas collection was performed using a custom-made plastic flux chamber (volume = 3.5 L), which was sealed to the SBR body. Sweep air was introduced into the chamber at a flow rate of 4 L/min, except

during transient oxygen inhibition, where the sum of the sweep gas flow rate and air (or oxygen) flow rate equaled 4 L/min. Real-time N_2O and NO concentrations (ppmv) in the flux-chamber were measured via gas-filter correlation (Teledyne API, San Diego, CA) and chemiluminescence (Ecophysics, Ann Arbor, MI), respectively. Nitrite (diazotization), nitrate (ion-selective electrode, Accumet®), pH, ORP and DO (Yellow Springs Instruments, Yellow Springs, OH) were measured at 30 min intervals. Reactor and effluent biomass COD concentrations were measured based on standard methods [125].

The fraction of influent nitrate emitted as N_2O or NO was determined by numerically integrating the real-time profile of N_2O or NO emission mass flux (Eqn. 3-1) and normalizing to mass of nitrate fed during a cycle.

$$M_N = Q \times C \times \frac{MW_N}{V_0} \times t_0 \qquad \text{(Equation 3-1)}$$

where, M_N is the mass of emitted nitrogen during a cycle as either NO or N_2O (mg-N), Q is the flow rate of sweep air and gas pumped into the flux chamber (4 L/min), C is the accumulated concentration of N_2O or NO during a cycle (ppmv), MW_N is the molecular weight of nitrogen in N_2O and NO (14 and 28 g/mol), V_0 is the molar volume of an ideal gas, 24.05 L/mol at 1atm and 22°C and t_0 is the duration of one cycle (6 h).

3.2.3 Extant biokinetics of denitrification

Batch experiments were conducted as described previously to determine denitrification kinetics with methanol and ethanol at ultimate state and exposure to three DO concentrations: 2, 5 and 9 mg O_2/L (comparable to DO concentrations transiently imposed upon the SBRs) [76]. Briefly, 500 ml biomass samples were

withdrawn from the SBRs towards the end of the react cycle, washed, and resuspended in nitrate and COD free medium and sparged with N_2 gas to render them anoxic (DO < 0.2 mg/L). Biokinetic assays were conducted by spiking the biomass samples with non-limiting concentrations of nitrate and COD (methanol or ethanol) and tracking the resulting nitrate and nitrite profiles over time. In selected assays, air or pure oxygen was introduced into the batch denitrification vessels, to achieve different DO concentrations. Specific denitrification rates (sDNR) were computed via linear regression of the nitrate depletion profiles *vs* time and normalizing to total biomass COD concentrations.

3.3 Results and Discussion

3.3.1 Ultimate state performance and emissions of N_2O and NO

During ultimate-state operation, near complete nitrate removal was observed in both SBRs (methanol: 92.5 ± 11.6 %, ethanol: 98.5 ± 2.5 %) with minimal nitrite accumulation (<1 mg-N/L). Little N_2O (methanol: 0.11 ± 0.02 %, ethanol: 0.10 ± 0.01 %) or NO (methanol: 0.02 ± 0.01%, ethanol: 0.01 ± 0.00%) was emitted (Figure 3-1). In keeping with the sequential production of the two species during denitrification, NO concentrations peaked before N_2O concentrations during any given SBR cycle (Figure 3-2, a1 and b1).

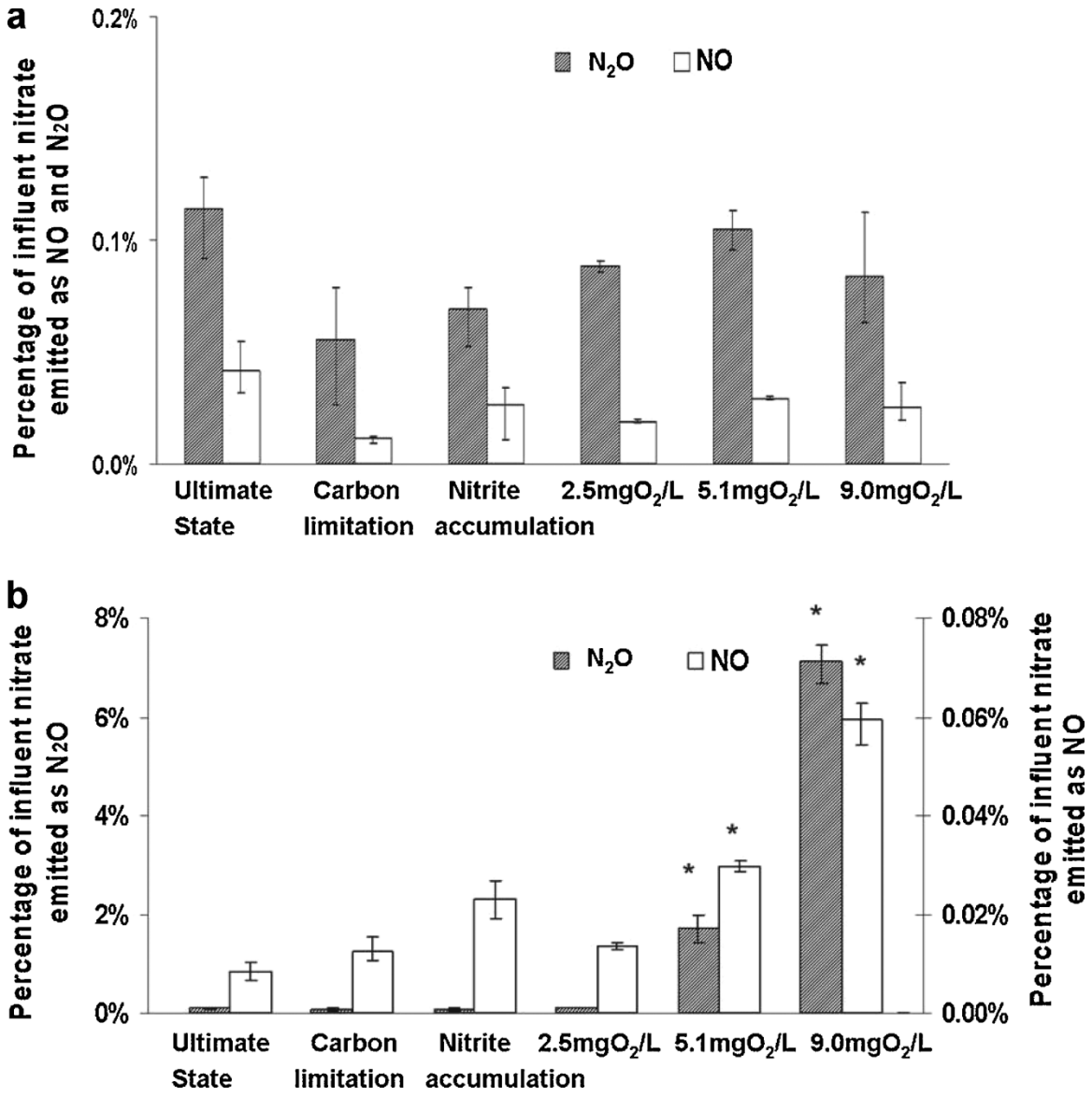

Figure 3-1: Fraction of influent nitrate load emitted as N_2O and NO in (a) methanol fed SBR and (b) ethanol fed SBR under ultimate state, carbon limitation, nitrite and DO inhibition. * indicates results significantly different from steady-state at $\alpha = 0.05$.

Under the ultimate-state operation, factors leading to incomplete denitrification have generally been attributed to N_2O production. For instance, in a recent study, complete denitrification resulted in 0.1% of the removed nitrate emitted as N_2O. In contrast, the extent of emissions was significantly higher (1.3%) as nitrate removal dropped to 66% [175]. These results are consistent with the low ultimate-

state N_2O and NO emissions from the either of both SBRs, wherein nitrate removals higher than 90% were observed without concomitant nitrite accumulation. The fraction of influent nitrate removed that was emitted as N_2O for methanol (0.12%) was comparable with previous results in the range of 0.2-1.3% with methanol [172]. Emissions with ethanol enriched denitrifying bacteria have not been reported previously and thus cannot be directly compared.

3.3.2 Impact of transient carbon limitation

Transient carbon limitation resulted in transient nitrate accumulation for both methanol and ethanol fed SBRs. Relatively lower nitrate accumulation was observed during ethanol limitation than during methanol limitation (data not shown), which can be explained by higher denitrification biokinetics for ethanol than methanol [77]. Nitrite accumulation was similar for both COD sources and much lower than nitrate accumulation (data not shown). However, owing to the long react phase and the operating SRT of 10 days, complete nitrate removal was eventually observed by the end of the overall cycle for both reactors. N_2O and NO emissions during a cycle were statistically lower than ultimate state control for the methanol fed SBR, but were largely similar in the ethanol fed SBR (Figure 3-1).

The lack of significant N_2O emissions during carbon limitation is in contrast to some previous reports [171, 176]. It has been postulated that the higher electron affinities of two upstream denitrification enzymes, NaR and NiR, relative to downstream NOR and N_2OR enzymes could be the reason for N_2O accumulation during carbon limitation [1, 39]. While specific enzyme affinities were not directly measured in this study, it is possible that the distinct populations fostered by methanol

and ethanol (as described previously [77]) might possess more uniform and high affinities across the sequential reductive nitrogen cascade, leading to the lack of N_2O and NO emissions during carbon limitation.

The possession of high affinities could be due to the high operating SRT of the SBRs for over 2 years, which could have resulted in long-term enzymatic adaptation to low substrate (carbon and nitrate) concentrations. Indeed, minimal N_2O emissions were observed from acetate-limited denitrifying reactors operated at high SRT values (10 days) [170]. Additionally, adaptation of *Alcaligenes faecalis* cultures to cycling between feast and famine resulting in lower N_2O production has also been shown [177]. Therefore, these results show that the link between carbon limitation and N_2O emission may not be universal for all carbon sources and operating conditions, and needs to be evaluated more specifically.

3.3.3 Impact of nitrite inhibition

Exposure to nitrite led to statistically higher nitrate accumulation at the end of the SBR cycle for both carbon sources, indicating feedback inhibition of nitrate reduction by nitrite (data not shown). However, near complete nitrite reduction was still achieved in the ethanol fed SBR, but not in the methanol fed SBR (76.5 ± 3.2 %). The nitrite transient also resulted in slightly elevated secondary peak of NO (Figure 3-2, a3 and b3) compared to ultimate-state (Figure 3-2, a1 and b1) for both SBRs. Nevertheless, N_2O emissions were not impacted and the resulting fractions of nitrate converted to N_2O and NO were statistically similar (α=0.05) to those at ultimate state (Figure 3-1).

It has been previously suggested that N_2OR is more sensitive to nitrite inhibition compared to other enzymes in denitrification, thus leading to N_2O production under nitrite exposure [1, 178]. Besides the direct impact of nitrite, N_2OR inhibition can also be due to NO, which is formed from nitrite reduction [179]. Indeed, accumulation of N_2O and NO during denitrification in the presence of nitrite was observed with acetate and yeast extract fed denitrifying cultures, with an inhibitory threshold nitrite concentration of approximately 10 mg-N/L [170, 173]. However, at the same nitrite concentration, little N_2O production was observed from activated sludge with sucrose as sole carbon source [165]. Another study using pure cultures of *Alcaligenes sp.* and *P. fluorescens* grown on nutrient broth as carbon source also reported no impact of nitrite pulses on N_2O accumulation [39]. The differences in N_2O production as a function of nitrite exposure in these different studies could be possibly due to the different carbon sources used or the mode of cultivation used. Therefore, the previous results and this study essentially underscore the lack of generality in the link between nitrite exposure and N_2O production, from denitrification using different carbon sources.

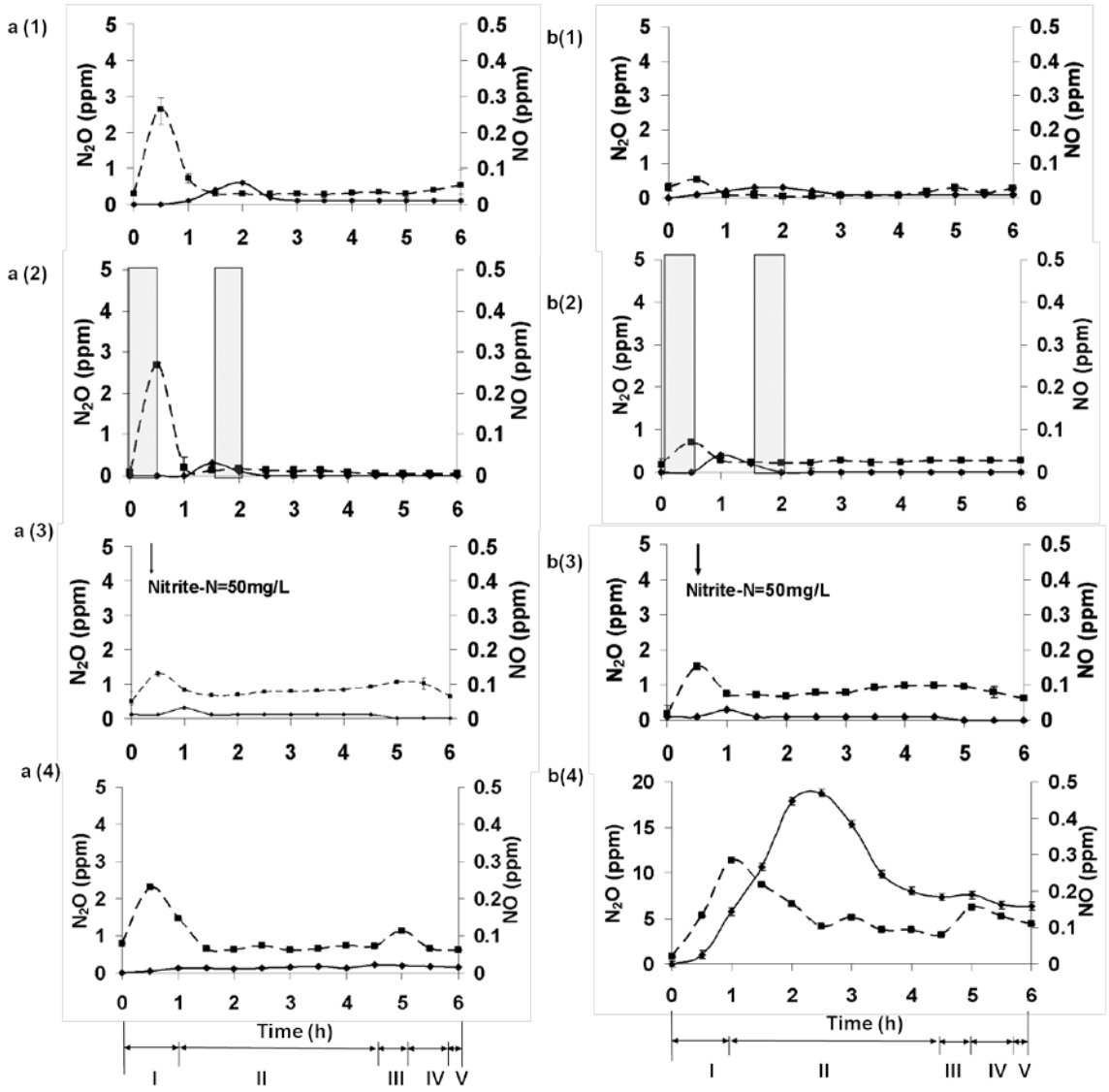

Figure 3-2: Representative N_2O and NO emissions from (a) methanol fed SBR and (b) ethanol fed SBR under ultimate state (1), carbon limitation (2, the 1h interval between two shadows indicates carbon limitation phase), nitrite inhibition (3), and DO inhibition at 9 mg O_2/L (4). Roman numerals, I-V represent: anoxic feed and react, anoxic react, aerobic mixing, settle and decant phases of the SBR cycle, respectively. ━■━ N_2O (primary axis); ━◆━ NO (secondary axis).

3.3.4 Impact of oxygen inhibition

In both methanol and ethanol fed SBRs, a rapid initial accumulation of nitrate was observed upon the introduction of air or oxygen (Figure 3-3). Higher inhibition of oxygen on nitrate reduction occurred in methanol fed SBR. In contrast, significant

(but delayed) nitrate removal occurred in the ethanol fed SBR at all DO concentrations.

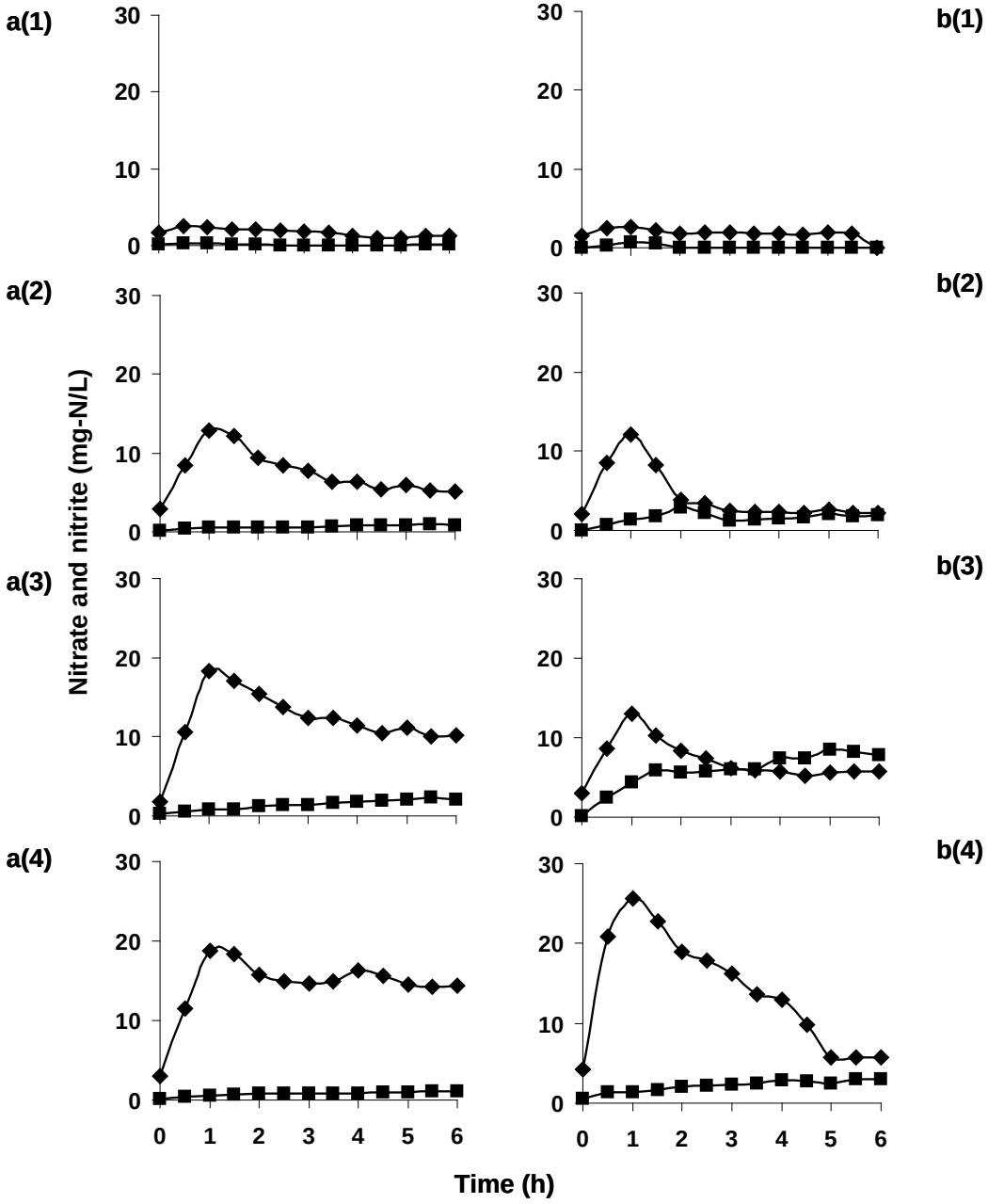

Figure 3-3: Representative nitrate and nitrite concentrations from (a) methanol fed SBR and (b) ethanol fed SBR under ultimate state (1) and different DO concentrations (2)-(4): DO=2.5, 5.1 and 9.0 mg/L respectively. The SBR cycle was the same as shown in Figure 3-2. ■ Nitrite; ◆ Nitrate

As expected, there was a positive correlation between DO concentration and the extent of nitrate accumulation for both carbon sources. High nitrite accumulation was also observed in both SBRs, but was more pronounced in the ethanol fed SBR due to ongoing nitrate reduction therein. N_2O emission was significant in the ethanol fed SBR (Figure 3-4, b-d) and the highest emissions were at DO = 9.0 mg/L, where as much as 7.1 % of influent nitrate load was emitted as N_2O (Figure 3-1b). NO emissions were much lower, but displayed a similar positive correlation with increasing DO concentrations. In contrast, methylotrophic denitrification did not result in significant N_2O or NO emissions at any DO concentration tested (Figure 3-1a).

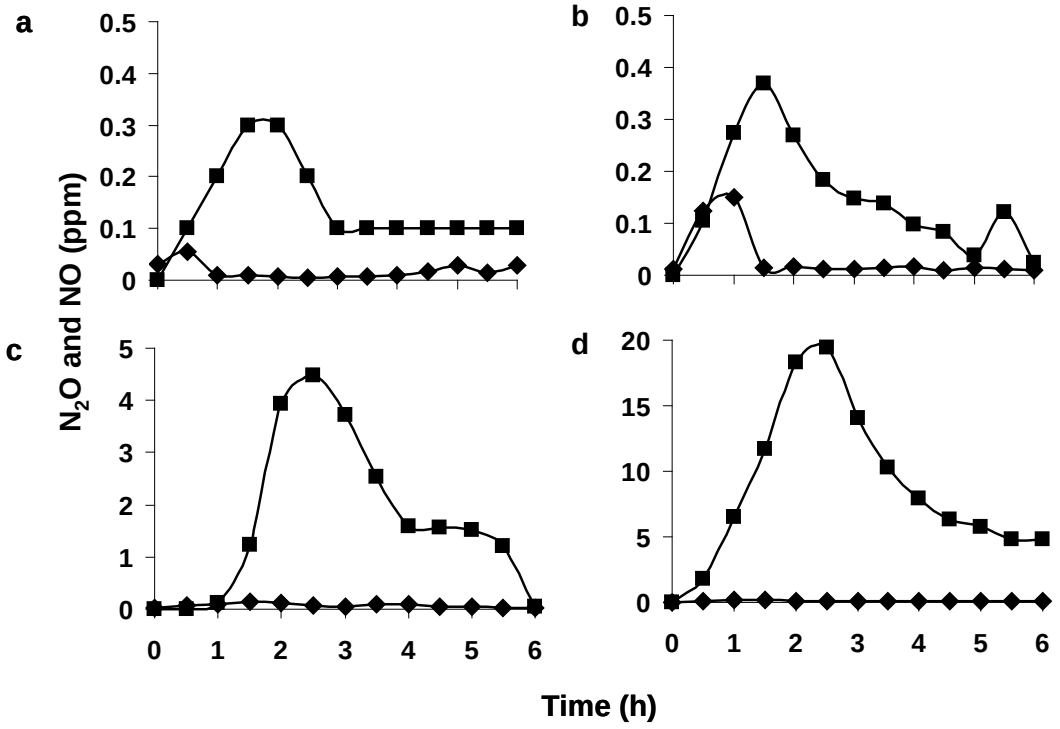

Figure 3-4: Representative N_2O and NO emissions from ethanol fed SBR. Ultimate state (a) and different DO concentrations (b-d: DO=2.5, 5.1 and 9.0 mg/L respectively). The SBR cycles were the same as shown in Figure 3-2. —■— N_2O; —◆— NO

The relative production of N_2O by the two SBRs could not be entirely described by a reduction in their specific nitrate depletion sDNR values (Figure 3-5). Though the sDNR values for the ethanol SBR were consistently higher than those for the methanol SBR, the extent of reduction due to oxygen inhibition was statistically similar ($p=0.79$) and not in correspondence with much higher N_2O production from the former (Figure 3-4). The inability of nitrate sDNR values to describe the extent of N_2O emissions is expected and can be attributed to inhibition of not just NaR but also the other nitrogen reductases by oxygen.

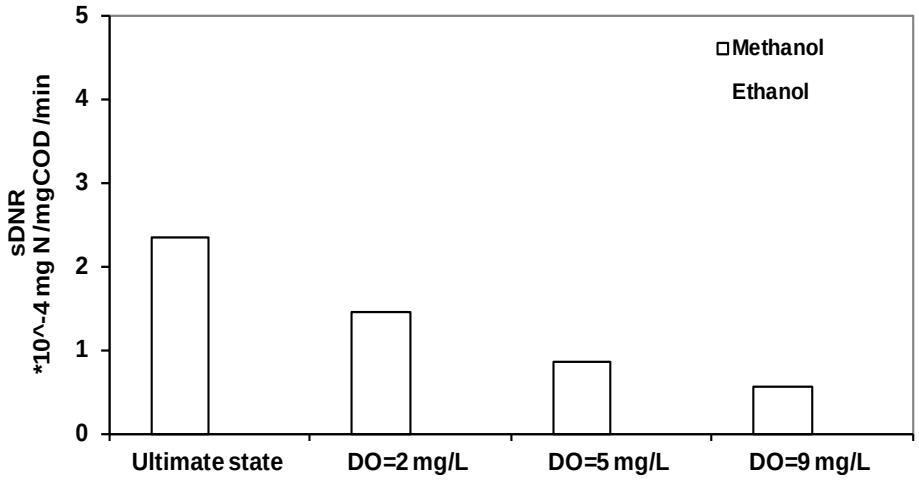

Figure 3-5: Impact of DO concentrations on biokinetics of methanol and ethanol based denitrification.

It is reported that N_2OR is more sensitive to oxygen inhibition than the remaining upstream nitrogen reductase enzymes, thus leading to selective N_2O production [1, 41]. Based on the results of this study, differential N_2O production could also be related to differential NaR inhibition by oxygen. In the methanol-fed SBR, complete cessation of NaR mediated nitrate reduction occurred at the highest oxygen concentration tested (Figure 3-3, a3). Therefore, the lower level of nitrite, N_2O

or NO production in the methanol-fed SBR was in fact mainly due to less upstream nitrate reduced than in the ethanol-fed SBR (Figure 3-2, a4). It should be pointed out that downstream nitrogen reductases (NOR and N_2OR enzymes) could also have been inhibited in the methanol-fed SBR, but could not be discerned due to the lack of accumulation of their substrates. On the other hand, the NaR system in the ethanol fed SBR was seemingly more robust, as reflected in near-complete albeit delayed nitrate reduction (Figure 3-3b). However, such ongoing nitrate reduction under oxygen inhibiting conditions resulted in N_2O production.

It is acknowledged that DO concentrations close to saturation are not common in most activated sludge systems. However, in several modular biological nitrogen removal (BNR) processes, such as non-optimally operated step-feed BNR or five-stage Bardenpho processes, the effluent end of the primary aerobic zone is typified by high DO concentrations as high as 4-5 mg O_2/L, especially during complete nitrification [166]. In such cases, in the absence of a swing-zone to scavenge oxygen concentrations, there is carry-over of non-limiting DO concentrations into the downstream zone of carbon addition.

Given increased evidence for autotrophic N_2O and NO production via nitrification, it could be also argued that the observed emissions were in fact from nitrifying populations in the two SBRs. However, the absence of ammonia oxidizing bacteria in the biomass in both SBRs was confirmed via endpoint polymerase chain reaction (PCR), conducted as per a variation of [180] (data not shown). Additionally, extant resporimetric assays conducted as per [126] revealed negligible ammonia oxidation related specific oxygen uptake rates (sOUR). The sOUR values for methanol and ethanol-

fed biomass were: $(1.1\pm0.2)\times10^{-4}$ and $(4.8\pm0.4)\times10^{-5}$ $mgO_2/gCOD/h$, both of which were close to endogenous uptake rates of $(8.7\pm1.3)\times10^{-5}$ ($p=0.18$) and $(2.9\pm1.8)\times10^{-5}$ $mgO_2/gCOD/h$ ($p=0.45$). Thus, the contribution of nitrification denitrification to observed N_2O and NO emissions was precluded.

Finally, it should be noted that these results may be unique to the specific microbial communities fostered in the two SBRs fed only with methanol and ethanol, respectively. Further, the emissions from anoxic zones of full scale BNR processes may not be as pronounced (as indeed shown recently [166]) given the presence of a broader non-methanol and ethanol degrading consortium therein. Nevertheless, these qualifying factors only underscore the lack of generality in denitrification related N_2O emissions from activated sludge and commonly investigated triggers thereof, especially when applied to different carbon sources.

3.4 Summary

In this study, the impact of three factors, organic carbon limitation, nitrite concentrations, and dissolved oxygen concentrations on gaseous N_2O and NO emissions from two sequencing batch reactors operated respectively with methanol and ethanol as electron donors was evaluated. During undisturbed ultimate-state operation, emissions of both N_2O and NO from either reactor were minimal and in the range of <0.2% of influent nitrate-N load. Subsequently, the two reactors were challenged with transient organic carbon limitation and nitrite pulses, both of which had little impact on N_2O or NO emissions for either electron donor. In contrast, transient exposure to oxygen led to increased production of N_2O (up to 7.1% of influent nitrate-N load) from ethanol grown cultures, owing to their higher kinetics

and potentially lower susceptibility to oxygen inhibition. A similar increase in N_2O production was not observed from methanol grown cultures. These results suggest that for dissolved oxygen, but not for carbon limitation or nitrite exposure, N_2O emission from heterotrophic denitrification reactors can vary as a function of the electron donor used. Therefore, N_2O and NO emissions from denitrification cannot be generalized for all carbon sources, and need to be addressed on a case-specific basis. Based on the differences observed, specific mechanisms and pathways of N_2O and NO production on different carbon sources also need to be elucidated. Additionally, dosing of ethanol to anoxic zones in BNR processes needs to be strictly controlled not only to minimize ethanol wastage but also to minimize the generation and emission of N_2O in downstream aerobic zones.

CHAPTER 4

DIAGNOSIS AND QUANTIFICATION OF GLYCEROL ASSIMILATING DENITRIFYING BACTERIA IN AN INTEGRATED FIXED-FILM ACTIVATED SLUDGE REACTOR VIA ^{13}C DNA STABLE-ISOTOPE PROBING

This chapter has been published as:

Lu H, Chandran K*. 2010. Diagnosis and quantification of glycerol assimilating denitrifying bacteria in an integrated fixed-film activated sludge reactor via ^{13}C DNA stable-isotope probing. *Environmental Science and Technology* 44(23):8943–8949.

4.1 Introduction

Methanol is one of the most widely used external organic carbon sources for enhancing denitrification at wastewater treatment plants [1, 129, 181]. Of late, glycerol has emerged as an alternative to methanol due to three factors. First, the price of methanol, which is tied to natural gas price has been increasing [182]. Second, the dramatic increase in biodiesel production as a means of moving away from petroleum as an energy source has given rise to significant quantities of glycerol as a waste product [183]. Third, glycerol has been previously shown to foster higher denitrification kinetics than those of methanol [184, 185]. Consequently, wastewater treatment plants today are intently considering glycerol as a supplement or replacement for methanol.

From the perspective of wastewater treatment process design, it is essential to determine the fraction of activated sludge bacteria assimilating any given carbon source. It has been shown previously that the type of electron donor applied can strongly impact nitrate removal rates, the molecular microbial ecology of denitrification [70, 77, 79, 116, 186, 187] as well as production of nitrous and nitric oxides in response to disturbances such as inhibition by nitrite or oxygen [188]. If it is determined that certain carbon sources can only be assimilated by a sub-population of activated sludge bacteria as in the case of methanol [77], then process models that adequately capture this specific assimilation capability need to be developed and employed. Recent studies have indeed focused on elucidating the ecology of bacteria assimilating other carbon sources such as methanol, acetate or ethanol [70, 76, 77, 79]. It has also been shown that only a fraction of activated sludge bacteria could assimilate methanol, and out of these, only some could assimilate ethanol as well [77]. Nevertheless, to date the microbial ecology

of glycerol assimilation in mixed microbial communities such as activated sludge has not received adequate attention, although several organisms in pure culture have been shown to grow anaerobically using glycerol as the sole carbon and energy source [183]. Therefore, diagnosing glycerol assimilating bacteria and comparing the microbial ecology of bacteria assimilating methanol and glycerol would be beneficial in evaluating the feasibility of maintaining denitrification performance and kinetics while switching from widely used carbon sources such as methanol to glycerol.

Accordingly, the overall focus of this study was to characterize the microbial ecology of glycerol assimilating bacteria in both the biofilm and suspended phases of a denitrifying integrated fixed-film activated sludge (IFAS) reactor. IFAS reactors are being adopted widely for post-denitrification using externally added carbon sources such as methanol, ethanol and glycerol [184, 189, 190]. IFAS reactors offer several advantages compared to conventional activated sludge since they can achieve comparable process performance, while operating at a lower footprint [191]. While the microbial ecology and kinetics of biofilms in IFAS reactors has been described previously [68, 75, 192], there exist few comparisons of community structures and activities in the two distinct phases (suspended and biofilm) based on *direct substrate assimilation*.

In an earlier study, *Methyloversatilis* spp. and *Hyphomicrobium* spp. related speices were identified as the dominant populations in a sequencing batch denitrifying reactor with methanol as carbon source via stable isotope probing [76]. It was hypothesized that the microbial ecology of glycerol enriched biomass would differ from that enriched by methanol, due to the metabolic specificity of methylotrophic

denitrification [77]. In addition, due to dissimilar nutrient concentration gradients expected in the suspended and biofilm phases, it was hypothesized that distinct glycerol-assimilating bacterial populations would dominate in these two phases. The specific objectives were to:

(1) *Identify glycerol assimilating denitrifying bacteria in the suspended and biofilm phases of a sequencing batch IFAS reactor (SB-IFAS) using ^{13}C-DNA stable isotope probing.*

(2) *Quantitatively track the abundance of dominant glycerol assimilating bacteria and two methylotrophic bacteria (Methyloversatilis spp. and Hyphomicrobium spp.) in the suspended and biofilm phases during start up and steady-state operation of the SB-IFAS reactor.*

(3) *Evaluate the extent of N-removal and kinetics of glycerol induced denitrification in the suspended and biofilm phases.*

4.2 Materials and Methods

4.2.1 Sequencing batch moving bed biofilm reactor operation

Biomass was obtained from the methanol-fed anoxic zone of a full-scale wastewater treatment process and used to seed an 8 L denitrifying SB-IFAS reactor containing 30 % by volume circular Kaldnes K1 polyethylene carriers (external diameter = 9 mm, specific surface area = 800 m^2/m^3, AnoxKaldnes^{TM} USA, Providence, RI). The choice of this methylotrophic inoculum also allowed for evaluating possible metabolic and ecological similarities between methanol and glycerol based denitrification. The SB-IFAS reactor was operated for 380 days at 21°C at a hydraulic retention time of 1 day and a targeted suspended phase solids

retention time of 10 days. Each SB-IFAS reactor cycle (6 h) consisted of 1 h anoxic feed and react, 3.5 h anoxic react, 0.5 h aerobic mixing (to strip out dinitrogen gas and improve settling), 0.75 h settle, and 0.25h decant periods and was automatically controlled via a digital controller (Chrontrol Corp, San Diego, CA) (Figure S-4 in the Supplementary Information). The pH was automatically controlled in the range of 7.3 ± 0.2 using concentrated hydrochloric acid. The feed medium was as described earlier [77] and contained (per liter): 0.2 g of $MgSO_4 \cdot 7H_2O$, 0.02 g of $CaCl_2 \cdot 2H_2O$, 0.087 g of K_2HPO_4, 1 mL of trace elements solution (10 mg of $Na_2MoO_4 \cdot 2H_2O$, 172 mg of $MnCl_2 \cdot 4H_2O$, 10 mg of $ZnSO_4 \cdot 7H_2O$, 0.4 mg of $CoCl_2 \cdot 6H_2O$ in a total volume made up to 100 mL with distilled water). The influent concentrations of glycerol and nitrate were 410 mg glycerol /L and 442 mg nitrate /L, respectively.

4.2.2 DNA stable isotope probing

DNA stable isotope probing (SIP) was conducted as described previously [77]. Briefly, on day 360, 500 mL of suspended biomass and 60 biofilm carrier particles were withdrawn from the SB-IFAS reactor just prior to the “settle” phase and washed individually by centrifugation (2050xg, 10 min) and re-suspension in 500 mL nitrate- and glycerol-free medium. The washed biomass samples were spiked with 205 mg [^{13}C3]-$C_3H_8O_3$ /L and 442 mg nitrate /L and incubated under anoxic conditions at room temperature. 50 ml suspended biomass samples were obtained from the batch incubations before the spike (t = 0, to characterize the overall SB-IFAS populations, S12) and at the point of carbon depletion (t = 20 h in Figure S-5 of SI, to characterize the ^{13}C glycerol assimilating populations, S13). Similarly, 6 biofilm carriers were harvested at t = 0 (A12) and t = 20 h (A13). ~ 10 μg Genomic DNA was extracted

from the 4 biomass samples (DNeasy Blood & Tissue Kit, Qiagen, Valencia, CA), stained with 0.5 μL 10,000X SYBR Green I (Invitrogen, Carlsbad, CA) and subjected to cesium chloride density gradient ultracentrifugation (45,000 rpm, 20°C, 70 h) [193]. The DNA fractions were visualized using UV trans-illumination at 365 nm and withdrawn from the centrifuge tube using a syringe. A single DNA fraction was withdrawn from the samples taken at time t=0 (S12 and A12), both light (unlabeled with ^{13}C) and heavy (labeled with ^{13}C) fractions were withdrawn from samples S13 and A13. In order to test the quality of the separation between the labeled and unlabeled fractions, one more sample was withdrawn at a position longitudinally between the two fractions (data shown in the SI, Figure S-6). DNA recovered from the samples (S12, A12, labeled fraction of S13 and A13) were amplified against eubacterial 16S rRNA primers 11f (5′-GTTTGATCCTGGCTCAG-3′) and 1392r (5′-ACGGGCGGTGTGTRC-3′) as per [121, 194]. Amplicons were cloned (TOPO TA Cloning® Kit for Sequencing, Invitrogen, Carlsbad, CA) and 21 colonies were randomly picked for sequencing (Macrogen USA, Rockville, MD). All 16S rRNA gene sequences were checked for chimera using Mallard [195]. Phylogenetic trees were generated using MEGA 4.0 Neighbor-joining method and the substitution model of Jukes-Cantor. Sequences with the highest number of BLAST hits were included in the tree, and *Methanosarcina thermophila* served as the outgroup. The sequence data generated in this study has been deposited in GenBank under accession nos. HQ232435-HQ232455.

4.2.3 Quantitative PCR assays for tracking glycerol assimilating biomass concentrations

Based on the identification of *Comamonas* spp., *Bradyrhizobium* spp. *Diaphorobacter* spp. and *Tessaracoccus* spp. as dominant glycerol assimilating populations, qPCR primers were designed to specifically target their abundance in both suspended and biofilm phases, using PrimerQuest software (Integrated DNA Technologies, Coralville, IA) (Table 4-I). Primer specificity was checked using Primer BLAST for both forward and reverse primers (http://www.ncbi.nlm.nih.gov/tools/primer-blast/). qPCR assays were employed in triplicate in 25 μL volumes, containing 12.5 μL iQ™ SYBR® Green Supermix (BioRad, Valencia, CA), 1 μL each of forward and reverse primers (final concentration of 0.25 μM), 1 μL of DNA template (10-20 ng), and 9.5 μL of dH_2O. For negative and no template controls, 1 μL of *Nitrosomonas europaea* genomic DNA and dH_2O were used, respectively. The optimized PCR conditions were as follows: 5 min at 95°C, followed by 35 cycles of 95°C for 1 min, 30 s at a specific annealing temperature (T_m, Table 4-I), and 72°C for 1 min and final extension at 72°C for 5 min. Standard curves for qPCR were constructed with serial decimal dilutions of plasmids containing the target amplicon inserts. PCR product specificity for each reaction was confirmed by the presence of a single peak during melt curve analysis and the presence of a single-band of expected molecular size by agarose gel electrophoresis.

In selected SBMBBR biomass samples, concentrations of two methylotrophic populations, *Methyloversatilis* spp. and *Hyphomicrobium* spp., previously found in methanol fed SBRs were also measured as described previously [77]. The fractions of the different bacterial populations were determined by normalizing the respective 16S rRNA copy number to the copy number of the total eubacterial 16S rRNA gene, which in

turn was determined using the primer set UNIf (5′-TCCTACGGGAGGCAGCAGT-3′), and UNIr (5′-GGACTACCAGGGTATCTAATCCTGTT-3′) as per [196].

Table 4-I. Real-time PCR primers employed to quantify glycerol assimilating bacteria

Target group	Primer name	Sequence (5' to 3')	T_m (°C)	Amplicon size (bp)
Comamonas spp.	CoF	AGTTGCTACGAAAGGGCACTCTGA	57	120
	CoR	TACCGGCCATTGTATGACGTGTGT		
Tessaracoccus spp.	TeF	GCATGCTACAATGGCCGGTACAAA	59	80
	TeR	AATCCGAACTGAGACCGGCTTTCT		
Diaphorobacter spp.	DiF	GCCGCAAGGTTGAAACTCAAAGGA	59	110
	DiR	TCCTGCCATGTCAAAGGTGGGTAA		
Bradyrhizobium spp.	BrF	ATGGATTCCTTCAGTTCGGCTGGA	56	88
	BrR	TGCGGGACTTAACCCAACATCTCA		

4.2.4 Performance and extant kinetics measurements

The performance of the SB-IFAS reactor was determined by measuring influent nitrate and effluent nitrite, nitrate, total and effluent soluble chemical oxygen demand (COD, expressed as g O_2 eq / L), all according to Standard Methods [125]. Denitrification kinetics were determined via extant batch assays [77]. For suspended phase kinetics, 500 mL mixed liquor samples were withdrawn from the SB-IFAS reactor, centrifuged and re-suspended in nitrogen and carbon free medium. Biofilm kinetic tests were conducted with 60 Kaldnes K1 carriers. The initial concentration of nitrate and glycerol in the batch kinetic assays were 442 mg nitrate / L and 205 mg glycerol /L, respectively, thereby rendering glycerol as the limiting nutrient based on a stoichiometric carbon:nitrate requirement of 500 mg O_2 eq :442 mg nitrate [197]. In

selected experiments, methanol was added *in lieu* of glycerol for comparing kinetics of denitrification with glycerol. The specific denitrification rate (sDNR) was computed by linear regression of the nitrate depletion profiles *vs* time and normalized to total suspended or biofilm biomass concentrations (expressed as g O_2 eq / L). The relative contributions of biomass in the two phases to the total nitrogen removal were approximated according to Eqn. 4-1 and 4-2:

$$Contribution_{suspended} = \frac{sDNR_{sus} \times M_{sus}}{sDNR_{sus} \times M_{sus} + sDNR_{biofilm} \times M_{biofilm}} \quad \text{(Equation 4-1)}$$

$$Contribution_{biofilm} = 1 - Contribution_{suspended} \quad \text{(Equation 4-2)}$$

where, M_{sus} and $M_{biofilm}$ are the mass inventories of total biomass in suspended and biofilm phases, respectively during steady state operation. M_{sus}= 7.6 ± 0.4 g O_2 eq (n=82) and $M_{biofilm}$= 3.9 ± 0.2 g O_2 eq (n=54).

4.3 Results and Discussion

4.3.1 Microbial ecology of glycerol assimilating denitrifying bacteria in suspended and biofilm phases

Based on retrieved clone library sequences, the bacteria assimilating glycerol in the suspended phase were most closely related to *Comamonas badia* (8/21) and *Diaphorobacter* GS1 (9/21) (Figure 4-1). Both *C. badia* and *Diaphorobacter* spp. belong to the family of *Comamonadaceae* in *β-Proteobacteria*. *C. badia* has been implicated in floc-formation in activated sludge [198]. *Diaphorobacter* spp. has been reported to denitrify using polyhydroxybutyrate as an electron donor [199]. *Diaphorobacter* spp. has also been implicated in simultaneous nitrification and denitrification under aerobic conditions [200]. However, the capacity of *C. badia* and

Diaphorobacter spp. to denitrify while assimilating glycerol has not been demonstrated.

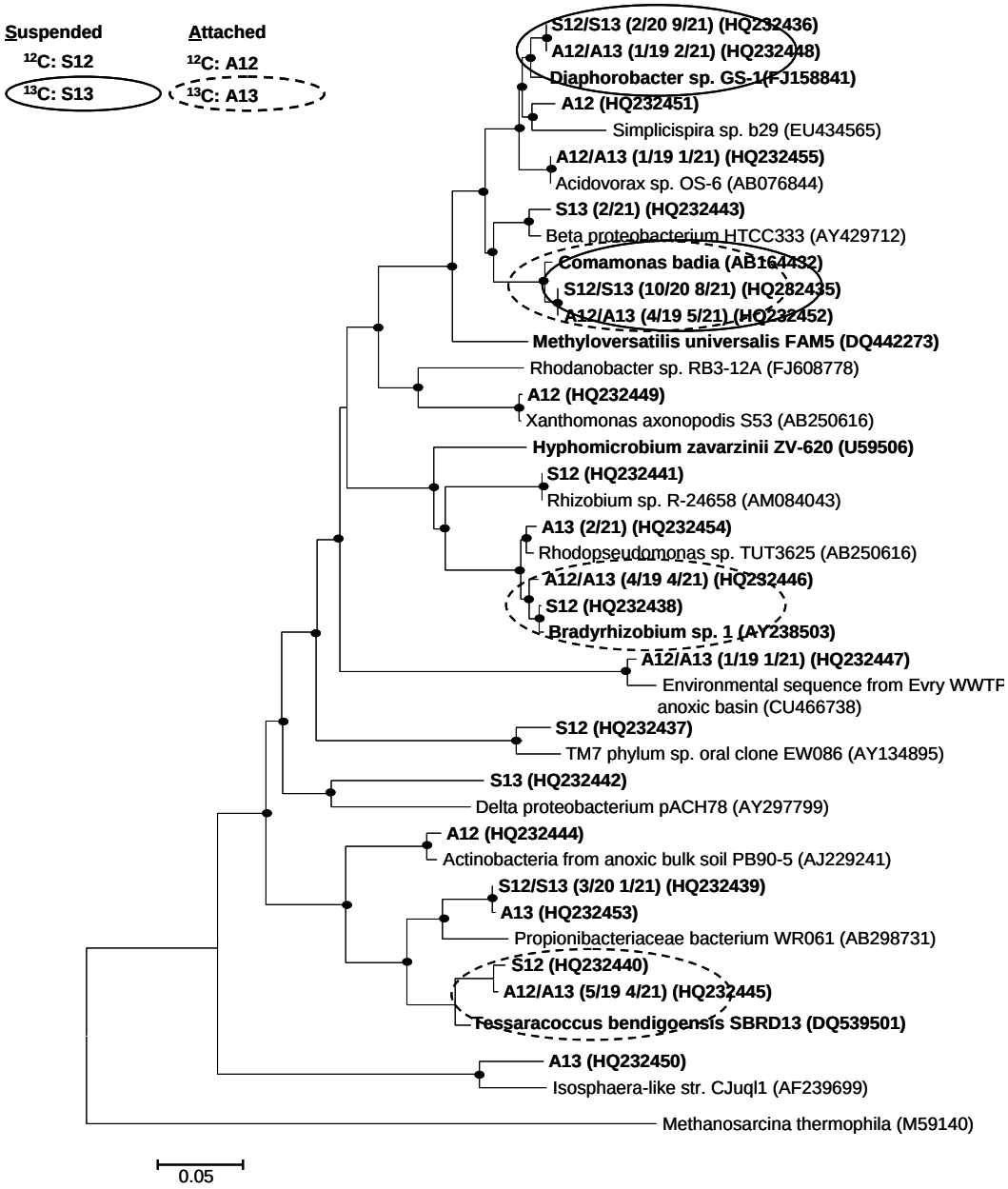

Figure 4-1: 16S rRNA based phylogenetic tree depicting (1) overall populations in suspended and attached biomass (denoted by "S12" and "A12", respectively); (2) populations assimilating ^{13}C glycerol in suspended and attached biomass ("S13" and "A13", respectively). Numbers in parentheses represent fraction of clones most closely associated with a given phylogenetic lineage (those with two fractions stand for ^{12}C and ^{13}C, respectively). Circles indicate dominant species found in suspended and attached biomass.

The ^{13}C DNA sequences of the biofilm samples were more diverse and dominated by *Comamonas badia* (5/21), *Bradyrhizobium* sp. 1 (4/21) and *Tessaracoccus bendigoensis* (4/21) related bacteria. *Bradyrhizobia* and *Tessaracocci* belong to the family of *Rhizobiales* in *α-proteobacteria* [201] and *Propionibacteriaceae* in *Actinobacteria* [202], respectively. Very little is known about the denitrification capability of these bacteria and or their ability to use glycerol as an electron donor.

It is notable that the glycerol assimilating bacteria diagnosed and quantified in this study have not been implicated in glycerol metabolism before (as reviewed by [183]). A possible explanation for this discrepancy is that the previous studies selected their strains *a priori* for examining glycerol metabolism. In contrast, this study was not biased towards any particular strain. Rather the focus was to elucidate the glycerol assimilating communities in the overall population of a denitrifying IFAS reactor.

It is acknowledged that during SIP, any incubation could lead to the production of labeled by-products, which might be taken by non-glycerol assimilating species via crossfeeding. However, short incubation time (20 h) and discrete ^{13}C and ^{12}C fractions obtained (data documented in the SI, Figure S-6) indicated little crossfeeding in this study. Therefore, the assumption that ^{13}C assimilating species also assimilate glycerol in this study can be made. In addition, with an oxidation reduction potential (ORP) of -100 ~ 50 mV in the SIP experiment, nitrate was preferably used as an electron acceptor as opposed to other alternatives. As a result, the majority of glycerol-assimilating species were engaged in denitrification.

By visually and quantitatively analyzing the ^{12}C clone libraries of the communities in two phases, relatively high overall microbial diversity in the biofilm phase than the suspended phase was inferred in keeping with past results [203-205]. It is generally speculated that the chemical heterogeneity (concentration gradients of substrates, metabolic intermediates and products within the biofilm, owning to biochemical reaction-transportation interactions) provides the opportunity for metabolic competition and cooperation between different bacterial groups, thereby allowing more diverse communities to coexist [206, 207]. In contrast, the relatively more uniform substrate concentrations in the bulk-suspended phase in the IFAS reactor may have contributed to a lower microbial diversity therein, as suggested by [207].

The concentrations of the four identified glycerol assimilating bacteria in the overall population increased from 19.8 ± 0.8%, based on the 16S rRNA gene fraction, on day 1 to 71.3 ± 1.2% (suspended phase) and 54.4 ± 0.7% (biofilm) on day 363 (Figure 4-2). The suspended phase was more enriched in glycerol-assimilating bacteria than the biofilm phase possibly due to the higher availability of glycerol in the suspended phase to which it was fed.

It was also observed that a significant fraction of the overall population was not related to the four glycerol-assimilating bacterial groups, e.g. *Simplicispira* sp., *Xanthomonas* sp., and *Rhizobium* sp.. Many of these species can reduce nitrate, but their denitrifying capacities with glycerol as carbon source are not tested [208-210]. This non-glycerol assimilating fraction possibly denitrified in the reactor via metabolic cross-feeding, either on glycerol degradation intermediates, such as acetate, butyrate, ethanol,

n-butanol [211] or on products of biomass decay. Additional data on specific glycerol assimilating bacterial fractions are provided in SI (Figure S-7).

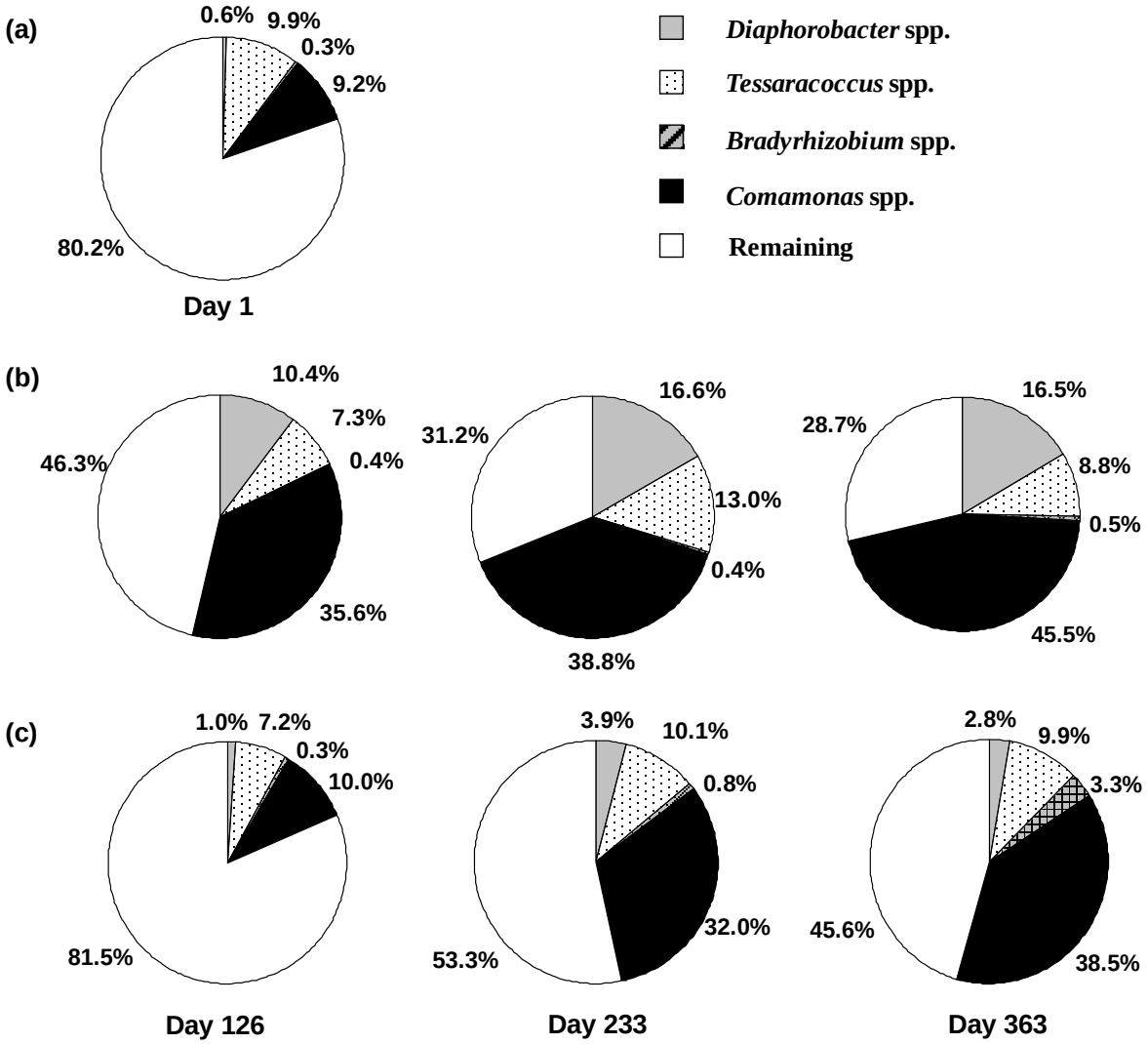

Figure 4-2: Variation in microbial community composition on (a) Day 1, and Day 126, 233, 363 in (b) suspended and (c) biofilm phases. Pie slices with fractional percentages represent relative abundance of each dominant species, as well as the "remaining" untargeted populations.

4.3.2 Differences in the microbial ecology of glycerol and methanol assimilation

Notably, glycerol assimilating bacteria enriched in both suspended and biofilm phases were not related to *Methyloversatilis* spp. or *Hyphomicrobium* spp, which were

the two principal methylotrophic populations identified in a methanol fed-SBR [77]. A lack of glycerol based denitrification by methanol enriched biomass has been shown earlier [58], but the direct inspection of glycerol assimilation during denitrification as performed herein is novel. The activated sludge sample used to inoculate the SB-IFAS reactor contained 1.99 ± 0.21% *Methyloversatilis* spp. and 4.32 ± 0.31% *Hyphomicrobium* spp. (as copies of 16S rRNA per copy of the total eubacterial 16S rRNA gene). During the course of exposure to glycerol, the two methylotrophic population concentrations decreased by factors of about 200-1000 (data shown in SI, Figure S-8). The washout of *Hyphomicrobium* spp. related population is in accordance with its obligately methylotrophic nutritional mode [77, 212]. Although *Methyloversatilis* spp. have been shown to assimilate both methanol and ethanol during denitrification [77], the results of this study show that they might be incapable of assimilating glycerol. Notwithstanding the absence of these two previously detected methylotrophs in the SB-IFAS reactor, the possibility remains that the reactor could have fostered other methylotrophs not characterized to date. However, owing to the focus of this study on glycerol assimilation, no attempts were made to explore ^{13}C methanol assimilation by the IFAS reactor bacterial communities.

Additionally, although denitrification can be conducted by archaea as well [213, 214], their abundance and contribution to wastewater denitrification processes are not well-documented. As a result, we also did not systematically evaluate the contribution of glycerol assimilating archaea in this study, and focused on bacteria alone.

4.3.3 Performance and kinetics of the denitrifying SB-IFAS reactor

Near-complete nitrate removal (92.7 ± 5.8%) with the absence of significant nitrite accumulation (< 0.6 mg nitrite /L) was achieved 50 days after initial inoculation of the SB-IFAS reactor (Figure S-9 in the SI). For suspended biomass, glycerol-sDNR values continuously increased from zero during the study and exceeded those of methanol (1.1 ± 0.4 mg nitrate /g O_2 eq / h, p = 8.19e-7 and therefore statistically significant at α=0.05) on and after day 99 (Figure 4-3). In general, the suspended-phase glycerol sDNR values measured in this study were higher than those previously reported in the range of 4.42 mg nitrate /g O_2 eq / h [215] and might be due to differences in the initial inoculum, reactor operation or just biological variability in the different systems. A significant decrease of sDNR values on methanol was also observed during this period. The reduction in methanol sDNR values, coupled with the low abundance of methylotrophic bacteria in the suspended and biofilm phases of the glycerol fed SB-IFAS reactor, reflected the progressively declining capacity of the reactor biomass for denitrification using methanol. Therefore, via a combination of SIP and kinetics measurements, the lack of glycerol assimilation by methanol assimilating bacteria was confirmed.

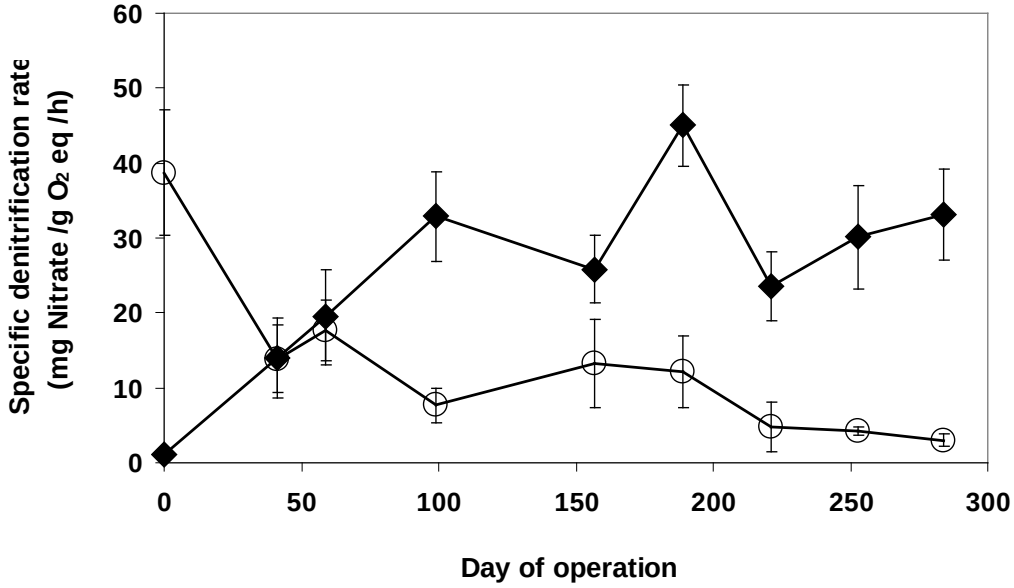

Figure 4-3: Time-series profiles of suspended biomass sDNR values with glycerol (—◆—) and methanol (—⊖—) as carbon sources. Error bars indicate one standard deviation of linear regression slopes.

In a side-by-side comparison, sDNR values obtained with suspended biomass on glycerol (20.4 ± 7.1 mg nitrate / g O_2 eq / h) were generally higher than those with biofilm biomass (17.3 ± 5.3 mg nitrate / g O_2 eq / h, p = 4.33e-4 and therefore statistically significant at α=0.05) during steady state operation. The suspended phase contributed to 69.7 ± 4.5 % of the total nitrogen removal, calculated using Equation 3a. The higher overall N removal in the suspended phase was likely because of higher glycerol availability and degradation therein [216]. Alternately, the utilization of exogenous and endogenous organic carbon compounds for the production of extracellular polymeric substances (EPS) by biofilm bacteria at the expense of lower energy for growth [217], might also have resulted in the lower N-removal therein.

4.4 Summary

In this study, the microbial ecology of glycerol assimilating denitrifying bacteria in a sequencing batch integrated fixed film activated sludge reactor (SB-IFAS) was investigated using ^{13}C-DNA stable isotope probing (SIP). Based on ^{13}C DNA clone libraries, bacteria related to *Comamonas* spp. and *Diaphorobacter* spp. dominated in the suspended phase communities. In contrast, the biofilm community were phylogenetically more diverse and the ^{13}C assimilating members therein were related to *Comamonas* spp., *Bradyrhizobium* spp., and *Tessaracoccus* spp.. Possibly owing to greater substrate availability in the suspended phase, the glycerol-assimilating denitrifying populations (quantified by real-time PCR) were more abundant than in the biofilm phase. Correspondingly, the biomass in the suspended phase had a higher specific denitrification rate than the biofilm phase (p = 4.33e-4), and contributed to 69.7 ± 4.5% of the overall N-removal on a mass basis. Previously identified methanol assimilating denitrifying bacteria were not associated with glycerol assimilation, thereby suggesting limited cross-utilization of these two substrates for denitrification in the systems tested. In sum, this study provides a better understanding of the diversity and activity of glycerol assimilating bacteria in denitrifying activated sludge, which could benefit the maintenance of efficient and stable denitrifying systems during carbon switch from methanol to glycerol.

4.5 Supplementary Information Available

Details pertaining to IFAS reactor operation (Figure S-4); a representative nitrate depletion curve for SIP experiments (Figure S-5); the extent of density gradient separation between ^{12}C and ^{13}C DNA fractions using SIP (Figure S-6); relative

concentrations of four dominant glycerol assimilating populations (Figure S-7) and two methylotrophic populations during the SB-IFAS operation (Figure S-8); SB-IFAS reactor performance (Figure S-9)

CHAPTER 5

ALCOHOL DEHYDROGENASE EXPRESSION AS A BIOMARKER OF DENITRIFICATION ACTIVITY IN ACTIVATED SLUDGE USING METHANOL AND GLYCEROL AS ELECTRON DONORS

This chapter has been published as:

Lu H, Nuruzzaman F, Ravindhar J and Chandran K*. 2011. Alcohol dehydrogenase expression as a biomarker of denitrification activity in activated sludge using methanol and glycerol as electron donors. *Environmental Microbiology* doi:10.1111/j.1462-2920.2011.02568.x

5.1 Introduction

Methanol is commonly used as a carbon source to enhance denitrification in wastewater treatment facilities [113]. However, with the price variability [182] and safety concerns associated with the low flash-point (49^{o}C, [25]) of methanol, alternative carbon sources need to be considered. Glycerol is especially appealing since it is a byproduct of biodiesel production [183], and expected to be increasingly available. There are also indications that glycerol can foster higher denitrification kinetics than methanol [184, 185].

Currently, denitrification kinetics and activity in activated sludge are commonly monitored using 'extant' specific denitrification assays (for instance, as described previously [77]. Such extant specific denitrification assays rely upon the interpretation and analysis of nitrate and nitrite depletion profiles to infer denitrification kinetics of the overall denitrifying population in activated sludge. However, these assays cannot be used to infer the contributions of different microbial sub-groups degrading different carbon sources to the overall observed nitrogen depletion profiles. Therefore, carbon source-specific biomarkers of denitrification need to be developed. Application of such biomarkers could not only help track carbon-specific denitrification activity but also prove to be a valid screening tool prior to the application of the carbon sources to enhance denitrification in wastewater treatment plants, typically as a final nitrate removal step in Modified Lutzak Ettinger or Bardenpho treatment configurations [22].

Biomarkers and assays targeting carbon metabolism genes could potentially implicate denitrification activity fostered by a certain carbon source. For instance, alcohol dehydrogenase (ADH) enzymes play a crucial role in the carbon metabolism of

many alcohols during denitrification. Methanol dehydrogenase carries out the oxidation of methanol to formaldehyde, a key intermediate, which feeds into both assimilative and dissimilative metabolism in gram negative methylotrophic bacteria [159, 160]. In particular, the gene encoding the large subunit of methanol dehydrogenase, *mxaF* is highly conserved among all gram negative methylotrophs and has been used as a functional marker to detect methylotrophs in the environment [159, 218, 219]. However, some methylotrophic bacteria lack *mxa* and instead possess other methanol dehydrogenases, such as *mdh2* [160].

Glycerol-based denitrification involves glycerol kinase (*glpK*) or glycerol dehydrogenase (*dhaD*) [220, 221]. Thus, either gene could be a valid possible biomarker of glycerol-based denitrification activity. Alternate fermentative glycerol pathways also exist, for example, encoded by glycerol dehydratase (*dhaB*) and 1,3-propanediol dehydrogenase (*dhaT*) as summarized in da Silva and colleagues 2009 and Figure S-10 in the Supplementary Information. However, these pathways and genes are not involved in glycerol-based denitrification and are thus not appropriate biomarker candidates for glycerol-based denitrification. Therefore, the expression of the dhaD gene, which catalyses the first step of glycerol oxidation during denitrification, was explored as a biomarker of glycerol assimilation activity.

Accordingly, the specific objectives were to:

(1) *characterize differences in microbial ecology and kinetics of a sequencing batch reactor (SBR) operated sequentially with methanol and glycerol as electron donors*

(2) *examine the applicability of using mdh2, mxaF and dhaD messenger RNA (mRNA) concentrations as biomarkers of carbon-specific denitrification activity*

5.2 Materials and Methods

5.2.1 Operation of denitrifying SBR

A methylotrophic enrichment consortium was cultivated at 21^{o}C in a methanol fed denitrifying SBR with a volume of 9.2 L, hydraulic retention time (HRT) of 1d, and solids retention time (SRT) of 10 d. The SBR was seeded with methylotrophic enrichment culture obtained from a previously described identically operated bioreactor [76, 77]. Each SBR cycle was six hours long and consisted of 1 h anoxic feed and react, 3.5 h anoxic react, 0.5 h aerobic mixing (to strip out dinitrogen gas and improve settling), 0.75 h settle and 0.25 h decant periods. SBR cycles were automatically controlled via a digital controller (Chrontrol Corp, San Diego, CA). The pH of the SBR was automatically controlled at 7.5 ± 0.1 using concentrated hydrochloric acid. The SBR was operated for 120 days with methanol (Phase I) and 90 days with glycerol (Phase II) as electron donors using nitrate as the terminal electron acceptor. For both phases, the influent electron donor and acceptor concentrations were 500 mg chemical oxygen demand (COD)/L and 100 mg-N/L, respectively. The SBR feed medium was made up with tap water and also contained (per liter), 0.2 g $MgSO_4$•$7H_2O$, 0.02 g $CaCl_2$•$2H_2O$, 0.087 g K_2HPO_4 and 1 mL trace elements solution (10 mg Na_2MoO_4•$2H_2O$, 172 mg $MnCl_2$•$4H_2O$, 10 mg $ZnSO_4$•$7H_2O$, 0.4 mg $CoCl_2$•$6H_2O$ in a total volume made up to 100 mL with distilled water).

5.2.2 Performance and extant denitrification kinetics measurements

SBR performance was determined by measuring effluent nitrate, nitrite and total reactor and effluent COD, all according to Standard Methods [125]. Denitrification kinetics were determined via extant batch assays as described previously [77]. Briefly,

500 mL biomass samples were withdrawn from the SBR just prior to the end of the react phase, centrifuged at 5000g for 5 min and re-suspended in nitrate and carbon free medium. The initial concentrations of denitrifying biomass in methanol and glycerol batch tests were 0.72 ± 0.12 and 0.68 ± 0.07 g volatile suspended solids (VSS)/L, respectively. The washed biomass samples were rendered anoxic with N_2 gas. The extant batch denitrification assays were initiated by adding sodium nitrate at t = 0 min to achieve an initial concentration of 100 mg N/L. After an initial endogenous period of 20 min, the electron donor (methanol or glycerol) was added at t = 21 min at an initial concentration of 250 mg COD/L, to render the electron donor the ultimate limiting nutrient based on a stoichiometric COD:N requirement of 4:1 for methanol [222] and 5:1 for glycerol [197]. The initial slope of the nitrate depletion profile (obtained during non-limiting carbon or nitrogen denitrification activity) was normalized to the initial biomass concentrations to obtain the specific denitrification rates (expressed as mg N/ g VSS/ d).

DNA extraction and phylogenetic analysis

Genomic DNA was extracted from 1 mL of SBR biomass (DNeasy Blood & Tissue Kit, Qiagen, Valencia, CA). The microbial community composition on day 100 (methanol fed, Phase I) and day 200 (glycerol fed, Phase II) was inferred via cloning and sequencing by amplifying sample DNA against eubacterial 16S rRNA primers 338f (5'-ACTCCTACGGGAGGCAGC-3') [88] and 1387r (5'-GGGCGGWGTGTACAAGGC-3') [223]. Amplicons were cloned (TOPO TA Cloning® Kit for Sequencing, Invitrogen, Carlsbad, CA), and 50 colonies for each sample were randomly picked for sequencing (Macrogen USA, Rockville, MD). Phylogenetic trees were generated using MEGA 4.0 with the neighbor-joining method and the substitution model of Jukes-Cantor.

Methanosarcina thermophila served as the outgroup. The sequence data generated in this study has been deposited in GenBank under accession nos. HQ596303-HQ596311 and HQ703513-HQ703545.

Quantification of dominant microbial populations in the SBR via qPCR

The concentrations of total bacteria, *Methyloversatilis* spp., *Hyphomicrobium* spp. and *Citrobacter* spp. were determined via triplicate qPCR assays performed using a Bio-Rad *iQ5* real-time PCR detection system in 25 μL volumes, containing 12.5 μL iQ™ SYBR® Green Supermix (BioRad, Valencia, CA), 1 μL each of forward and reverse primers (final concentration of 200 nM), 1 μL of DNA template (10-20 ng), and 9.5 μL of dH_2O. For negative and no template controls, 1 μL of *Nitrosomonas europaea* genomic DNA and dH_2O were used, respectively. The qPCR conditions were as follows: 5 min at 95°C, followed by 40 cycles of 94°C for 30 s, 30 s at specific annealing temperature (T_a, Table 5-I.), and 72°C for 45 s and final extension at 72°C for 5 min. Standard curves were constructed with serial decimal dilutions of plasmids containing the target amplicon inserts. PCR product specificity was confirmed by the presence of a single peak during melt curve analysis and a single-band of expected molecular size by agarose gel electrophoresis. The fractions of *Methyloversatilis* spp., *Hyphomicrobium* spp. and *Citrobacter* spp. in the reactor were determined by dividing their respective concentrations by the eubacterial concentrations.

RNA extraction and quantification of ADH mRNA concentrations

Total RNA was isolated from 1 ml of SBR biomass, stabilized with 250 μL RNA Protect™ Bacteria Reagent (Qiagen, Valencia, CA) and stored at -80°C using the PureLink RNA Mini Kit (Invitrogen, Carlsbad, CA). cDNA synthesis was performed

using the QuantiTect® Reverse Transcriptase kit (Qiagen, Valencia, CA). qPCR primers were designed to specifically target the cDNA of *Methyloversatilis* spp. *mdh2* (GenBank: EU548062) [160], *Hyphomicrobium* spp. *mxaF* [224] (GenBank: Y08080), and *Citrobacter* spp. *dhaD* [225] (GenBank: U09771) using the PrimerQuest® online software from Integrated DNA Technologies (Coralville, LA) (Table 5-I.). BLAST searches using both forward and reverse primers indicated that these biomarkers could not target other methanol or glycerol utilizing bacteria based on currently available genomic data. The mRNA concentrations of the three alcohol dehydrogenase genes were normalized to the corresponding 16S rRNA concentrations. All qPCR assays were performed in triplicate with conditions as described above. The potential of gene expression as a surrogate of denitrification activity was evaluated by tracking and correlating *mdh2*, *mxaF* and *dhaD* mRNA concentrations during several extant batch denitrification tests over Phases I and II of SBR operation (as shown in Eqn. S-1 in the Supplementary Information).

Table 5-I. qPCR primers developed and employed in this study

Target group	Primer name	Sequence (5' to 3')	T_a (^oC)	Source
Eubacteria (16S rRNA)	EubF	TCCTACGGGAGGCAGCAGT	58	[196]
	EubR	GGACTACCAGGGTATCTAATCCTGTT		
Methyloversatilis spp. (16S rRNA)	MuF	AAGGCCTACCAAGGCAACGA	55	[76]
	MuR	ACCGTTTCGTTCCTGCCGAA		
Hyphomicrobium spp. (16S rRNA)	HzF	ACAATGGGCAGCAACACAGC	57	[76]
	HzR	ATTCACCGCGCCATGCTGAT		
Citrobacter spp. (16S rRNA)	CfF	AGCGCAACCCTTATCCTTTGTTGC	58	This study
	CfR	TCGCGAGGTCGCTTCTCTTTGTAT		
Methyloversatilis spp. (*mdh2*)	Mu_mdh2	TGCTGTTCGAGTACAAGGATCCGA	58	This study
	Mu_mdh2	TCACGAAGAAGTAGCCATTGCGGT		
Hyphomicrobium spp. (*mxaF*)	Hz_mxaF	TGGACCACAAGGGCAAGGAAATCT	58	This study
	Hz_mxaR	ATTCGTGCAGATGTGGTTGATGCC		
Citrobacter spp. (*dhaD*)	Cf_dhaF	TGGAAGAGATCGAAACCGTGCTGA	56	This study
	Cf_dhaR	TCACCGAGAACGGCATATTGTGGA		

5.3 Results and Discussion

5.3.1 Microbial ecology of SBR biomass fed sequentially with methanol and glycerol

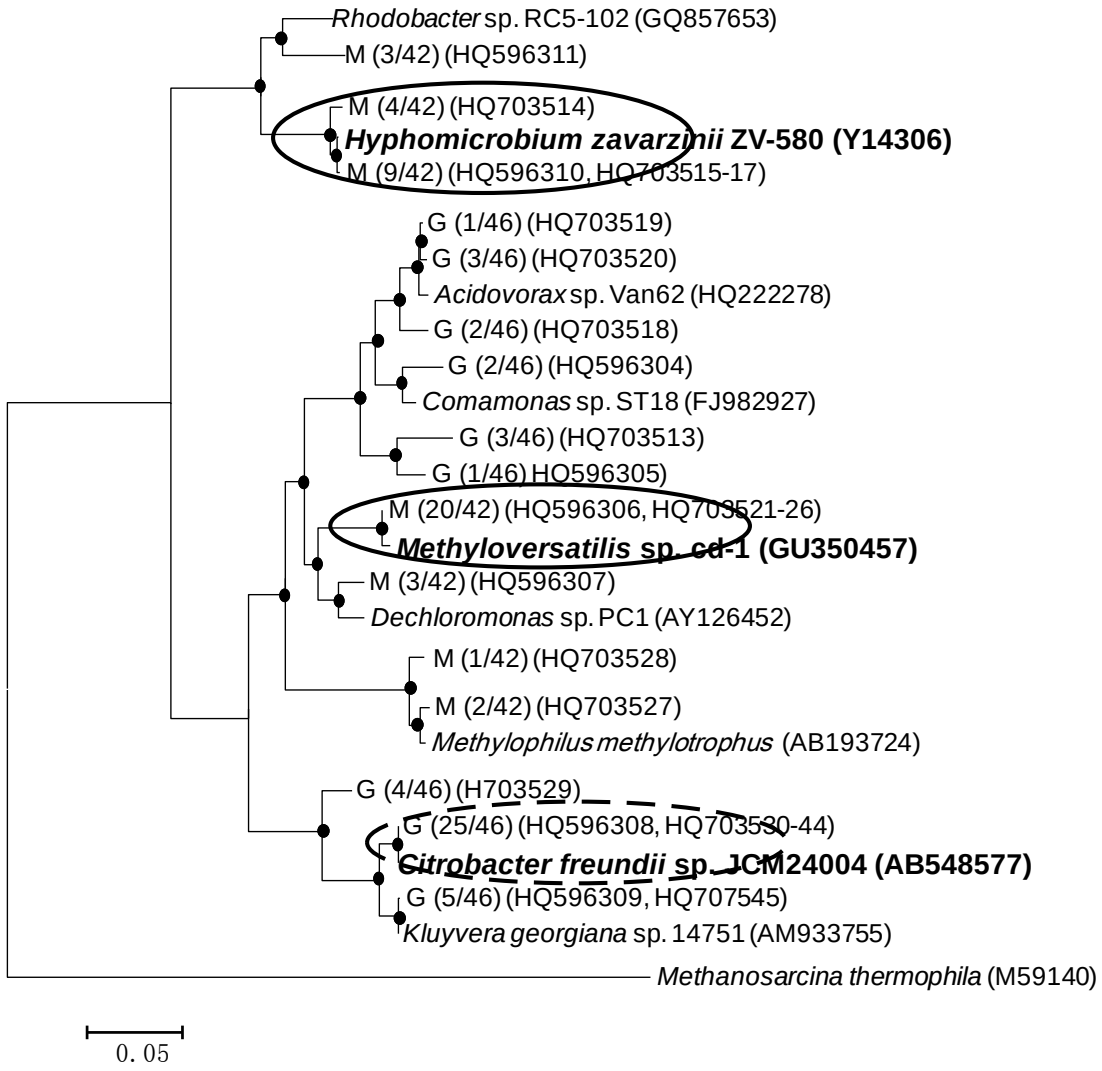

Figure 5-1: 16S rRNA based phylogenetic tree depicting overall populations in the denitrifying reactor with methanol (M) and glycerol (G) as carbon sources. Numbers in parentheses represent fraction of clones most closely associated with a given phylogenetic lineage, and circles indicate dominant species found in the reactor with methanol (⬭) and glycerol (⬭) as carbon sources.

Based on 16S rRNA gene clone libraries constructed using biomass samples obtained on day 100 (methanol fed, Phase I) and day 200 (glycerol fed, Phase II), the

microbial community supported by these two carbon sources was substantially different (Figure 5-1). During Phase I, bacteria closely related to *Methyloversatilis* spp. (20/42) and *Hyphomicrobium* spp. (13/42) were enriched in the SBR as inferred from the clone libraries. These two methylotrophic populations were not found in the clone libraries of Phase II, which were in turn enriched in *Citrobacter* spp. related bacteria (25/46, Figure 5-1). The enrichment of the SBR in *Methyloversatilis* spp. and *Hyphomicrobium* spp., relative to *Citrobacter* spp. during Phase 1 was confirmed by qPCR (Figure 5-2). However, both population fractions decreased even during Phase 1, possibly reflecting the build-up of non-methylotrophic bacteria within the reactor sustained via secondary degradation of the active methylotrophic biomass (Figure 5-2). During Phase II, the fractions of *Hyphomicrobium* spp. and *Methyloversatilis* spp. decreased even further, while the fraction of *Citrobacter* spp. related species rose rapidly subsequently stabilized at approximately 90% of the total bacterial concentration (Figure 5-2).

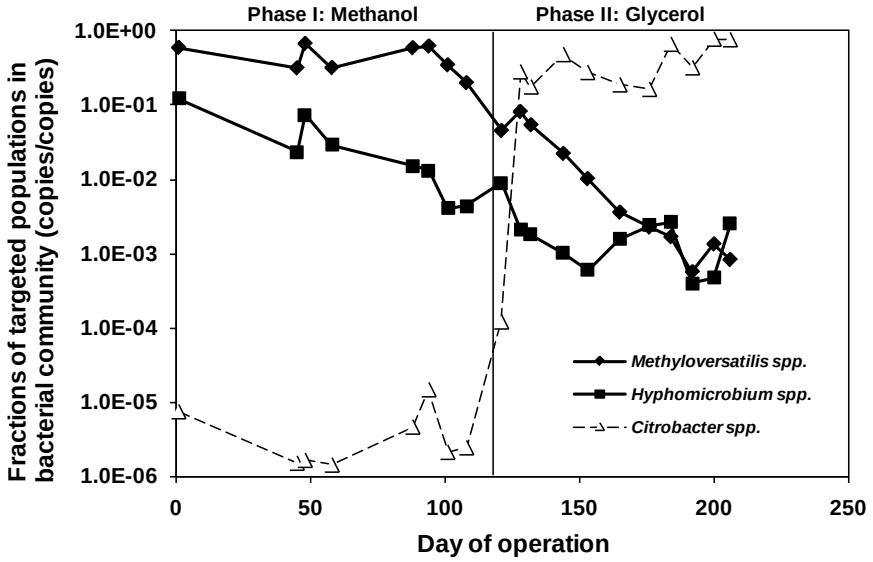

Figure 5-2: Fractions of *Methyloversatilis* spp. ( ), *Hyphomicrobium* spp. ( ), *Citrobacter* spp. ( ) in the overall bacterial community during methanol and glycerol fed phases of SBR operation (population concentrations normalized to total eubacterial concentration). Error bars represent standard deviation from triplicate qPCR assays.

The enrichment of the two methylotrophic populations during Phase I of this present study was in good agreement with a previous study, wherein methanol assimilation in a methanol fed denitrifying SBR was primarily attributed via stable isotope probing (SIP), to *Methyloversatilis* spp. and *Hyphomicrobium* spp. [76, 77]. A quantitative comparison to the previous study in terms of fractions is precluded by the lack of eubacterial concentrations in the previous study [76, 77]. Nevertheless, *Methyloversatilis* spp. were more abundant than *Hyphomicrobium* spp. in both Phase I of this present study as well as the previous study referenced [76, 77]. The higher fraction of *Methyloversatilis* spp. (44.5 ± 17.3%) relative to *Hyphomicrobium* spp. (3.8 ± 2.3%, Figure 5-2) was likely due to the higher affinity of the former for methanol as also observed and suggested recently [77]. In terms of metabolism, some *Hyphomicrobium* spp. only utilize C1 compounds for energy and biomass synthesis [128, 212] whereas other *Hyphomicrobium* strains can indeed grow on multicarbon compounds, including glycerol [226]. *Methyloversatilis* spp. can also grow on methanol as well as multi-carbon sources, including glycerol [227]. However, the significant decrease of both *Hyphomicrobium* spp. and *Methyloversatilis* spp. during Phase II (glycerol fed, Figure 5-2) can potentially be attributed either to their out-competition by more rapidly growing glycerol assimilating species such as *Citrobacter* spp., which were enriched during the glycerol feeding phase. *Citrobacter* spp. can indeed grow anaerobically on glycerol as the sole carbon and energy source [228]. *Citrobacter* spp. also possess some metabolic flexibility as demonstrated by their ability to denitrify under both aerobic and anaerobic conditions [229]. The ecology of glycerol based denitrification in activated sludge is

only just emerging and the ability of *Citrobacter* spp. to denitrify using glycerol has not been demonstrated elsewhere.

Among additionally identified species in the clone libraries of Phase II (Figure 5-1), *Comamonadaceae* spp. related strains, such as *Acidovorax* spp. and *Comamonas* spp., were relatively enriched (12/46) and can denitrify using glycerol as the carbon source [81, 230]. The *Comamonas* spp. 16S rRNA gene sequences detected in this study were more than 98% similar to those of *C. badia* that were found to assimilate ^{13}C glycerol in a denitrifying biofilm reactor [81]. Thus, the presence of these additional bacteria in the glycerol fed SBR was also consistent with their reported metabolic capacities. As inferred from their respective genome sequences, bacteria such as *Comamonas testosteroni* KF-1 (http://genome.jgi-psf.org/comte/comte.info.html) , *Comamonas testosteronii* CNB-2 [231] and *Acidovorax* sp. JS42 [232] employ the glycerol kinase pathway (encoded by the *glp* system) to transform glycerol instead of the *dha* encoded pathway. Therefore, it is acknowledged that by tracking the mRNA concentrations of *dha*D, the activity of *Comamonadaceae* was likely not included. Nevertheless, based on the positive results obtained herein with the *mxaF, mdh2* and *dhaD* genes, it might be possible to track the glycerol degradation pathways of *Comamonadaceae* as well.

5.3.2 Impact of varying electron donors on denitrification performance and kinetics

During methanol feed (Phase I), a high degree of nitrate removal (95.4 ± 5.9 %, n = 21) with minimal nitrite accumulation (< 1 mg-N/L) was achieved. After changing the carbon source from methanol to glycerol (Phase II), transient nitrate accumulation in the range of 20-30 mg N/L was observed (data shown in the SI, Figure S-11). However, near

complete nitrate removal was rapidly achieved subsequently within 6 days and sustained thereafter through the end of the study (97.3 ± 3.5 %, n = 24) with minimal nitrite accumulation. During Phase I, the methanol specific denitrification rate (sDNR) values were in the range 1078 ± 236 mg N/ g volatile suspended solids (VSS)/ d (n = 11). Upon switching to glycerol, the methanol sDNR values decreased significantly (at α=0.05) to 332 ± 198 mg N/ g VSS/ d (n = 14) (Figure 5-3a). Concurrently, the glycerol sDNR values increased approximately 26-fold, from to 36 ± 13 mg N/g VSS/ d (n = 11) to 938 ± 434 mg N/g VSS/ d (n = 14) (Figure 5-3b). These inverse trends in sDNR values for methanol and glycerol corresponded well with the washout of known methanol assimilating bacteria in the SBR, and their replacement with a distinct population fostered on glycerol (Figure 5-2).

From an engineering perspective, the above results also suggest that despite long term operation with methanol, denitrifying wastewater treatment plants should be able to rapidly adapt to glycerol as a new carbon source. Additionally, minimal re-sizing of anoxic bioreactors for denitrification (which depends on denitrification kinetics) could be expected after the switch to glycerol given the statistically similar (α=0.05) steady-state sDNR values on methanol and glycerol during their respective feeding periods.

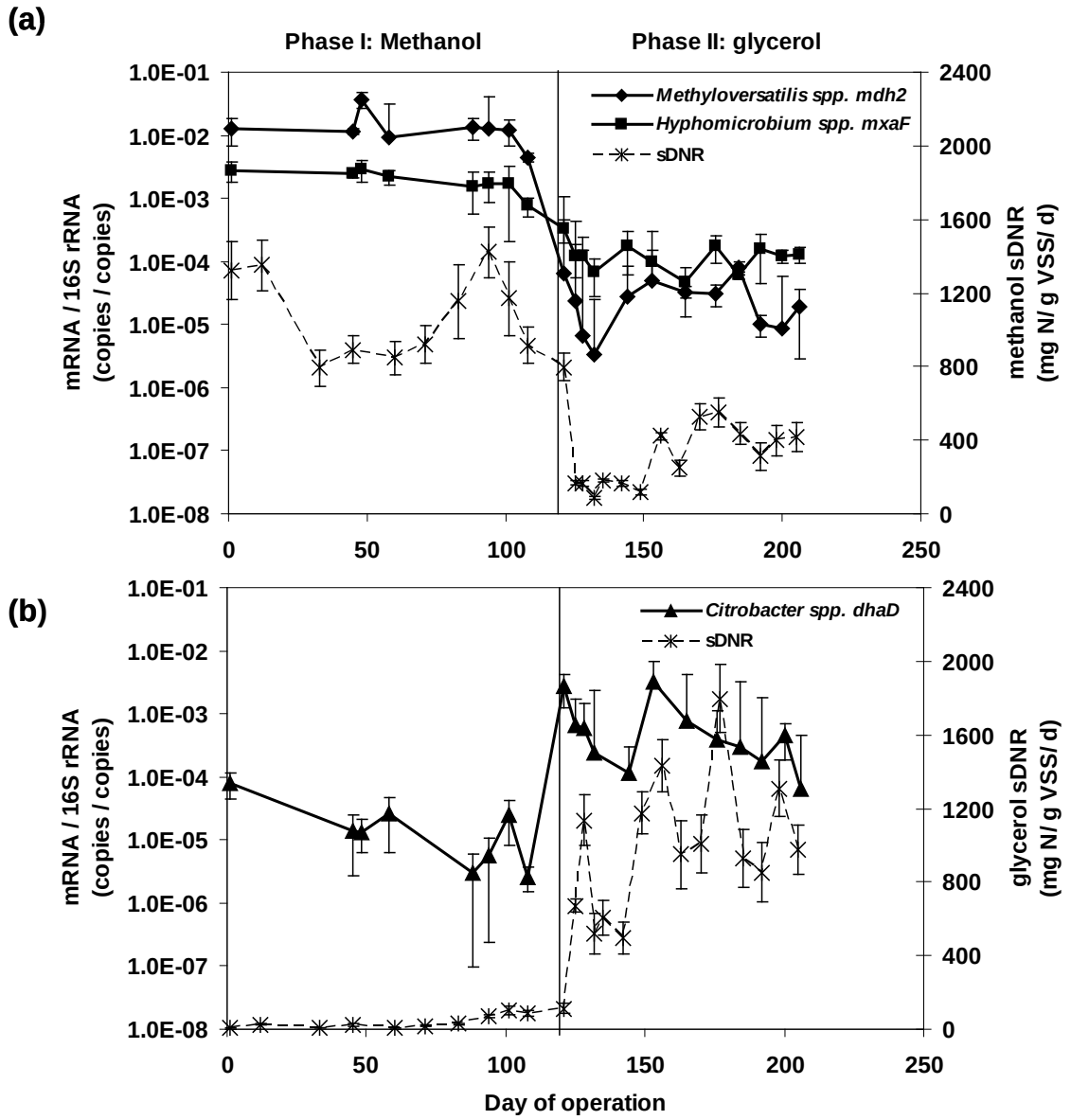

Figure 5-3: Time-series profiles during long term SBR operation of (a) *Methyloversatilis* spp. *mdh2* ( ) and *Hyphomicrobium* spp. *mxaF* ( ) mRNA concentrations and methanol sDNR values ( ); (b) *Citrobacter* spp. *dhaD* ( ) mRNA concentrations and glycerol sDNR values ( ). Error bars represent standard deviation from triplicate qPCR assays.

mdh2, mxaF and dhaD mRNA profiles during extant batch denitrification assays

Addition of glycerol to SBR biomass samples to initiate the batch sDNR assays during phase II (glycerol fed) significantly stimulated the transcription of *Citrobacter dhaD,* but not *Methyloversatilis mdh2* and *Hyphomicrobium mxaF,* (Figure 5-4, a2). The

rapid increase in *Citrobacter* spp. *dhaD* mRNA concentrations after the addition of glycerol is consistent with previous studies, which showed induction of *dhaD* and other genes of the *dha* regulon in cultures exposed to glycerol or dihydroxyacetone, an intermediate of glycerol oxidation [221, 233]. Notably, the short term *dhaD* mRNA profile (which is related to glycerol oxidation *sensu-stricto*) also paralleled the nitrate reduction profile (Figure 5-4, a1), thereby reflecting a close metabolic link between nitrate reduction and glycerol oxidation. When the rate of nitrate depletion slowed down presumably in response to glycerol limitation (around t=10 h, Figure 5-4, a1) *dhaD* mRNA concentrations also reverted back to their initial level of about 10^{-5} copies / copies (Figure 5-4, a2). In contrast the mRNA concentrations of *mdh2* and *mxaF*, were mostly unresponsive to the glycerol spike (Figure 5-4, a2), reflecting mutually exclusive and carbon source-specific stimulation of the respective alcohol dehydrogenase genes.

During the methanol batch tests, *Methyloversatilis* spp. *mdh2* and *Hyphomicrobium* spp. *mxaF* mRNA concentrations increased by factors of 2.2 ± 0.6 and 2.3 ± 0.1, respectively after the addition of methanol (Figure 5-4, b2). The lower increase in *mdh2* and *mxaF* mRNA concentrations (in contrast to the nearly 100 fold increase in *dhaD* mRNA concentrations) were presumably owing to the minimal methanol oxidation capability of the SBR during the glycerol feeding phase, during which these tests were conducted. There was no significant change in *Citrobacter* spp. *dhaD* mRNA concentrations during the entire methanol batch test (Figure 5-4, b2). The marginal increase of *mdh2* and *mxaF* expression was paralleled by a gradual decrease in nitrate concentrations during the batch methanol spike to the glycerol enriched biomass (Figure 5-4, b1), again underlining the lack of overlap between glycerol oxidation and methanol

oxidation capacities in the microbial community within the SBR. This lack of functional overlap is also in parallel with the lack of structural overlap in the microbial communities in the SBR during the two phases of operation (Figure 5-1). A similar exclusivity in glycerol and methanol based denitrifying bacterial populations in activated sludge using ^{13}C DNA SIP has also been recently demonstrated [81].

Long-term tracking of denitrification activity via alcohol dehydrogenase gene expression

The parallel trends between expression of genes coding for methanol or glycerol oxidation and denitrification activity using these carbon sources, which was observed during short-term biokinetic assays were repeated over long-term SBR operation as well.

During phase I, *Methyloversatilis* spp. *mdh2* and *Hyphomicrobium* spp. *mxaF* mRNA concentrations were higher than that of *Citrobacter* spp. *dhaD* (α=0.05**,** Figure 5-3). During Phase II, the *mdh2* and *mxaF* mRNA concentrations decreased by factors of 525.0 ± 58.7 and 17.3 ± 9.3, respectively (Figure 5-3a). In parallel, the methanol sDNR values also decreased significantly except a slight increase around 150-200 days of operation. The increase in methanol sDNR and accompanying increase of *Hyphomicrobium mxaF* around 150-200 days could possibly indicate the adaption of methanol dehydrogenase expression to new substrates, such as glycerol or byproducts from glycerol metabolism in the SBR [234]. In direct contrast, the *Citrobacter* spp. *dhaD* mRNA concentrations increased 37.7 ± 5.3 times and paralleled the trend in glycerol sDNR values (Figure 5-3b).

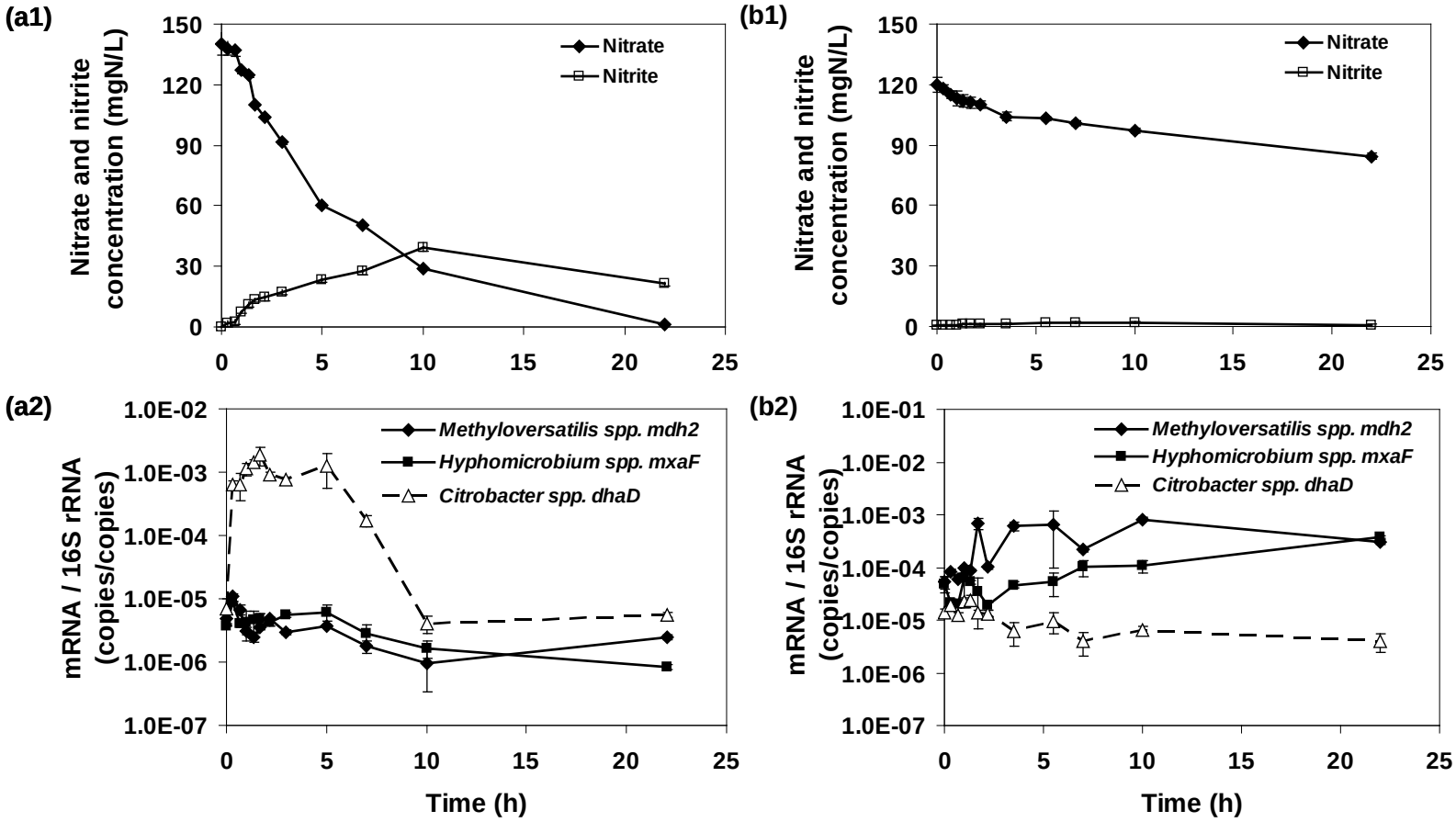

Figure 5-4: Time-series profiles of nitrate (◆) and nitrite (□) concentrations, and *Methyloversatilis* spp. *mdh2* (◆), *Hyphomicrobium* spp. *mxaF* (■), *Citrobacter* spp. *dhaD* (△) mRNA concentrations during a representative extant batch denitrification test with (a) glycerol and (b) methanol as external carbon source. Error bars represent standard deviation from triplicate qPCR assays.

Specific denitrification rates and corresponding weighted biomarker concentrations (calculated based on Equation S1 provided in Supplementary Information), showed statistically significant positive correlations at α=0.05 (Table II). The strong correlations underscore the potential link between functional gene transcription and corresponding carbon specific denitrification activity. Notwithstanding these observations, mechanism based inferences may not be drawn from these correlations and further studies linking ADH gene transcription and ADH enzyme activity are needed.

Table 5-II. Bivariate correlation analysis of denitrification activities and weighted potential biomarker concentrations

	Methanol sDNR and *Hyphomicrobium mxaF*	**Methanol sDNR and *Methyloversatilis mdh2***	**Glycerol sDNR and *Citrobacter dhaD***
r	0.505	0.609	0.513
p	0.023	0.004	0.021

r, Pearson correlation; p, p-value (two-tailed); sample size = 20.

These results are significant, since they suggest that the biomarkers developed herein provide a functional activity indicator of the overall SBR population in terms of either methanol or glycerol oxidation activities. This is rather positive also from a wastewater treatment perspective, where the focus is specifically on maximizing microbial functionality (*in casu*, ability to oxidize methanol or glycerol during denitrification and corresponding activity) and determination of specific activity measures to describe the different microbial active fractions [22]. Use of the biomarkers developed herein could also potentially help to address the impact of intermittent aeration (which is typically employed during wastewater treatment, [22]) on carbon-specific denitrification rates and ultimately result in better informed bioreactor designs for engineered denitrification. Additionally, despite the presence of downstream steps in the

overall process of carbon source oxidation and energy synthesis, it is significant that the genes coding for one of the first steps in this oxidation process (alcohol dehydrogenation to aldehyde) could still correlate well with the rate of electron acceptor (*in casu*, nitrate) reduction.

Notwithstanding the positive results obtained herein, some limitations must be considered. For example, the prospect of other genes coding for methanol oxidation in some bacteria as yet not detected cannot be overlooked. Additionally, given differences in the structural and functional ecology of different denitrifying wastewater treatment plants, it might be appropriate to develop more broadly targeted biomarkers to detect the concentrations and activity of methanol and glycerol assimilating bacteria therein. Furthermore, methanol dehydrogenase can oxidize a wide range of primary alcohols and aldehydes, albeit at lower rates [71]. As a result, expression of methanol dehydrogenase could also be correlated with denitrification fostered by other carbon sources, especially in bioreactors or other natural and engineered environments exposed to these alternate substrates. Therefore, further studies directed towards additional biomarker development and application, are recommended, particularly with additional carbon sources and their mixtures.

5.4 Summary

In this study, the applicability of genes coding for methanol dehydrogenase (*mdh2* and *mxaF*) and glycerol dehydrogenase (*dhaD*) as potential biomarkers of denitrification using methanol and glycerol was explored and confirmed using a two-pronged approach. First, during short-term spikes of activated sludge biomass with glycerol, the ability of *dhaD* mRNA concentrations to closely track nitrate depletion

profiles was demonstrated. Second, a high-degree of correlation of the mRNA concentrations of *mdh2, mxaF* and *dhaD* with methanol and glycerol based denitrification kinetics during long term bioreactor operation using these substrates was also shown. The basis for the link between selected alcohol dehydogenase gene mRNA concentrations and *in-situ* denitrification activity is that changes in gene transcription are one of the most fundamental responses of a cell to changes in the extracellular environment such as stress or substrate availability. Based on these results, expression of *mdh2, mxaF* and *dhaD* genes are promising biomarkers of *in situ* denitrification activity on methanol and glycerol respectively, in mixed-culture engineered wastewater treatment processes.

5.5 Supplementary Information Available

Metabolism of glycerol under oxidative and reductive conditions (Figure S-10); .Effluent concentrations of nitrate and nitrite from the SBR (Figure S-11)

CHAPTER 6

COMPARATIVE PROTEOMIC AND TRANSCRIPTIONAL ANALYSIS OF *Methyloversatilis universalis* FAM5 GROWN ON METHANOL AND ETHANOL UNDER ANOXIC CONDITIONS

This chapter is the basis of the paper:

Lu H[1], Kalyuzhnaya M[2], and Chandran K[1]*. 2011. Comparative proteomic and transcriptional analysis of *Methyloversatilis universalis* FAM5 grown on methanol and ethanol under anoxic conditions. (In preparation)

Affiliation:

1. Department of Earth and Environmental Engineering, Columbia University, New York, NY 10027
2. Department of Microbiology, University of Washington, Seattle, WA 98105

6.1 Introduction

The addition of organic carbon sources such as methanol is widely practiced to enhance denitrification in biological wastewater processes. However, due to the price variability and safety concerns of methanol, the potential of utilizing other alternatives, such as ethanol is of interest to many treatment facilities [235]. Several studies have been conducted to investigate the effects of the carbon source employed on denitrification process. Some focus areas include: performance and biokinetics [134, 236], microbial community structure [81, 137, 237], function of specific carbon assimilating populations [77, 79, 238], and greenhouse gas emissions [170, 175, 188]. However, mechanistic explanations for the functional responses of denitrifying bacteria to different carbon sources remain limited. Modern transcriptional and proteomic approaches allow a comprehensive view of microbial gene expression, metabolic pathways and adaptation to the environment [239-241]. The information gained from such transcriptional and proteomic analysis could potentially lead to a better understanding of the responses of denitrifying activated sludge communities to different carbon sources. Such understanding could be possibly extended to enable better operation and control of engineered denitrifying systems.

In a recent investigation using DNA-based stable isotope probing, *Methyloversatilis universalis* related populations were found to be dominant methanol and ethanol assimilating populations in lab-scale denitrifying reactors [77]. *M. universalis* is a Gram-negative, facultative methylotroph under the order of *Rhodocyclales* in Beta-Proteobacteria. *M. universalis* cultures can grow on C1 as well as multicarbon compounds [136]. Some essential genes for C1 assimilation have been identified in a

representative strain, *M. universalis* FAM5. The recently sequenced genome of *M. universalis FAM5* ([242], summarized in Figure 6-1) features nitrogen uptake pathways for energy metabolism, H_4MPT and H_4F linked C1-transfer, complete serine and Calvin cycles for C1 assimilation, and superpathway of glyoxylate cycle and TCA cycle for central metabolism. Therefore, *M. universalis* FAM5 could serve as a model organism to characterize the effects of different carbon sources on global gene expression patterns of facultative methylotroph under anoxic conditions.

As specialized enzymes are required for growth on C1 substrates, multiple energy generation and carbon assimilating pathways are normally present in the genome of the organisms capable of utilizing both C1 and multi-carbon compounds [123, 243]. Proteomic studies on one of the well-characterized facultative methylotrophs, *Methylobacterium extorquens* AM1, also confirmed the significant differences in the expression of carbon assimilatory pathways under single carbon and multi-carbon growth [244, 245]. Therefore, it was hypothesized that the growth of *M. universalis* FAM5 using methanol and ethanol would also elicit a widespread difference at the proteomic and gene transcription levels, especially for enzymes involved in the energy generation and biosynthesis from C1 and C2 compounds, such as the methanol dehydrogenase (methanol oxidation to formaldehyde) and formate dehydrogenase (formate oxidation to CO_2). It was also hypothesized that genes encoding N metabolic enzymes, such as the respiratory nitrate reductase (nitrate reduction to nitrite), and assimilatory nitrite reductase (nitrite reduction to ammonia for cell growth) would be transcribed at different levels depending on the carbon sources applied. In this study, the proteomic and transcriptional changes of *M. universalis* to growth on methanol and ethanol were measured in a pure-culture

chemostat, where growth rate-dependent gene expression variations can be avoided and thus allow the investigation under steady state and during carbon source transition. The specific objectives were to:

(1) *track the performance and denitrification kinetics of M. universalis upon switching the electron donor from methanol to ethanol;*

(2) *compare the proteome of M. universalis during growth on methanol and ethanol;*

(3) *quantify mRNA concentrations of genes encoding methanol/ethanol dehydrogenase (mdh2), formate dehydrogenase (fdh2A), respiratory nitrate reductase (narG) and assimilatory nitrite reductase (nasB) during growth on methanol and ethanol*

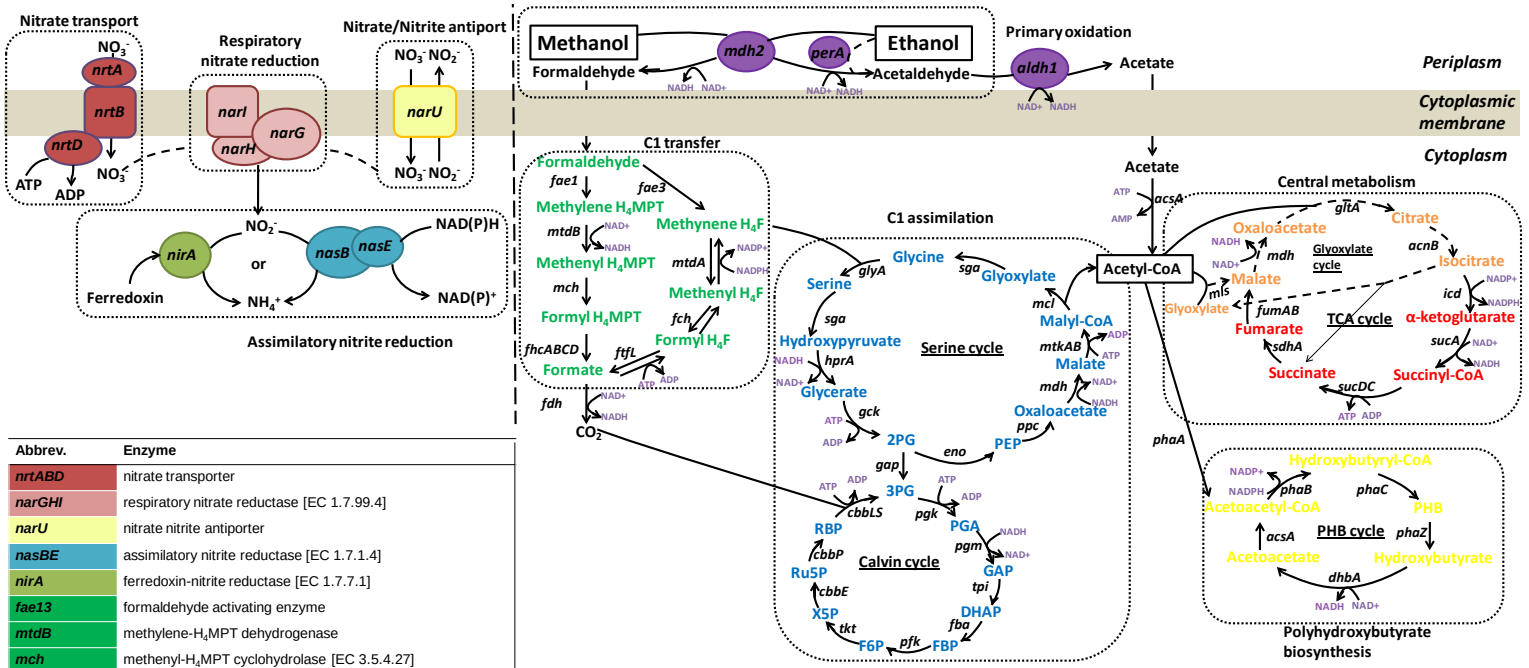

Abbrev.	Enzyme
nrtABD	nitrate transporter
narGHI	respiratory nitrate reductase [EC 1.7.99.4]
narU	nitrate nitrite antiporter
nasBE	assimilatory nitrite reductase [EC 1.7.1.4]
nirA	ferredoxin-nitrite reductase [EC 1.7.7.1]
fae13	formaldehyde activating enzyme
mtdB	methylene-H_4MPT dehydrogenase
mch	methenyl-H_4MPT cyclohydrolase [EC 3.5.4.27]
fhcABCD	formyltransferase/hydrolase complex
fdh	formate dehydrogenase [EC 1.2.1.2]
fch	methenyl-H_4F cyclohydrolase [EC 3.5.4.9]
ftfL	formate-tetrahydrofolate ligase [EC 6.3.4.3]
mtdA	bifunctional protein methylene-H_4MPT dehydrogenase and methylene-H_4-folate dehydrogenase [EC 1.5.1.5]
glyA	serine hydroxymethyltransferase [EC 2.1.2.1]
sga	serine-glyoxylate aminotransferase [EC 2.6.1.45]
hprA	hydroxypyruvate reductase [EC 1.1.29]
gck	glycerate kinase [EC 2.7.1.31]
eno	enolase [EC 4.2.1.11]
ppc	phosphoenolpyruvate carboxylase [EC 4.1.1.31]
mdh	malate dehydrogenase [EC 1.1.1.37]
mtkAB	malate thiokinase [EC 6.2.1.5]
mcl	malyl-CoA lyase [EC 4.1.3.24]
gap	glyceraldehyde 3-phosphate dehydrogenase [EC 1.2.1.12]

Abbrev.	Enzyme
cbbLS	ribulose bisphosphate carboxylase [EC 4.1.1.39]
pgk	phosphoglycerate kinase [EC 2.7.2.3]
pgm	phosphoglycerate mutase [EC 5.4.2.1]
tpi	triosephosphate isomerase [EC 5.3.1.1]
fba	fructose-bisphosphate aldolase [EC 4.1.2.13]
pfk	phosphofructokinase [EC 2.7.1.90]
tkt	transketolase [EC 2.2.1.1]
cbbE	ribulose-phosphate 3-epimerase [EC 5.1.3.1]
perA	peroxisomal catalase [EC 1.11.1.6]
mdh2	PQQ dependent methanol ethanol dehydrogenase [EC 1.1.1.244]
aldh1	acetaldehyde dehydrogenase 1 [EC 1.2.1.3]
mls	malate synthase A [EC 2.3.3.9]

Abbrev.	Enzyme
acnB	aconitate hydratase 2 [EC 4.2.1.3]
aceA	isocitrate lyase [EC 4.1.3.1]
icd	isocitrate dehydrogenase, NADP+ dependent [EC 1.1.1.42]
sucA	alpha-ketoglutarate dehydrogenase [EC 1.2.4.2]
sucDC	succinyl-CoA synthetase, alpha/beta subunits [EC 6.2.1.5]
sdhA	succinate dehydrogenase [EC 1.3.99.1]
fumAB	fumarate hydratase [EC 4.2.1.32]
phaA	acetyl-CoA acetyltransferase [EC 2.3.1.9]
phaB	acetoacetyl-CoA reductase [EC 1.1.1.36]
phaC	poly-beta-hydroxybutyrate polymerase
phaZ	poly(3-hydroxybutyrate) depolymerase
dhbA	d-3-hydroxybutyrate dehydrogenase [EC 1.1.1.30]

Figure 6-1. Nitrogen and carbon related electron transfer and metabolic pathways in *Methyloversatilis universalis* FAM5

6.2 Materials and Methods

6.2.1 Culture cultivation

M. universalis FAM5 cultures (American Type Culture Collection, ATCC BAA-1314) were grown in chemostat mode in a BioFlo® 115 fermentor (V= 2 L, T=25°C). Triplicate chemostats were operated at a hydraulic residence time (HRT) of 4 days. The pH of the reactor was automatically controlled in the range of 7.5 ± 0.1 using a sterile solution of 0.5 M sulfuric acid. Nitrogen gas was continuously sparged through the reactor at a flow rate of 0.5 L/min to maintain anoxic conditions (dissolved oxygen ≤ 0.01 mg/L). Each chemostat was sequentially operated with methanol (phase I), ethanol (phase II) and methanol (phase III) as organic electron donors (approximately 16 days for each phase) and nitrate as the electron acceptor. The influent concentrations of organic carbon (600 mg methanol or ethanol chemical oxygen demand (COD, explained in the Supplementary Information) /L) and nitrate-nitrogen (100 mg N/L) were determined based on the stoichiometric COD:NO_3^--N requirements of about 5~6:1 for methanol- and ethanol-fed denitrifying bacteria [22, 246]. In addition, the feed medium also contained (per liter): 0.4 g of NH_4Cl, 0.25 g of $MgSO_4 \cdot 7H_2O$, 0.102 g of KH_2PO_4, 0.261 g of K_2HPO_4, 0.1 mg vitamin B12 (filter sterilized), and 0.6 mL of trace elements solution (0.5 g of $FeSO_4 \cdot 7H_2O$, 0.101 g of $(NH_4)_6Mo_7O_{24} \cdot 4H_2O$, 0.5 g $MnSO_4 \cdot H_2O$, 0.125 g $CuCl_2 \cdot 2H_2O$, 0.45 of $ZnSO_4 \cdot 7H_2O$, 0.085 g $NiSO_4 \cdot 6H_2O$ in a total volume made up to 100 mL with distilled water).

6.2.2 Performance and denitrification kinetics measurements

Culture purity was checked daily by phase-contrast microscopy. Chemostat performance was monitored by measuring effluent nitrate (ion-selective electrode,

Accumet®), nitrite (diazotization), organic carbon (methanol and ethanol) concentration and cell concentration (direct microscopic counts) [125]. Methanol and ethanol concentrations were determined in quintuplicate using an SRI Model 8610C gas chromatography (SRI Instruments, Las Vegas, NV) equipped with a flame ionization detector (FID) and a HayeSep D stainless-steel column (SRI Instruments, Las Vegas, NV). The column had an initial temperature of 50°C, initial hold time of 1 min, program ramp of 20°C/min and a final temperature of 150°C. Under these conditions, the retention times for standard methanol and ethanol were 2.32 and 4.39 min, respectively. .

Nitrate reduction kinetics were determined via extant batch assays as described previously [76]. Briefly, 1 L cell suspensions were collected from the effluent of the chemostat at the end of each phase, centrifuged at 5000*g for 5 min and re-suspended in 500 mL sterile, nitrate and carbon free medium (same as the feed medium described above). The initial biomass COD concentrations in the batch tests were measured according to Standard Methods [125]. The extant batch assays (continuously sparged with N_2) were initiated by adding sodium nitrate and electron donor (methanol or ethanol) at t=0 to achieve an initial concentration of 100 mg N/L and 250 mg COD/L. Nitrate and nitrite concentrations were measured every 4 hours for 20 hours. The slope of the nitrate depletion profile was obtained during the non-carbon limiting phase and was normalized to the initial biomass concentrations to obtain the specific nitrate reduction rates (expressed as mg N/ g COD/ h).

6.2.3 RNA extraction and functional gene transcription

40 mL cell suspensions from the chemostat were collected and centrifuged at 5000*g for 10min. Cell pellets were stabilized with 250 µL RNA Protect™ Bacteria

Reagent (Qiagen, Valencia, CA) and stored at -80 °C. Total RNA was isolated using the PureLink™ RNA Mini Kit (Invitrogen, Carlsbad, CA) and then reverse transcribed using the Qiagen QuantiTect® Reverse Transcription Kit. qPCR primers were designed to specifically target genes encoding pyrroloquinoline quinone (PQQ)- dependent methanol/ethanol dehydrogenase (*mdh2*, METUNv1_590049), NAD-dependent formate dehydrogenase alpha subunit (*fdh2A*, METUNv1_700259), nitrate reductase large subunit (*narG*, METUNv1_700095) and respiratory nitrite reductase large subunit (*nasB*, METUNv1_470272) using the PrimerQuest® online software from Integrated DNA Technologies (Coralville, LA) (Table 6-I).

Table 6-I. qPCR primers and conditions to quantify functional gene transcription

Target gene	**Primer name**	**Sequence (5' to 3')**	**T_a (^{o}C)**	**Source**
16S	MuF	AAGGCCTACCAAGGCAACGA	55	[76]
	MuR	ACCGTTTCGTTCCTGCCGAA		
Mdh2	Mdh2F	TGCTGTTCGAGTACAAGGATCCGA	57	This study
	Mdh2R	TCACGAAGAAGTAGCCATTGCGGT		
Fdh2A	FdhF	AGCTGGGACGAAGCGATCAATTAC	56	This study
	FdhR	TAGGTTTCTTCATTGGTGCAGCGG		
NarG	NarF	AGAACGATCTCAACACCAGCGACA	57	This study
	NarR	GACGCACACCTCGCTGAATTTCTT		
NasB	NirF	TTCAAGAGCGGCGAAACCATTCC	57	This study
	NirR	ATCGTAGGTCTGCAGCGTGTCATT		

The mRNA concentrations of targeted functional genes were normalized to *M. universalis* FAM5 16S rRNA concentrations. All qPCR assays were performed in triplicate with the following conditions: 5 min at 95°C, followed by 40 cycles of 94 °C

for 30 s, 30 s at specific annealing temperature (Ta, Table I), and 72 °C for 45 s, and final extension at 72 °C for 5 min. The specificity of all qPCR products was confirmed by melt curve analysis and agarose gel electrophoresis.

6.2.4 Protein extraction and sample preparation

100 mL culture (~10^8 cells/mL) was withdrawn during three phases of the chemostat operation under steady state. Cells were centrifuged at 5000*g for 10 min, washed twice with 50 mL 1X PBS buffer (all at 4 °C) and then lysed in 250 µL lysis buffer, containing 0.1% Rapigest™ (Waters Corp.), 50 mM ammonium bicarbonate and 1% Protease Inhibitor Cocktail (Sigma-Aldrich). The solution was sonicated 3 times (30 s each time) on ice and the lysate was centrifuged at 15,000*g for 30 min at 4 °C to remove insoluble material. To further concentrate proteins, 300 µL of methanol and 75 µL of chloroform were added to 200 µL of lysate, mixed and centrifuged 5 min at 5,000* g for phase separation. The upper layer of methanol/water was aspirated using a micropipette and 225 µL methanol was added to form a uniform chloroform/methanol phase with precipitated protein floating. Supernatant was removed after centrifuging the mixture at 16,000*g for 5 min. 20 µL of lysis buffer (as described above) and 1.2 µL of dithiothreitol solution (0.1M, Sigma-Aldrich) was added to the pellets, which were further dissolved by sonication, then by heating for 5 min at boiling temperature. Protein content was estimated using the Bio-Rad Bradford total protein assay [247] and the target protein concentration was 1-5 µg/µL for all samples.

6.2.5 Mass spectrometry and data analysis

Protein extracts were heated to 80 ºC for 15 min. Cysteines were reduced in 2.8 mM dithiothreitiol at 60 ºC for 30 min and alkylated in 8.1 mM iodoacetamide for 30 min

at 25 ºC in the dark. Proteins were then digested with trypsin (6 ng/µL, Promega Corp.) in 50 mM NH_4HCO_3) for 16 h at 37 ºC and 75 fmol of a digest of yeast alcohol dehydrogenase was added as an internal standard. Prior to analytical separation on a NanoAcquity UPLC (Waters Corp.), peptides were trapped on a Symmetry C18 Trap column, 5 µm, 180 µm × 20 mm (Waters Corp.) for 2 min at 10 µL/minute in 1% solvent B (0.3% formic acid in acetonitrile) and 99% solvent A (0.3% formic acid, aqueous). Peptides were separated by a 34-min chromatographic separation with a 5 to 40% linear gradient of solvent B on a NanoAcquity UPLC at 300 nL/min using HSS T3 1.8 µm, 75 µm × 25 cm reversed phase column operated at 45 ºC. Mass spectra were recorded with a Synapt G2 QTOF mass spectrometer equipped with an ion mobility separation (IMS) cell (Waters Corp.), which alternated low- and high-energy scans (MS^E data-independent acquisition) with a scan time of 0.6 s. A reference mass of [Glu^1]-fibrinopeptide was infused at 500 nL/min and sampled every 30 s. All spectra were collected in resolution IMS mode.

Spectra were analyzed with ProteinLynx Global Server™ (PLGS 2.5, Waters Corp.) and searched against the *M. universalis* FAM5 protein sequence database. The database also contained sequences of yeast alcohol dehydrogenase, porcine trypsin and human keratin. Some of the default settings for PLGS analysis include: fixed modification was carbamidomethylation of cysteines, maximum false identification rate was 4%, the minimum fragment ion matches were 3 per peptide and 7 per protein, minimum peptide matches per protein was 1. A PLGS score was reported using a Monte Carlo algorithm to indicate the accuracy of assignment [248], and only proteins with PLGS scores higher than 300 were used for comparative analysis.

6.3 Results

6.3.1 Chemostat culture performance and biokinetics

During steady state operation, near complete nitrate removal was achieved under both methanol (phase I and III, 91.66 ± 3.13 %, n = 13) and ethanol (phase II, 92.52 ± 1.77 %, n = 7) feeding conditions (Table 6-II). However, most of the nitrate was only reduced to nitrite (92.40 ± 5.03%, n = 13 for methanol and 96.67 ± 2.27 %, n=7 for ethanol, respectively). The reactor effluent nitrate and nitrite concentrations during growth on methanol and ethanol were not statistically significant at α=0.05 as depicted by a representative performance profile (Supplementary Information, Figure S-12).

Table 6-II. Summary of the performance data from triplicate chemostat operation

Phase	% of nitrate removal	% of reduced nitrate to nitrite	ΔCOD/ΔN (mg COD/mg NO_3-N)	Estimated yield (mg COD/ mgCOD)	Cell density (10^8 cells/ mL)
I	93.97 ± 0.97	93.23 ± 4.19	2.32 ± 0.43	0.49 ± 0.10	2.33 ± 1.33
II	92.52 ± 1.77	96.67 ± 2.27	2.88 ± 0.35	0.60 ± 0.05	3.68 ± 2.18
III	89.36 ± 2.76	89.36 ± 2.77	2.43 ± 0.49	0.51 ± 0.11	2.66 ± 1.89

The observed biomass yield was calculated from the carbon to nitrogen ratio using Eq. 6-1. The higher estimated yield during ethanol feeding phase (0.60 ± 0.05, compared to 0.51 ± 0.09 mg biomass COD/ mg carbon COD for methanol) reflected 1.5 times more biomass grown on ethanol (3.68 ± 0.22 × 10^8 cells/ mL) than methanol (2.49 ± 0.23 × 10^8 cells/ mL), given near complete removal of the influent methanol or ethanol.

$$Y = 1 - \frac{1.14}{\Delta COD / \Delta N} \qquad \text{(Equation 6-1)}$$

During the methanol fed phase I, methanol induced specific nitrate reduction rates (16.9 ± 3.3 mg N/ g COD/ h) were higher than that of ethanol (12.7 ± 2.2 mg N/ g COD/ h) (n=3, p=0.15) (Figure 6-2). In the following ethanol feeding phase II, the methanol specific nitrate reduction rates decreased to 10.1 ± 1.4 mg N/ g COD/ h, and were statisticallylower (at α=0.05) than that of ethanol (17.4 ± 2.2 mg N/ g COD/ h), which in turn increased compared to numbers in phase I. These results were in agreement with previous studies on a mixed-culture denitrifying reactor dominated by *Methyloversatilis* spp., where nitrate sDNR values significantly decreased after switching the carbon source from methanol to ethanol [77]. At the end of the recovery phase (phase III, switching back to methanol feed), the ethanol specific nitrate reduction rates (12.7 ± 4.8 mg N/ g COD/ h) reverted back to its original level, but methanol specific nitrate reduction rates (13.8 ± 2.8 mg N/ g COD/ h) remained lower than in phase I, the initial methanol feeding phase (n=3, p=0.28).

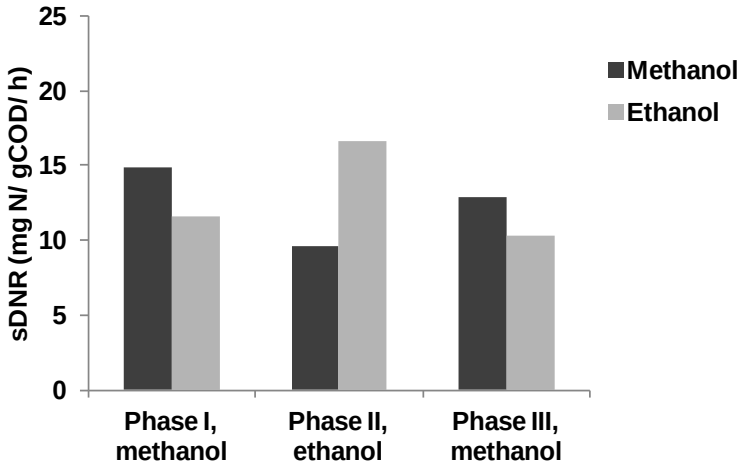

Figure 6-2: Specific nitrate reduction rates during three phases of chemostat operation

6.3.2 Transcription of several key functional genes involved in C and N metabolism

Profiling of mRNA provided several insights into the carbon and nitrogen metabolism pathways in *M. universalis* FAM5 in response to changing electron donors. PQQ dependent methanol ethanol dehydrogenase (*mdh2*), which primarily oxidizes the two alcohols to corresponding aldehydes, showed the highest transcription levels (normalized to 16S rRNA) among the four genes tested, and its mRNA concentration during ethanol feeding phase was about 5 times higher than that of methanol (Figure 6-3). The response time of *mdh2* transcription to carbon transition was on average 6 days (1.5 HRT). In contrast, relative transcript abundances of *narG*, *fdh2A* and *nasB* stayed at similar levels during the three phases, indicating little impact of different carbon sources on the transcription of these three genes.

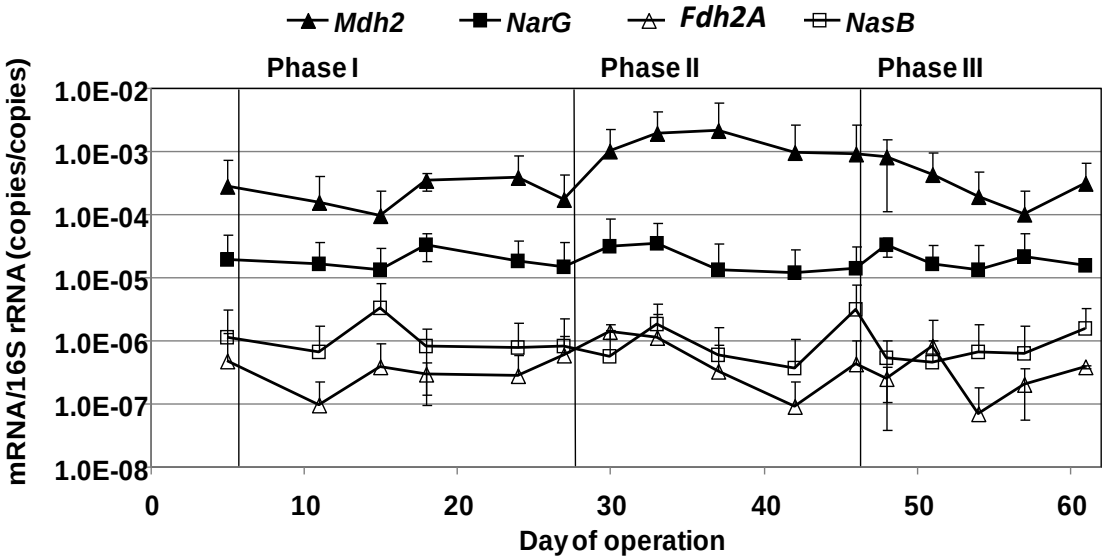

Figure 6-3: Time-series profiles during a representative chemostat operation of methanol/ethanol dehydrogenase (*mdh2*, ▲), nitrate reductase (*narG*, ■), formate dehydrogenase (*fdh2A*, △) and nitrite reductase (*nasB*, □) mRNA concentrations. Error bars represent standard deviation from triplicate qPCR assays

6.3.3 Comparative proteome under methanol and ethanol growth conditions

A total of 6000-7000 peptides with approximately 600 corresponding proteins were detected in each sample. The overall proteome coverage was about 15% out of the 3957 predicted CDSs in the *M. universalis* FAM5 genome. Concentrations (in fmol/μg total protein) of essential proteins for carbon oxidation, C1 transfer and assimilation, central metabolism and nitrogen metabolism are listed by category in Table 6-III . Fold changes of protein quantity from methanol to ethanol feeding condition have been calculated by dividing the averaged protein concentrations in phase II (E, ethanol feeding) by those in phase I (M, methanol feeding) for all biological replicates (therefore expressed as E/M). Therefore, a value less than 1 indicates induction under methanol growth, and greater than 1 indicates induction under ethanol growth.

PQQ dependent methanol ethanol dehydrogenase (*mdh2*) exhibited increased expression levels during growth on ethanol, and was consistent with the changes in its mRNA concentration (Figure 6-3). All enzymes involved in C1 transfer from formaldehyde to formate were uniformly up-regulated under methylotrophic condition (a fold change of 7 on average, during both phase I and the recovery phase III). Likewise, the serine pathway specific enzymes, except enolase (*eno*) and malate dehydrogenase (*mdh*), were expressed at significantly higher levels when methanol was used. Only a few enzymes that participate in the Calvin cycle were detected and their expressions appeared to be unaffected by carbon sources. Another significant difference between cells under the two growth conditions was the up-regulation of central metabolism enzymes by ethanol. These proteins catalyze the glyoxylate cycle and the majority of the TCA cycle,

with the exception of fumarate hydratase (*fumABC*), which was not detected in any sample.

Nitrate reductase gamma subunit (*narI*) showed decreased expression during growth on ethanol. The other two subunits of the nitrate reductase, as well as the nitrate nitrite antiporter were expressed regardless of the carbon sources supplied (changes were not significant at α=0.05). Assimilatory nitrite reductases (*nasBE* and *nirA*) were not detected in any sample. Differential expression (significant at α=0.05) of 15 other proteins, in addition to those catalyzing the N and C metabolic pathways displayed in Figure 6-1, was observed. These proteins are broadly involved in stress adaptation, poly-hydroxybutyrate (PHB), ATP and tRNA synthesis, and basic cellular functioning (e.g., ribosomal proteins) (Table 6-III).

Table 6-III. Relative changes in protein concentration under methanol versus ethanol feeding conditions. Normalized quantity represents the mean and standard deviation of biological triplicate experiments. Asterisk (*) indicates the difference in protein expression under the two growth conditions was significantly different at $\alpha = 0.05$.

Protein	Description	Accession number (METUNv1)	Normalized quantity (fmol/µg)			Fold change E/M
			Phase I	Phase II	Phase III	
C1 and C2 oxidation						
mdh2	methanol/ethanol dehydrogenase	590049	369.73 ± 55.17	461.06 ± 109.03	358.25 ± 43.26	1.25
fdh1A	formate dehydrogenase 1, alpha subunit	570005	9.87 ± 1.49	5.08 ± 0.59	15.45 ± 8.45	0.51
fdh1B	formate dehydrogenase 1, beta subunit	570006	13.18 ± 2.20	7.81 ± 0.97	12.21 ± 0.75	0.59
fdh3B	formate dehydrogenase 3, beta subunit	770386	65.85 ± 28.74	47.72 ± 16.28	25.66 ± 8.66	0.72
fdh3C	formate dehydrogenase 3, gamma subunit	770388	43.31 ± 17.85	19.34 ± 3.56	11.32 ± 1.03	0.41
perA	peroxisomal catalase	590008	87.43 ± 6.51	99.17 ± 36.47	56.39 ± 14.16	1.13
acsA	acetate-CoA ligase	470129	93.67 ± 22.62	115.04 ± 43.14	81.81 ± 7.13	1.65
C1 transfer (H_4MPT and H_4F pathways)						
fae1	formaldehyde-activating enzyme	580096	602.58 ± 77.22	510.55 ± 86.93	475.99 ± 34.53	0.84
mtdA	bifunctional protein mtdA	460310	63.17 ± 8.84	19.16 ± 5.99	37.59 ± 9.77	0.30*
mtdB	methylene-H_4MPT dehydrogenase	580091	77.33 ± 17.52	19.86 ± 6.29	68.62 ± 5.31	0.26*
mch	methenyl-H_4MPT cyclohydrolase	580093	16.46 ± 5.77	13.47 ± 4.26	14.74 ± 3.48	0.82
fch	methenyl-H_4F cyclohydrolase	460309	46.81 ± 14.77	14.48 ± 3.38	47.52 ± 8.70	0.31
fhcA	formyltransferase hydrolase complex, subunit A	580087	22.78 ± 13.06	7.59 ± 4.13	6.13 ± 0.55	0.27
fhcB	formyltransferase hydrolase complex, subunit B	580088	18.19 ± 6.90	8.69 ± 2.02	11.12 ± 1.52	0.48
fhcC	formyltransferase hydrolase complex, subunit C	580085	17.67 ± 5.52	5.19 ± 0.47	3.13 ± 1.14	0.29
fhcD	formyltransferase hydrolase complex, subunit D	580086	21.05 ± 9.41	7.06 ± 2.13	7.67 ± 2.08	0.33
ftfL	formate-tetrahydrofolate ligase	460318	121.97 ± 26.34	21.36 ± 3.11	116.03 ± 17.68	0.17*

C1 assimilation (Serine and Calvin cycle)						
glyA	serine hydroxymethyltransferase	460313	168.51 ± 28.70	28.29 ± 14.91	136.38 ± 26.03	0.17*
sga	serine-glyoxylate aminotransferase	460312	258.41 ± 81.05	20.26 ± 1.45	236.75± 29.99	0.07*
hprA	hydroxypyruvate reductase	460311	83.44 ± 21.64	84.09 ± 10.56	72.48 ± 12.14	1.01
gck	glycerate kinase	770329	18.38 ± 5.94	3.05 ± 1.21	20.29 ± 1.09	0.17
eno	enolase	460302	51.83 ± 3.58	80.38 ± 15.87	76.97 ± 37.83	1.55
ppc	phosphoenolpyruvate carboxylase	770169	12.98 ± 3.58	6.66 ± 4.91	34.63 ± 16.20	0.51*
mdh	malate dehydrogenase	520009	97.58 ± 11.95	201.97 ± 9.32	74.41 ± 23.29	2.07*
mtkA	malate thiokinase, large subunit	460314	190.19 ± 22.11	57.93 ± 34.19	196.89 ± 23.98	0.30*
mtkB	malate thiokinase, small subunit	460315	146.92 ± 32.67	34.75 ± 18.14	147.48 ± 13.39	0.23*
mcl	malyl-CoA lyase	460317	129.02 ± 20.79	18.37 ± 12.07	140.98 ± 13.92	0.14*
pgk	phosphoglycerate kinase	700106	15.02 ± 0.14	17.02 ± 3.55	14.88 ± 3.76	1.13
gap	glyceraldehyde 3-phosphate dehydrogenase	700107	43.32 ± 8.81	33.99 ± 4.27	38.84 ± 8.04	0.78
tkt	transketolase	700108	20.79 ± 3.33	15.88 ± 2.16	14.94 ± 4.53	0.76
fba	fructose-bisphosphate aldolase	700104	38.35 ± 3.58	53.03 ± 9.32	32.32 ± 2.14	1.38
pgm	phosphoglycerate mutase	710053	11.19 ± 2.06	27.79 ± 9.74	10.65 ± 4.08	2.48
tpi	triosephosphate isomerase	460124	6.45 ± 0.36	7.59 ± 2.08	6.96 ± 1.66	1.18
Central metabolism (Glyoxylate and TCA cycle)						
mls	malate synthase	620020	46.02 ± 6.13	66.00 ± 20.33	20.56 ± 16.19	1.43
gltA	citrate synthase	520016	56.08 ± 23.61	116.97 ± 37.91	31.92 ± 12.42	2.08
acnB	aconitate hydratase 2	610186	51.72 ± 11.77	74.90 ± 9.69	52.70 ± 8.98	1.45*
aceA	isocitrate lyase	620018	354.87 ± 111.51	403.19 ± 44.78	284.71 ± 22.73	1.14
icd	isocitrate dehydrogenase	620013	41.30 ± 9.22	42.64 ± 7.95	23.58 ± 8.28	1.03
sucA	alpha ketoglutarate dehydrogenase	520017	49.34 ± 15.10	94.70 ± 19.69	40.61 ± 4.31	1.92*
sucC	succinyl-CoA synthetase, beta subunit	700186	42.76 ± 16.47	138.21 ± 31.91	34.10 ± 13.67	3.23*
sucD	succinyl-CoA ligase, alpha subunit	700187	22.69 ± 8.87	87.65 ± 20.59	16.70 ± 7.29	3.86*
sdhA	succinate dehydrogenase	520013	48.89 ± 17.85	113.69 ± 47.89	45.01 ± 3.42	2.33

mdh	malate dehydrogenase	520009	97.58 ± 11.95	201.97 ± 9.32	74.41 ± 23.29	2.07*
Nitrogen metabolism						
narG	nitrate reductase, alpha subunit	700095	96.08 ± 10.30	88.78 ± 42.80	103.20 ± 19.61	0.92
narH	nitrate reductase, beta subunit	700094	62.06 ± 4.55	78.71 ± 7.05	54.34 ± 9.97	1.27
narI	nitrate reductase, gamma subunit	700092	52.18 ± 8.18	31.68 ± 9.63	30.62 ± 4.37	0.61
narU	nitrate nitrite antiporter	700096	85.37 ± 23.75	54.99 ± 10.48	70.81 ± 9.57	0.64
Some other differentially expressed proteins						
phaB	acetoacetyl-CoA reductase	460202	67.55 ± 0.86	145.61 ± 20.75	29.81 ± 10.42	2.16*
phaC	poly beta hydroxybutyrate polymerase	750111	15.89 ± 4.12	46.33 ± 10.31	18.88 ± 2.88	2.91*
phaP	granule associated protein phasin	770162	275.88 ± 48.04	878.91 ± 132.33	565.12 ± 50.58	3.18*
ppiB	peptidyl-prolyl cis-trans isomerase B	460087	35.33 ± 11.77	84.82 ± 15.73	43.04 ± 3.47	2.40*
phaR	Polyhydroxyalkanoate synthesis repressor	460203	33.54 ± 7.92	50.49 ± 9.50	45.75 ± 1.88	1.51*
ftfL	formate tetrahydrofolate ligase	460318	121.97 ± 26.35	21.36 ± 3.11	116.03 ± 17.68	0.18*
abpA	2-dehydropantoate 2-reductase	660147	36.89 ± 6.32	11.11 ± 4.92	32.85 ± 2.83	0.30*
hppA	pyrophosphate-energized proton pump	580036	54.60 ± 20.41	130.2 ± 20.29	49.63 ± 8.08	2.39*
etfA	electron transfer flavoprotein alpha-subunit	590059	60.18 ± 5.49	91.87 ± 17.43	46.93 ± 17.89	1.53*
rplR	50S ribosomal subunit protein L6	700018	85.89 ± 5.98	56.87 ± 16.70	59.06 ± 9.58	0.66*
ilvI	Acetolactate synthase large subunit	700216	92.51 ± 9.11	55.52 ± 13.62	66.74 ± 11.25	0.60*

6.4 Discussion

6.4.1 Carbon oxidation, C1 transfer and assimilation

The PQQ dependent methanol ethanol dehydrogenase oxidizes a wide range of primary alcohols, and has similar affinity for methanol and ethanol in *M. universalis* FAM5 [160]. In addition, the peroxisomal ethanol degradation to acetaldehyde, catalyzed by peroxydise (*perA*) [249] is also feasible as inferred from the genome of the strain. During the ethanol feed phase, both *mdh2* and *perA* were slightly up-regulated, resulting in a higher consumption of ethanol than methanol. In contrast to *M. universalis* FAM5, methanol dehydrogenase (encoded by *mxaF*) in another facultative methylotroph, *Methylobacterium extorquens* AM1, was expressed at significantly higher levels under methylotrophic (methanol feed) compared to nonmethylotrophic (succinate feed) conditions [244, 245]. This inconsistency can be explained by the different affinities of *mdh2*- and *mxa*-type dehydrogenase for the growth substrates tested [160, 250]. Surprisingly, acetaldehyde dehydrogenase (*aldh1*), which oxidizes acetaldehyde to acetate, was not detected in any sample. It has been shown that $NADP^+$-dependent alcohol dehydrogenase could possibly oxidize both ethanol and acetaldehyde in methanogenic bacteria [251]. Therefore, *mdh2* might catalyze the oxidation of acetaldehyde to acetate in *M. universalis* FAM5 instead of *aldh1*, as it possesses a broad substrate specificity (including aldehyde) [71]. As expected, acetyl-CoA synthetase (*acsA*), which further oxidizes acetate to the central metabolic intermediate acetyl-CoA, was induced during the ethanol feeding phase but not in the following methanol feeding recovery phase III.

Cytoplasmic formaldehyde is the crucial central intermediate for C1 metabolism, and formaldehyde activating enzyme (*fae*) catalyzes the first step of its oxidation and/or detoxification via either tetrahydromethanopterin (H_4MPT) or tetrahydrofolate (H_4F) dependent pathways. In agreement with previous enzyme assays [245, 252], all C1 transfer related proteins were found to be methanol-induced according to the proteomics data. Moreover, although H_4MPT-linked pathway has been shown to contribute to the majority of formaldehyde conversions [253], proteins involved in the two pathways were induced to comparable levels.

The three types of formate dehydrogenase identified in the genome of *M. universalis* FAM5 are homologous to those found in *M. extorquens*: NAD-dependent, tungsten-containing type I (*fdh1AB*), molybdenum-dependent type II (*fdh2ABCD*); cytochrome-linked type III (*fdh3ABC*) [73, 254] (a molybdenum-dependent type IV formate dehydrogenase (*fdh4AB*) was recently found in *M. extorquens* [255]). *fdh1AB* and *fdh3BC* in *M. universalis* FAM5 were up-regulated by methanol. In contrast, the expression of *fdh2* could only be assessed at the mRNA level, suggesting that it might be dispensable during the conversion from formate to CO_2.

The upregulation of nearly all the components of the serine cycle but not the Calvin cycle confirmed that the former was the favored C1 assimilation pathway in heterotrophic methylotrophs [218]. Malate dehydrogenase (*mdh*) and enolase (*eno*) were found to be ethanol-induced, since apart from serine cycle, they also function in the TCA and glycolysis cycle, respectively. The latter two pathways play important roles during growth on multicarbons [117]. The regulatory patterns of proteins involved in the serine

cycle were in good accordance with those detected in methanol and acetate grown *M. extorquens* cells [244, 256].

The higher yield coefficient for denitrifying bacteria grown on ethanol than ethanol was previously observed using activated sludge [61, 257]. More energy is needed during the utilization of methanol for biosynthesis, as it requires the input of NADH [55, 56]. As a result, yields for organisms using C1 compounds are generally less than those using multi-carbons [55].

Central metabolism

The glyoxylate bypass of TCA cycle requires two key enzymes, isocitrate lyase (*aceA*) and malate synthase (*mls*), and is used to regenerate glyoxylate for the serine cycle during C1 assimilation [258]. For most serine-cycle methylotrophs that lack *aceA*, alternative pathways exist for converting acetyl-CoA to glyoxylate [117]. The glyoxylate shunt is also essential for growth on C2 compounds as a replenishing pathway to the TCA cycle to prevent the loss of acetate carbon as CO_2 [259]. Meanwhile, the two cycles compete with each other in that *aceA* and isocitrate dehydrogenase (*icd*) share a common substrate, isocitrate. Based on the proteomics data, the expression of *aceA* was consistently higher than the TCA cycle enzyme *icd* under both growth conditions. As a result, it is speculated that more isocitrate was channeled through the glyoxylate cycle rather than the TCA cycle.

For methylotrophic bacteria that have isocitrate lyase, the expression of glyoxylate cycle enzymes under C1 and C2 feeding conditions have not been studied. The TCA cycle plays a strict assimilatory role and is not involved in energy generation during C1 metabolism [73, 117]. Therefore, it is not surprising that most enzymes in this

cycle were expressed at lower levels during growth on methanol. The function of class I (*fumAB*) and II fumarate hydratase (*fumC*) in TCA cycle requires further investigation, since the concentrations of these membrane associated proteins were both below the detection limit of proteomic analysis.,

Nitrogen metabolism

Dissimilatory nitrate reduction occurs via two pathways in prokaryotes, and both are initiated by respiratory nitrate reductase. Denitrification is the sequential reduction of nitrate to nitrogen gas via nitrite, nitric oxide and nitrous oxide [1]. The other pathway, termed ammonification, is carried out by bacteria such as *Escherichia coli*, which reduce nitrate to nitrite by respiratory nitrate reductase, and then to ammonia via assimilatory nitrite reduction [260]. Nitrate-ammonifying bacteria coexist with heterotrophic denitrifiers in activated sludge, marine and soil sediments [17, 18, 164]. The competition between these two groups of bacteria for carbon and nitrate is a function of the C:N ratio [261], and high carbon availability and/or low nitrate availability would favor ammonification over denitrification [262, 263].

Although *M. universalis* spp. related populations could assimilate methanol and ethanol effectively with nitrate as the electron acceptor [77], a lack of coding genes for dissimilatory nitrite reductase (*nirK* or *nirS*), nitric oxide reductase (*nor*) and nitrous oxide reductase (*nos*) results in the inability of *M. universalis* FAM5 to denitrify. Instead, its genome predicts that the strain is able to ammonify nitrate by means of periplasmic nitrate reductase (*nar*) and cytoplasmic nitrite reductase (*nasBE* and *nirA*, Figure 6-1). The significant amount of nitrite accumulated in this study could be attributed to the repression of assimilatory nitrite reductases, evidenced by the fact that neither *nasBE* nor

nirA were detectable in proteomic analysis. Presumably, nitrite reductase was subjected to end-product repression by non-limiting ammonia concentrations in the chemostat cultures, as observed similarly for other bacteria [264-266]. Assimilatory nitrite reduction is not favored herein because more reducing equivalents are required to reduce nitrite to ammonia for biosynthesis.

It has been shown that the synthesis of membrane-bound nitrate reductase (*nar*) can be induced to different levels under anaerobic conditions depending on the carbon sources utilized [267]. Nevertheless, the same study demonstrated that the induction level did not follow the same regulatory patterns for periplasmic nitrate reductase (*nap*), i.e., more reduced carbon sources lead to higher levels of synthesis under aerobic conditions [268]. Methanol and ethanol, which have the same degree of reduction (i.e., the number of electron equivalents in a mole of the compound divided by the number of carbon atoms, which equals to 6 for methanol and ethanol), led to similar *narGH* expression (Table 6-III) and specific nitrate reduction rates (induced by methanol in phase I and ethanol in phase II, Figure 6-2). These results re-confirmed previous findings that carbon sources have little effect on the expression of the *nar* operon. Nevertheless, due to a limited understanding of the biochemistry and regulation of the gamma subunit *narI*, its decreased expression during phase II cannot be interpreted mechanistically.

6.4.2 Differentially expressed proteins in other pathways-an example of PHB synthesis

Polyhydroxyalkanoates (PHAs) accumulate as granules in the bacterial cytoplasm for carbon and energy storage purposes under unfavorable growth conditions (such as limitation of nitrogen, phosphorus and magnesium) or in the presence of excess carbon source [269, 270]. Polyhydroxy β-butyrate (PHB), the best known PHA can accumulate

to as high as 80% of cell dry weight in methylotrophic bacteria depending on the C1 assimilation pathway utilized [271]. Therefore, a significant amount of carbon flux could be in the direction of PHB synthesis. In this study, analysis of the *M. universalis* FAM5 proteome revealed that four out of five PHB cycle proteins (except the PHB depolymerase (*phaZ*) in Figure 6-1), were consistently detected under both carbon feeding conditions (data not shown), among which acetoacetyl-CoA (*phaB*) and PHB polymerase (*phaC*) in the cycle were expressed at significantly higher levels under ethanol growth. The biosynthesis of PHB in most bacteria is initiated by the condensation of two molecules of acetyl-CoA to acetoacetyl-CoA, which then enters the PHB cycle [269]. It is speculated that more available acetyl-CoA generated from ethanol metabolism than that of methanol possibly led to the induction of polymer biosynthesis under ethanol growth. Granule associated protein (phasin, *phaP*) was also upregulated by ethanol, which was in accordance with its function as both a growth and polymer accumulation promoter [272]. *phaP* expression can also increase the resistance of *E. coli* cells to oxidative and heat stresses [273] by affecting the expression of stress-related genes during PHB production, such as the two encoding heat-shock protein promoters, *ibpA* and *dhaK* [273].

During the methanol recovery phase (phase III), most proteins that were up- or down-regulated in the ethanol phase (phase II) reverted to similar levels as those in phase I (methanol), suggesting that the changes caused by varying electron donors were reversible. The carbon metabolic flexibility of *M. universalis* may explain its continuous dominance found in the methanol and ethanol fed mixed-culture reactor [77]. Other proteins that are differentially expressed during growth on methanol and ethanol

suggested that carbon variation elicits stress, and basic regulatory responses that have not been characterized herein. Further work needs to be conducted for elucidating how these enzymes are impacted by different carbon sources, and the subsequent effects on denitrification.

6.5 Summary

In this study, the global proteomics and specific transcriptional responses of a newly isolated and sequenced facultative methylotroph, *Methyloversatilis universalis* FAM5, to the growth on different electron donors were characterized. During the anoxic chemostat growth of *M. universalis* FAM5 on nitrate as the electron acceptor, and methanol and ethanol as the electron donors, over 90% of influent nitrate was reduced and accumulated as nitrite irrespective of carbon sources utilized. Lower cell growth yield was found using methanol as the electron donor, possibly due to the energy loss during C1 transfer and assimilation. Based on label-free, quantitative mass spectrometry, methanol grown cells displayed elevated concentrations of the enzymes involved in C1 transfer (H_4MPT and H_4F pathways), formate oxidation and C1 assimilation (serine cycle). In contrast, primary alcohol oxidation, central metabolism (glyoxylate and tri-carboxylic acid cycle) and polyhydroxy β-butyrate (PHB) synthesis related proteins were generally induced during growth on ethanol. Notably, the expression of respiratory nitrate reductase and assimilatory nitrite reductase was not affected by the carbon sources applied at either proteome or transcript level. This study expands the understanding of the regulation of dissimilatory and assimilatory enzymes in facultative methylotrophs, and provides insights into the strategies employed by wastewater denitrifying bacteria when growing on different carbon sources.

6.6 Supplementary Information Available

Representative performance profiles during three phases of chemostat operation using methanol (Phase I), ethanol (Phase II) and methanol (Phase III) as electron donors (Figure S-12)

CHAPTER 7

CONCLUDING REMARKS

7.1 Carbon source selection criteria - balancing cost, yield and kinetics

During the past decade, increasingly stringent discharge limits of nitrogen species had been imposed across the US. Although methanol is still the most widely applied carbon source to enhance denitrification efficiency, the safety issues associated with using methanol make alternative carbon sources, such as ethanol and glycerol, of interest to many treatment facilities. Some considerations need to be taken into account when making a choice of carbon source for denitrification, such as nitrogen removal performance, kinetics, cost, sludge production and operational practice. In this study, cost, yield and kinetics based comparisons (Table 7-I) for the three tested compounds imply that methanol is still the most cost-effective carbon source for denitrification process. Although it has been suggested that the lower kinetics of methanol assimilating denitrifying bacteria may result in incomplete nitrate removal during low temperature operation, the two alternative carbon sources (ethanol and glycerol) did not exhibit better kinetics than methanol. In addition to the currently higher cost of biodiesel than methanol for reducing per kg of nitrate, another disadvantage of using glycerol-containing waste is that the higher growth yields of glycerol assimilating species could cause excess waste sludge to handle.

From the cost and kinetics perspectives, ethanol is not a favorable carbon source for denitrification. Lower ethanol kinetics compared to the other carbon sources contrasted with results found elsewhere [109, 257]. This divergence in findings can be explained by the fact that the community enriched by ethanol was developed after a

prolonged exposure to methanol. Consequently, the ethanol induced kinetics after carbon switch might not be representative of the dentirification potential of systems with more diverse ethanol utilizers.

Table 7-I. Comparison of the cost, growth yield and sDNR values of methanol, ethanol and glycerol fostered denitrification process

	Cost ($/ kg COD)[a]	**Yield (g VSS/ g COD)**	**COD/N (g COD/ g N)[c]**	**Cost of N removal ($/ kg N)**	**sDNR (mg N/ g VSS/ h)[b]**	
Methanol	0.44	0.35 ± 0.07[b]	5.61	2.24	44.3 ± 9.8	
Ethanol	0.57	0.42 ± 0.04[b]	7.15	4.07	38.9 ± 6.2	
Glycerol	1.19	0.50[d]	5.72	5.95	**SBR**	**SB-IFAS**
					42.6 ± 16.7	29.1 ± 10.1 (suspended) 24.6 ± 3.7 (biofilm)

a) Source: [257] and http://www.eosenvironmental.com/
b) Results obtained from this dissertation research
c) COD/N ratio calculated based on COD/N=2.86/(1-Y)
d) Assumed growth yield on glycerol [274]

7.2 Water quality and air quality: exclusive or compatible?

From the perspective of improving water and air quality, denitrification processes under oxygen inhibition condition using methanol and ethanol as carbon sources will be illustrative for further discussion. As observed in this study, the first step of methylotrophic denitrification was largely inhibited by oxygen, resulting in a significant increase of effluent nitrate concentrations. Notwithstanding the fact that all accumulated nitrate due to oxygen inhibition was eventually removed using ethanol as electron donor, the capacity of denitrification was sustained at the cost of deteriorating the air quality, since a large amount of N_2O was emitted. In practice, some single sludge BNR systems are characterized by the internal recirculation streams from the downstream anoxic

reactors to upstream aerobic reactors (post-denitrification), where denitrifying species are exposed to high DO concentrations (> 2 mg/L). Therefore, despite the potentially higher denitrification kinetics fostered by ethanol, dosing it into the post-denitrification zone should be avoided in order to eliminate the potential of N_2O emissions.

7.3 Future directions - integrating ecology into wastewater process engineering

One of the long outstanding questions in denitrification ecology relates to the structure-function link of the different communities within an overall denitrifying population. ^{13}C DNA-SIP based identification and qPCR based quantification techniques provided new insights into the "active" fraction of the denitrifying communities that involve in methanol, ethanol and glycerol metabolism. Only a small portion of bacteria could quickly assimilate these electron donors, leaving the others to grow on their metabolic intermediates or products. It is noteworthy that the distribution, abundance and function of the identified carbon assimilating populations can be integrated into both conceptual and quantitative models of wastewater treatment processes. For example, the carbon-specific stoichiometric and kinetic parameters can be incorporated into the design and assimilation software, such as Biowin^{TM} (EnviroSim Associates, Ltd., Flamborough, Ontario, Canada) to model denitrification processes using different carbon sources.

For plants with limiting methylotrophic growth and associated denitrification rates during low temperature operation, alternate carbon sources, such as biodiesel that could potentially induce higher denitrification kinetics at low temperature, can be added to replace a portion of methanol. As a result of adding the mixture of methanol and glycerol (in biodiesel waste), methylotrophic bacteria could be sustained in the system which can thus quickly adapt to the switch back to methanol when temperature increases.

By doing so, the biological denitrification system will become more efficient, stable and flexible to various carbon sources. In addition, the biomarkers developed in this study can be applied to predict the carbon-specific denitrification kinetics using the mixture of methanol and biodiesel waste during operation with different carbon sources. However, the ADH gene primers might need to be redesigned according to the composition of the communities existed in the real systems. The next step is to develop biomarkers to indicate denitrification kinetics in treatment facilities using even additional carbon sources (not only alcohols).

In the current version of Biowin 3.1, the growth of methylotrophs is limited to the anoxic zone, where methanol is supplemented. However, if methanol dosage is in excess, or the denitrification process is operated at sub-optimal conditions in the anoxic zone, methylotrophs may use the leftover methanol to grow in the aerobic zone. Except aerobic growth, some denitrifying bacteria can also perform denitrification in the presence of oxygen, such as ethanol utilizing bacteria as indicated by this study, resulting in increased emissions of NO and N_2O. Therefore, it is suggested that: 1) the dosing of these carbon sources to the anoxic zones needs to be strictly controlled to avoid potential emissions of nitrogenous gases in the downstream aerobic zone; 2) the aerobic growth and denitrification process of certain carbon fostered populations need to be considered in the Biowin^{TM} modeling.

Wastewater denitrification processes have been largely modeled as a black box in activated sludge. However, as shown in this study, the knowledge of denitrifying microorganisms could greatly help us to predict reactor performance, solve specific design or practical problems, or to implement novel treatment techniques. This study was

one of the first that systematically explored the link between denitrifying microbial community structure and function using molecular analysis at DNA, mRNA and protein levels. The high-resolution and community-wide molecular techniques provided wealthy information on the composition and activities of denitrifying communities. Combining this information with the principles and tools employed by microbial ecologists can provide wastewater engineers with added flexibility to fulfill their objectives in activated sludge process design, operation and control.

REFERENCES

[1] Knowles, R., Denitrification. *Microbiol Rev* 1982, *46*, 43-70.

[2] Zumft, W., Cell biology and molecular basis of denitrification. *Microbiol Mol Biol Rev* 1997, *61*, 533-616.

[3] IPCC, Intergovernmental Panel on Climate Change (IPCC). Special Report on Emissions Scenarios. *Cambridge University Press* 2000.

[4] Ward, B. B., Arp, D. J., Klotz, M. G., *Nitrification*, ASM Press, Washington, DC 2011.

[5] Gerardi, M. H., *Wastewater Bacteria*, Wiley-Interscience, Hoboken, New Jersey 2006.

[6] Purkhold, U., Pommerening-Roser, A., Juretschko, S., Schmid, M. C., *et al.*, Phylogeny of all recognized species of ammonia oxidizers based on comparative 16S rRNA and *amoA* sequence analysis: implications for molecular diversity surveys. *Appl Environ Microbiol* 2000, *66*, 5368-5382.

[7] Moreno-Vivián, C., Cabello, P., Martínez-Luque, M., Blasco, R., Castillo, F., Prokaryotic nitrate reduction: molecular properties and functional distinction among bacterial nitrate reductases. *J Bacteriol* 1999, *181*, 6573-6584.

[8] Hochstein, L. I., Tomlinson, G. A., The enzymes associated with denitrification. *Annu Rev Microbiol* 1988, *42*, 231-261.

[9] Bertero, M. G., Rothery, R. A., Boroumand, N., Palak, M., *et al.*, Structural and biochemical characterization of a quinol binding site of *Escherichia coli* nitrate reductase A. *J Biol Chem* 2005, *280*, 14836-14843.

[10] Coyne, M. S., Arunakumari, A., Averill, B. A., Tiedje, J. M., Immunological identification and distribution of dissimilatory heme cd1 and nonheme copper nitrite reductases in denitrifying bacteria. *Appl Environ Microbiol* 1989, *55*, 2924-2931.

[11] Yoshida, M., Ishii, S., Otsuka, S., Senoo, K., *nirK*-harboring denitrifiers are more responsive to denitrification- inducing conditions in rice paddy soil than *nirS*-harboring bacteria. *Microbes Environ* 2010, *25*, 45-48.

[12] Kukimoto, M., Nishiyama, M., Tanokura, M., Horinouchi, S., Gene organization for nitric oxide reduction in *Alcaligenes faecalis* S-6. *Biosci Biotechnol Biochem* 2000, *64*, 852-857.

[13] Sakurai, N., Sakurai, T., Genomic DNA cloning of the region encoding nitric oxide reductase in *Paracoccus halodenitrificans* and a structure model relevant to cytochrome oxidase. *Biochem Biophys Res Commun* 1998, *243*, 400-406.

[14] Cramm, R., Siddiqui, R. A., Friedrich, B., Two isofunctional nitric oxide reductases in *Alcaligenes eutrophus* H16. *J Bacteriol* 1997, *179*, 6769-6777.

[15] Rheinheimer, G., *Aquatic Microbiology*, John Wiley and Sons, New York, NY 1985.

[16] Robertson, L. A., Kuenen, J. G., in: Fry, J. C., Gadd, G. M., Herbert, R. A., Jones, C. W., Watson-Craik, I. A. (Eds.), *Microbial control of pollution* 1992, pp. 227-267.

[17] Sorensen, J., Capacity for denitrification and reduction of nitrate to ammonia in a coastal marine sediment. *Appl Environ Microbiol* 1978, *35*, 301-305.

[18] Keeney, D. R., Chen, R. L., Graetz, D. A., Importance of denitrification and nitrate reduction in sediments to the nitrogen budgets of lakes. *Nature* 1971, *233*, 66-67.

[19] Smith, V. H., Tilman, G. D., Nekola, J. C., Eutrophication: impacts of excess nutrient inputs on freshwater, marine, and terrestrial ecosystems. *Environ Pollut* 1999, *100*, 179-196.

[20] Kuba, T., van Loosdrecht, M. C. M., Heijnen, J. J., Phosphorus and nitrogen removal with minimal COD requirement by integration of denitrifying dephosphatation and nitrification in a two-sludge system. *Wat Res* 1996, *30*, 1702-1710.

[21] Metcalf and Eddy, *Wastewater Engineering: Treatment, Disposal, Reuse*, McGraw-Hill Book Company, New York, NY 1979.

[22] Grady, C. P. L., Daigger, G. T., Lim, H. C., *Biological Wastewater Treatment*, Marcel Dekker, New York 1999.

[23] US-EPA, *Nitrogen Control Manual, EPA-625/R-93-010*, Office of Research and Development, U.S. Environmental Protection Agency, Washington D.C. 1993.

[24] Lee, N. M., Welander, T., The effect of different carbon sources on respiratory denitrification in biological wastewater treatment. *J Ferment Bioeng* 1996, *82*, 277-285.

[25] Flick, E. W., *Industrial Solvents Handbook*, Data Corp, Park Ridge, NJ 1998.

[26] Rittmann, B. E., McCarty, P. L., *Environmental Biotechnology: Principles and Applications*, Mc-Graw Hill, New York 2001.

[27] Sobieszuk, P., Szewczyk, K. W., Estimation of (C/N) ratio for microbial denitrification. *Environ Technol* 2006, *27*, 103-108.

[28] Li, Y. M., Li, J., Zheng, G. H., Luan, J. F., *et al.*, Effects of the COD/NO_3-N ratio and pH on the accumulation of denitrification intermediates with available pyridine as a sole electron donor and carbon source. *Environ Technol* 2008, *29*, 1297-1306.

[29] Chiu, Y. C., Chung, M. S., Determination of optimal COD/nitrate ratio for biological denitrification. *Int Biodeterioration Biodegrad* 2003, *51*, 43-49.

[30] Monod, J., The growth of bacterial cultures. *Annu Rev Microbiol* 1949, *3*, 371-394.

[31] Gaudy, A. F. J., Gaudy, E. T., *Microbiology for Environmental Scientists and Engineers*, McGraw Hill, New York, NY 1980.

[32] Stensel, H. D., Loehr, R. C., Lawrence, A. W., Biological kinetics of suspended-growth denitrification. *Journal (Water Pollution Control Federation)* 1973, *45*, 249-261.

[33] Wild, D., von Schulthess, R., Gujer, W., Structured modelling of denitrification intermediates. *Wat Sci Tech* 1995, *31*, 45-54.

[34] Marazioti, C., Kornaros, M., Lyberatos, G., Kinetic modeling of a mixed culture of *Pseudomonas denitrificans* and *Bacillus subtilis* under aerobic and anoxic operating conditions. *Wat Res* 2003, *37*, 1239-1251.

[35] Dawson, R. N., Murphy, K. L., The temperature dependency of biological denitrification. *Wat Res* 1972, *6*, 71-83.

[36] Christensen, M. H., Harremoes, P., Biological denitrification of sewage: A literature review. *Progr Water Tech* 1977, *8*, 509-555.

[37] Berks, B. C., Baratta, D., Richardson, D. J., Ferguson, S. J., Purification and characterization of a nitrous oxide reductase from *Thiosphaera pantotropha*. *Eur J Biochem* 1993, *212*, 467-476.

[38] Oh, J., Silverstein, J., Oxygen inhibition of activated sludge denitrification. *Water Research* 1999, *33*, 1925-1937.

[39] Betlach, M. R., Tiedje, J. M., Kinetic explanation for accumulation of nitrite, nitric oxide, and nitrous oxide during bacterial denitrification. *Appl Environ Microbiol* 1981, *42*, 1074-1084.

[40] Hernandez, D., Rowe, J. J., Oxygen inhibition of nitrate uptake is a general regulatory mechanism in nitrate respiration. *J Biol Chem* 1988, *263*, 7937-7939.

[41] Korner, H., Zumft, W. G., Expression of denitrification enzymes in response to the dissolved oxygen level and respiratory substrate in continuous culture of *Pseudomonas stutzeri*. *Appl Environ Microbiol* 1989, *55*, 1670-1676.

[42] Thorndycroft, F. H., Butland, G., Richardson, D. J., Watmough, N. J., A new assay for nitric oxide reductase reveals two conserved glutamate residues form the entrance to a proton-conducting channel in the bacterial enzyme. *Biochem J* 2007, *401*, 111-119.

[43] Kornaros, M., Lyberatos, G., Kinetic modelling of *Pseudomonas denitrificans* growth and denitrification under aerobic, anoxic and transient operating conditions. *Wat Res* 1998, *32*, 1912-1922.

[44] Almeida, J. S., Julio, S. M., Reis, M. A., Carrondo, M. J., Nitrite inhibition of denitrification by *Pseudomonas fluorescens*. *Biotechnol Bioeng* 1995, *46*, 194-201.

[45] Glass, C., Silverstein, J., Oh, J., Inhibition of denitrification in activated sludge by nitrite. *Wat Env Res* 1997, *69*, 1086-1093.

[46] Neubauer, H., Gotz, F., Physiology and interaction of nitrate and nitrite reduction in *Staphylococcus carnosus*. *J Bacteriol* 1996, *178*, 2005-2009.

[47] Baumann, B., van der Meer, J. R., Snozzi, M., Zehnder, A. J. B., Inhibition of denitrification activity but not of mRNA induction in *Paracoccus denitrificans* by nitrite at a suboptimal pH. *Antonie van Leeuwenhoek* 1997, *72*, 183-189.

[48] Abeling, U., Seyfried, C., Anaerobic-aerobic treatment of high-strength ammonium wastewater--nitrogen removal via nitrite. *Wat Sci Tech* 1992, *26*, 1007-1015.

[49] Frunzke, K., Zumft, W. G., Inhibition of nitrous-oxide respiration by nitric oxide in the denitrifying bacterium *Pseudomonas perfectomarina*. *BBA-Bioenergetics* 1986, *852*, 119-125.

[50] Carr, G. J., Ferguson, S. J., Nitric oxide formed by nitrite reductase of *Paracoccus denitrificans* is sufficiently stable to inhibit cytochrome oxidase activity and is reduced by its reductase under aerobic conditions. *Biochim Biophys Acta* 1990, *1017*, 57-62.

[51] Kucera, I., The release of nitric oxide from denitrifying cells of *Paracoccus denitrificans* by an uncoupler is the basis for a new oscillator. *FEBS Letters* 1989, *249*, 56-58.

[52] Zumft, W. G., The biological role of nitric oxide in bacteria. *Arch Microbiol* 1993, *160*, 253-264.

[53] Onnis-Hayden, A., Gu, A. Z., *81st Annual Water Environment Federation Technical Exposition and Conference*, Water Environment Federation: Alexandria, Virginia, Chicago, Illinois 2008.

[54] White, D., *The Physiology and Biochemistry of Prokaryotes*, Oxford University Press, New York 1995.

[55] McCarty, P. L., Thermodynamic electron equivalents model for bacterial yield prediction: Modifications and comparative evaluations. *Biotechnol Bioeng* 2007, *97*, 377-388.

[56] Minkevich, I. G., Estimation of available efficiency of microbial growth on methanol and ethanol. *Biotechnol Bioeng* 1985, *27*, 792-799.

[57] Foglar, L., Briški, F., Wastewater denitrification process-the influence of methanol and kinetic analysis. *Process Biochem* 2003, *00*, 1-9.

[58] Akunna, J. C., Bizeau, C., Moletta, R., Nitrate and nitrite reductions with anaerobic sludge using various carbon sources: glucose, glycerol, acetic acid, lactic acid and methanol. *Water res* 1993, *27*, 1303-1312.

[59] Christensson, M., Lie, E., Welander, T., A comparison between ethanol and methanol as carbon sources for denitrification. *Wat Sci Tech* 1994, *30*, 83-90.

[60] Mokhayeri, Y., Nichols, A., Murthy, S., Riffat, R., *et al.*, Examining the influence of substrates and temperature on maximum specific growth rate of denitrifiers. *Water Sci Technol* 2006, *54*, 155-162.

[61] Peng, Y.-z., Ma, Y., Wang, S.-y., Denitrification potential enhancement by addition of external carbon sources in a pre-denitrification process. *J Environ Sci* 2007, *19*, 284-289.

[62] McCarty, P. L., Beck, L., Amant, P. S., *24th Industrial Waste Conference (Engineering Extension Series)*, 24th Industrial Waste Conference (Engineering Extension Series), Purdue University 1969, pp. 1271-1285.

[63] Kujawa, K., Klapwijk, B., A method to estimate denitrification potential for predenitrification systems using NUR batch test. *Wat Res* 1999, *33*, 2291-2300.

[64] Muller, A., Wentzel, M. C., Loewenthal, R. E., Ekama, G. A., Heterotroph anoxic yield in anoxic aerobic activated sludge systems treating municipal wastewater. *Wat Res* 2003, *37*, 2435-2441.

[65] Ramalingam, K., Fillos, J., Deur, A., Beckmann, K., *2nd External Carbon Source WERF Workshop*, Washington, D.C. 2007.

[66] Sperl, G. T., Hoare, D. S., Denitrification with methanol: a selective enrichment for *Hyphomicrobium* species. *J Bacteriol* 1971, *108*, 733-736.

[67] Nurse, G. R., Denitrification with methanol: microbiology and biochemistry. *Wat Res* 1980, *14*, 531-537.

[68] Labbe, N., Laurin, V., Juteau, P., Microbiological community structure of the biofilm of a methanol-fed, marine denitrification system, and identification of the methanol-utilizing microorganisms. *Microb Ecol* 2007, *53*, 621-630.

[69] Anthony, C., How half a century of research was required to understand bacterial growth on C1 and C2 compounds; the story of the serine cycle and the ethylmalonyl-CoA pathway. *Sci Prog* 2011, *94*, 109-137.

[70] Ginige, M. P., Hugenholtz, P., Daims, H., Wagner, M., *et al.*, Use of stable-isotope probing, full-cycle rRNA analysis, and fluorescence *in situ* hybridization-microautoradiography to study a methanol-fed denitrifying microbial community. *Appl Environ Microbiol* 2004, *70*, 588-596.

[71] de Vries, G. E., Kües, U., Stahl, U., Physiology and genetics of methylotrophic bacteria. *FEMS Microbiol Lett* 1990, *75*, 57-101.

[72] O'Keeffe, D. T., Anthony, C., The two cytochromes c in the facultative methylotroph *Pseudomonas* AM1. *J Biochem* 1980, *192*, 411-419.

[73] Chistoserdova, L., Chen, S.-W., Lapidus, A., Lidstrom, M. E., Methylotrophy in *Methylobacterium extorquens* AM1 from a genomic point of view. *J Bacteriol* 2003, *185*, 2980-2987.

[74] Blaszczyk, M., Galka, E., Sakowicz, E., Mycielski, R., Denitrification of high concentrations of nitrites and nitrates in synthetic medium with different sources of organic carbon. III. Methanol. *Acta Microbiol Pol* 1985, *34*, 195-205.

[75] Lemmer, H., Zaglauer, A., Neef, A., Meier, H., Amann, R., Denitrification in a methanol-fed fixed-bed reactor. Part 2: Composition and ecology of the bacterial community in the biofilms. *Water Res* 1997, *31*, 1903-1908.

[76] Baytshtok, V., Kim, S., Yu, R., Park, H., Chandran, K., Molecular and biokinetic characterization of methylotrophic denitrification using nitrate and nitrite as terminal electron acceptors. *Water Sci Technol* 2008, *58*, 359-365.

[77] Baytshtok, V., Lu, H., Park, H., Kim, S., *et al.*, Impact of varying electron donors on the molecular microbial ecology and biokinetics of methylotrophic denitrifying bacteria. *Biotechnol Bioeng* 2009, *102*, 1527-1536.

[78] Hwang, C., Wu, W. M., Gentry, T. J., Carley, J., *et al.*, Changes in bacterial community structure correlate with initial operating conditions of a field-scale denitrifying fluidized bed reactor. *Appl Microbiol Biotechnol* 2006, *71*, 748-760.

[79] Osaka, T., Yoshie, S., Tsuneda, S., Hirata, A., *et al.*, Identification of acetate- or methanol-assimilating bacteria under nitrate-reducing conditions by stable-isotope probing. *Microb Ecol* 2006, *52*, 253-266.

[80] Ginige, M. P., Keller, J., Blackall, L. L., Investigation of an acetate-fed denitrifying microbial community by stable isotope probing, full-cycle rRNA analysis, and

fluorescent *in situ* hybridization-microautoradiography. *Appl Environ Microbiol* 2005, *71*, 8683-8691.

[81] Lu, H., Chandran, K., Diagnosis and quantification of glycerol assimilating denitrifying bacteria in an integrated fixed-film activated sludge reactor via ^{13}C DNA stable-isotope probing. *Environ Sci Technol* 2010, *44*, 8943–8949.

[82] Nakatsu, C. H., Carmosini, N., Baldwin, B., Beasley, F., *et al.*, Soil microbial community responses to additions of organic carbon substrates and heavy metals (Pb and Cr). *Appl Environ Microbiol* 2005, *71*, 7679-7689.

[83] Etchebehere, C., Errazquin, I., Barrandeguy, E., Dabert, P., *et al.*, Evaluation of the denitrifying microbiota of anoxic reactors. *FEMS Microbiol Ecol* 2001, *35*, 259-265.

[84] Nyberg, U., Aspegren, H., Andersson, B., Jansen, J. l. C., Villadsen, I. S., Full-scale application of nitrogen removal with methanol as carbon source. *Wat Sci Tech* 1992, *26*, 1077-1086.

[85] Isaacs, S. H., Henze, M., Søeberg, H., Kümmel, M., External carbon source addition as a means to control an activated sludge nutrient removal process. *Wat Res* 1994, *28*, 511-520.

[86] Hallin, S., Pell, M., Metabolic properties of denitrifying bacteria adapting to methanol and ethanol in activated sludge *Wat Res* 1998, *32*, 13-18.

[87] Hallin, S., Rothman, M., Pell, M., Adaptation of denitrifying bacteria to acetate and methanol in activated sludge. *Wat Res* 1996, *30*, 1445-1450.

[88] Amann, R. I., Binder, B. J., Olson, R. J., Chisholm, S. W., *et al.*, Combination of 16S rRNA-targeted oligonucleotide probes with flow cytometry for analyzing mixed microbial populations. *Appl Environ Microbiol* 1990, *56*, 1919-1925.

[89] Smith, C. J., Nedwell, D. B., Dong, L. F., Osborn, A. M., Diversity and abundance of nitrate reductase genes (NarG and NapA), nitrite reductase genes (NirS and NrfA), and their transcripts in estuarine sediments. *Appl Environ Microbiol* 2007, *73*, 3612-3622.

[90] Braker, G., Ayala-del-Rio, H. L., Devol, A. H., Fesefeldt, A., Tiedje, J. M., Community structure of denitrifiers, bacteria, and archaea along redox gradients in pacific northwest marine sediments by terminal restriction fragment length polymorphism analysis of amplified nitrite reductase (*nirS*) and 16S rRNA genes. *Appl Environ Microbiol* 2001, *67*, 1893-1901.

[91] Rich, J. J., Heichen, R. S., Bottomley, P. J., Cromack, K., Jr., Myrold, D. D., Community composition and runctioning of denitrifying bacteria from adjacent meadow and forest soils. *Appl Environ Microbiol* 2003, *69*, 5974-5982.

[92] Radajewski, S., Ineson, P., Parekh, N. R., Murrell, J. C., Stable-isotope probing as a tool in microbial ecology. *Nature* 2000, *403*, 646-649.

[93] Liu, W.-T., Jansson, J. K., *Environmental Molecular Microbiology*, Caister Academic Press, Norfolk, UK 2010.

[94] Becker, S., Boger, P., Oehlmann, R., Ernst, A., PCR bias in ecological analysis: a case study for quantitative Taq nuclease assays in analyses of microbial communities. *Appl Environ Microbiol* 2000, *66*, 4945-4953.

[95] Taroncher-Oldenburg, G., Griner, E. M., Francis, C. A., Ward, B. B., Oligonucleotide microarray for the study of functional gene diversity in the nitrogen cycle in the environment. *Appl Environ Microbiol* 2003, *69*, 1159-1171.

[96] Cho, J.-C., Tiedje, J. M., Quantitative detection of microbial genes by using DNA microarrays. *Appl Environ Microbiol* 2002, *68*, 1425-1430.

[97] Philippot, L., Hallin, S., Finding the missing link between diversity and activity using denitrifying bacteria as a model functional community. *Curr Opin Microbiol* 2005, *8*, 234-239.

[98] Petrosino, J. F., Highlander, S., Luna, R. A., Gibbs, R. A., Versalovic, J., Metagenomic pyrosequencing and microbial identification. *Clin Chem* 2009, *55*, 856-866.

[99] Liu, Z., Lozupone, C., Hamady, M., Bushman, F. D., Knight, R., Short pyrosequencing reads suffice for accurate microbial community analysis. *Nucleic Acids Res* 2007, *35*, e120.

[100] Wang, Z., Gerstein, M., Snyder, M., RNA-Seq: a revolutionary tool for transcriptomics. *Nat Rev Genet* 2009, *10*, 57-63.

[101] Wilmes, P., Wexler, M., Bond, P. L., Metaproteomics provides functional insight into activated sludge wastewater treatment. *PLoS ONE* 2008, *3*, e1778.

[102] Park, C., Helm, R. F., Application of metaproteomic analysis for studying extracellular polymeric substances (EPS) in activated sludge flocs and their fate in sludge digestion. *Water Sci Technol* 2008, *57*, 2009-2015.

[103] Mulder, A., Graaf, A. A., Robertson, L. A., Kuenen, J. G., Anaerobic ammonium oxidation discovered in a denitrifying fluidized bed reactor. *FEMS Microbiol Ecol* 1995, *16*, 177-184.

[104] Third, K. A., Sliekers, A. O., Kuenen, J. G., Jetten, M. S., The CANON system (Completely Autotrophic Nitrogen-removal Over Nitrite) under ammonium limitation: interaction and competition between three groups of bacteria. *Syst Appl Microbiol* 2001, *24*, 588-596.

[105] Kuai, L., Verstraete, W., Ammonium removal by the oxygen-limited autotrophic nitrification-denitrification system. *Appl Environ Microbiol* 1998, *64*, 4500-4506.

[106] Siezen, R. J. a. G., Marco, Genomics of biological wastewater treatment. *Microb Biotechnol* 2008, *1*, 333-340.

[107] Strous, M., Pelletier, E., Mangenot, S., Rattei, T., *et al.*, Deciphering the evolution and metabolism of an anammox bacterium from a community genome. *Nature* 2006, *440*, 790-794.

[108] Louzeiro, N. R., Mavinic, D. S., Oldham, W. K., Meisen, A., Gardner, I. S., Process Control and Design Considerations for Methanol-Induced Denitrification in a Sequencing Batch Reactor. *Environ Technol* 2003, *24*, 161-169.

[109] dos Santos, S. G., Amâncio Varesche, M. B., Zaiat, M., Foresti, E., Comparison of methanol, ethanol, and methane as electron donors for denitrification. *Environ Eng Sci* 2004, *21*, 313-320.

[110] Gauntlett, R. B., Denitrification kinetics in a fluidised bed using methanol as the carbon source. *Biotechnol Lett* 1979, *1*, 391-396.

[111] Her, J.-J., Huang, J.-S., Denitrifying kinetics involving the distributed ratio of reductases. *J Chem Technol Biot* 1995, *62*, 261-267.

[112] Janning, K. F., Harremoës, P., Nielsen, M., Evaluating and modelling the kinetics in a full scale submerged denitrification filter. *Water Sci Technol* 1995, *32*, 115-123.

[113] Louzeiro, N. R., Mavinic, D. S., Oldham, W. K., Meisen, A., Gardner, I. S., Methanol-induced biological nutrient removal kinetics in a full-scale sequencing batch reactor. *Wat Res* 2002, *36*, 2721-2732.

[114] Mulcahy, L. T., Shieh, W. K., LaMotta, E. J., Experimental determination of intrinsic denitrification kinetic constants. *Biotechnol Bioeng* 1981, *23*, 2403-2406.

[115] Purtschert, I., Gujer, W., Population dynamics by methanol addition in denitrifying wastewater treatment plants. *Wat Sci Tech* 1999, *39*, 43-50.

[116] Osaka, T., Ebie, Y., Tsuneda, S., Inamori, Y., Identification of the bacterial community involved in methane-dependent denitrification in activated sludge using DNA stable-isotope probing. *FEMS Microbiol Ecol* 2008, *64*, 494-506.

[117] Anthony, C., *The Biochemistry of Methylotrophs*, Academic Press, New York 1982.

[118] Neufeld, J. D., Vohra, J., Dumont, M. G., Lueders, T., *et al.*, DNA stable-isotope probing. *Nat Protocols* 2007, *2*, 860-866.

[119] Suzuki, M. T., Taylor, L. T., DeLong, E. F., Quantitative analysis of small-subunit rRNA genes in mixed microbial populations via 5'-nuclease assays. *Appl Environ Microbiol* 2000, *66*, 4605-4614.

[120] Ahn, J. H., Yu, R., Chandran, K., Distinctive microbial ecology and biokinetics of autotrophic ammonia and nitrite oxidation in a partial nitrification bioreactor. *Biotechnol Bioeng* 2008, *100*, 1078-1087.

[121] Kane, M. D., Poulsen, L. K., Stahl, D. A., Monitoring the enrichment and isolation of sulfate-reducing bacteria by using oligonucleotide hybridization probes designed from environmentally derived 16S rRNA sequences. *Appl Environ Microbiol* 1993, *59*, 682-686.

[122] Weisburg, W. G., Barns, S. M., Pelletier, D. A., Lane, D. J., 16S ribosomal DNA amplification for phylogenetic study. *J Bacteriol* 1991, *173*, 697-703.

[123] Vuilleumier, S., Chistoserdova, L., Lee, M.-C., Bringel, F., *et al.*, *Methylobacterium* genome sequences: A reference blueprint to investigate microbial metabolism of C1 compounds from natural and industrial sources. *PLoS ONE* 2009, *4*, e5584.

[124] Saitou, N., Nei, M., The neighbor-joining method: a new method for reconstructing phylogenetic trees. *Mol. Biol. Evol.* 1987, *4*, 406-425.

[125] Eaton, A., Clesceri, L., Greenberg, A., Standard Methods for the Examination of Water and Wastewater. 21st Ed. Washington, DC: APHA, AWWA and WEF. 2005.

[126] Chandran, K., Smets, B. F., Single-step nitrification models erroneously describe batch ammonia oxidation profiles when nitrite oxidation becomes rate limiting. *Biotechnol Bioeng* 2000, *68*, 396-406.

[127] Attwood, M., Harder, W., A rapid and specific enrichment procedure for *Hyphomicrobium spp*. *Antonie van Leeuwenhoek* 1972, *38*, 369-377.

[128] Harder, W., Attwood, M. M., Biology, physiology and biochemistry of *Hyphomicrobia*. *Adv Microb Physiol* 1978, *17*, 303-359.

[129] Timmermans, P., Van Haute, A., Denitrification with methanol: Fundamental study of the growth and denitrification capacity of *Hyphomicrobium* sp. *Wat Res* 1983, *17*, 1249-1255.

[130] Gliesche, C. G., Fesefeldt, A., Monitoring the denitrifying *Hyphomicrobium* DNA/DNA hybridization group HG 27 in activated sludge and lake water using MPN cultivation and subsequent screening with the gene probe Hvu-1. *Syst Appl Microbiol* 1998, *21*, 315-320.

[131] Holm, N. C., Gliesche, C. G., Hirsch, P., Diversity and structure of hyphomicrobium populations in a sewage treatment plant and its adjacent receiving lake. *Appl Environ Microbiol* 1996, *62*, 522-528.

[132] Kloos, K., Fesefeldt, A., Gliesche, C. G., Bothe, H., DNA-probing indicates the occurrence of denitrification and nitrogen fixation genes in *Hyphomicrobium*. Distribution of denitrifying and nitrogen fixing isolates of *Hyphomicrobium* in a sewage treatment plant. *FEMS Microbiol Ecol* 1995, *18*, 205-213.

[133] Neef, A., Zaglauer, A., Meier, H., Amann, R., *et al.*, Population analysis in a denitrifying sand filter: conventional and in situ identification of *Paracoccus* spp. in methanol-fed biofilms. *Appl Environ Microbiol* 1996, *62*, 4329-4339.

[134] Mokhayeri, Y., Riffat, R., Takacs, I., Dold, P., *et al.*, Characterizing denitrification kinetics at cold temperature using various carbon sources in lab-scale sequencing batch reactors. *Water Sci Technol* 2008, *58*, 233-238.

[135] McDonald, I., Doronina, N., Trotsenko, Y., McAnulla, C., Murrell, J., *Hyphomicrobium chloromethanicum* sp. nov. and *Methylobacterium chloromethanicum* sp. nov., chloromethane-utilizing bacteria isolated from a polluted environment. *Int J Syst Evol Microbiol* 2001, *51*, 119-122.

[136] Kalyuzhnaya, M. G., De Marco, P., Bowerman, S., Pacheco, C. C., *et al.*, *Methyloversatilis universalis* gen. nov., sp. nov., a novel taxon within the Betaproteobacteria represented by three methylotrophic isolates. *Int J Syst Evol Microbiol* 2006, *56*, 2517-2522.

[137] Hallin, S., Throback, I. N., Dicksved, J., Pell, M., Metabolic profiles and genetic diversity of denitrifying communities in activated sludge after addition of methanol or ethanol. *Appl Environ Microbiol* 2006, *72*, 5445-5452.

[138] Cheneby, D., Hallet, S., Mondon, M., Martin-Laurent, F., *et al.*, Genetic characterization of the nitrate reducing community based on *narG* nucleotide sequence analysis. *Microb Ecol* 2003, *46*, 113-121.

[139] Flanagan, D. A., Gregory, L. G., Carter, J. P., Karakas-Sen, A., *et al.*, Detection of genes for periplasmic nitrate reductase in nitrate respiring bacteria and in community DNA. *FEMS Microbiol Lett* 1999, *177*, 263-270.

[140] Gregory, L. G., Karakas-Sen, A., Richardson, D. J., Spiro, S., Detection of genes for membrane-bound nitrate reductase in nitrate-respiring bacteria and in community DNA. *FEMS Microbiol Lett* 2000, *183*, 275-279.

[141] Braker, G., Fesefeldt, A., Witzel, K.-P., Development of PCR primer systems for amplification of nitrite reductase genes (*nirK* and *nirS*) to detect denitrifying bacteria in environmental samples. *Appl Environ Microbiol* 1998, *64*, 3769-3775.

[142] Hallin, S., Lindgren, P.-E., PCR detection of genes encoding nitrite reductase in denitrifying bacteria. *Appl Environ Microbiol* 1999, *65*, 1652-1657.

[143] Liu, X., Tiquia, S. M., Holguin, G., Wu, L., *et al.*, Molecular diversity of denitrifying genes in continental margin sediments within the oxygen-deficient zone off the Pacific coast of Mexico. *Appl Environ Microbiol* 2003, *69*, 3549-3560.

[144] Nogales, B., Timmis, K. N., Nedwell, D. B., Osborn, A. M., Detection and diversity of expressed denitrification genes in estuarine sediments after reverse transcription-PCR amplification from mRNA. *Appl Environ Microbiol* 2002, *68*, 5017-5025.

[145] Prieme, A., Braker, G., Tiedje, J. M., Diversity of nitrite reductase (*nirK* and *nirS*) gene fragments in forested upland and wetland soils. *Appl Environ Microbiol* 2002, *68*, 1893-1900.

[146] Song, B., Ward, B. B., Nitrite reductase genes in halobenzoate degrading denitrifying bacteria. *FEMS Microbiol Ecol* 2003, *43*, 349-357.

[147] Yoshie, S., Noda, N., Tsuneda, S., Hirata, A., Inamori, Y., Salinity decreases nitrite reductase gene diversity in denitrifying bacteria of wastewater treatment systems. *Appl Environ Microbiol* 2004, *70*, 3152-3157.

[148] Braker, G., Tiedje, J. M., Nitric oxide reductase (*norB*) genes from pure cultures and environmental samples. *Appl Environ Microbiol* 2003, *69*, 3476-3483.

[149] Scala, D. J., Kerkhof, L. J., Nitrous oxide reductase (*nosZ*) gene-specific PCR primers for detection of denitrifiers and three *nosZ* genes from marine sediments. *FEMS Microbiol Lett* 1998, *162*, 61-68.

[150] Scala, D. J., Kerkhof, L. J., Diversity of nitrous oxide reductase (*nosZ*) genes in continental shelf sediments. *Appl Environ Microbiol* 1999, *65*, 1681-1687.

[151] Lee, N., Nielsen, P. H., Andreasen, K. H., Juretschko, S., *et al.*, Combination of fluorescent *in situ* hybridization and microautoradiography-a new tool for structure-function analyses in microbial ecology. *Appl Environ Microbiol* 1999, *65*, 1289-1297.

[152] Nielsen, J. L., Nielsen, P. H., Advances in microscopy: microautoradiography of single cells. *Methods Enzymol* 2005, *397*, 237-256.

[153] Radajewski, S., Webster, G., Reay, D. S., Morris, S. A., *et al.*, Identification of active methylotroph populations in an acidic forest soil by stable-isotope probing. *Microbiology* 2002, *148*, 2331-2342.

[154] Singleton, D. R., Hunt, M., Powell, S. N., Frontera-Suau, R., Aitken, M. D., Stable-isotope probing with multiple growth substrates to determine substrate specificity of uncultivated bacteria. *J Microbiol Methods* 2007, *69*, 180-187.

[155] Singleton, D. R., Powell, S. N., Sangaiah, R., Gold, A., *et al.*, Stable isotope probing of bacteria capable of degrading salicylate, naphthalene, or phenanthrene in a bioreactor treating contaminated soil. *Appl Environ Microbiol* 2005, *71*, 1202-1209.

[156] Manefield, M., Whiteley, A. S., Griffiths, R. I., Bailey, M. J., RNA stable isotope probing, a novel means of linking microbial community function to phylogeny. *Appl Environ Microbiol* 2002, *68*, 5367-5373.

[157] Kalyuzhnaya, M. G., Lidstrom, M. E., Chistoserdova, L., Utility of environmental pimers trgeting acient ezymes: Methylotroph detection in Lake Washington. *Microb Ecol* 2004, *48*, 463-472.

[158] Nercessian, O., Noyes, E., Kalyuzhnaya, M. G., Lidstrom, M. E., Chistoserdova, L., Bacterial populations active in metabolism of C1 compounds in the sediment of Lake Washington, a freshwater lake. *Appl Environ Microbiol* 2005, *71*, 6885-6899.

[159] McDonald, I., Murrell, J., The methanol dehydrogenase structural gene *mxaF* and its use as a functional gene probe for methanotrophs and methylotrophs. *Appl Environ Microbiol* 1997, *63*, 3218-3224.

[160] Kalyuzhnaya, M. G., Hristova, K. R., Lidstrom, M. E., Chistoserdova, L., Characterization of a novel methanol dehydrogenase in representatives of burkholderiales: Implications for environmental detection of methylotrophy and evidence for convergent evolution. *J Bacteriol* 2008, *190*, 3817-3823.

[161] Pianka, E., On r and K selection. *Amer Nat* 1970, *104*, 592-597.

[162] Ravishankara, A. R., Daniel, J. S., Portmann, R. W., Nitrous oxide (N_2O): the dominant ozone-depleting substance emitted in the 21st century. *Science* 2009, *326*, 123-125.

[163] Seinfeld, J. H., Pandis, S. N., *Atmospheric Chemistry and Physics: From Air Pollution to Climate Change*, Wiley, New York 1998.

[164] Tallec, G., Garnier, J., Billen, G., Gousailles, M., Nitrous oxide emissions from denitrifying activated sludge of urban wastewater treatment plants, under anoxia and low oxygenation. *Bioresource Technol* 2008, *99*, 2200-2209.

[165] Thn, M., Sensson, F., Variation of nitrous oxide formation in the denitrification basin in a wastewater treatment plant with nitrogen removal. *Wat Res* 1996, *30*, 1543-1547.

[166] Ahn, J. H., Kim, S., Katehis, D., Pagilla, K., Chandran, K., Spatial and temporal variability in N_2O generation and emission from wastewater treatment plants. *Proceedings of the 2nd Water Environment Federation Nutrient Management Conference, Washington, D.C., 2009* 2009.

[167] Kampschreur, M. J., van der Star, W. R., Wielders, H. A., Mulder, J. W., *et al.*, Dynamics of nitric oxide and nitrous oxide emission during full-scale reject water treatment. *Wat Res* 2008, *42*, 812-826.

[168] Lidstrom, M. E., Genetics of carbon metabolism in methylotrophic bacteria. *FEMS Microbiol Lett* 1990, *87*, 431-436.

[169] Focht, D. D., The effect of temperature, pH and aeration on the production of nitrous oxide and gaseous nitrogen: A zero-order kinetic model. *Soil Sci* 1974, *118*, 173-179.

[170] Hanaki, K., Production of nitrous oxide gas during denitrification of wastewater. *Water Sci Technol* 1992, *26*, 1027-1036.

[171] Chung, Y.-C., Chung, M.-S., BNP test to evaluate the influence of C/N ratio on N_2O production in biological denitrification. *Water Sci Technol* 2000, *42*, 23-27.

[172] Park, K. Y., Inamori, Y., Mizuochi, M., Ahn, K. H., Emission and control of nitrous oxide from a biological wastewater treatment system with intermittent aeration. *J Biosci Bioeng* 2000, *90*, 247-252.

[173] Schulthess, R. v., Kuhni, M., Gujer, W., Release of nitric and nitrous oxides from denitrifying activated sludge. *Water Res* 1995, *29*, 215-226.

[174] Chandran, K., Characterization of Nitrogen Greenhouse Gas Emissions from Wastewater Treatment Operations (U4R07). Field Protocol and Quality Assurance Plan. Water Environment Research Foundation, Alexandria, VA. 2009.

[175] Tallec, G., Garnier, J., Gousailles, M., Nitrogen removal in a wastewater treatment plant through biofilters: nitrous oxide emissions during nitrification and denitrification. *Bioprocess Biosyst Eng* 2006, *29*, 323-333.

[176] Itokawa, H., Hanaki, K., Matsuo, T., Nitrous oxide production in high-loading biological nitrogen removal process under low COD/N ratio condition. *Wat Res* 2001, *35*, 657-664.

[177] Schalk-Otte, S., Seviour, R. J., Kuenen, J. G., Jetten, M. S. M., Nitrous oxide (N_2O) production by *Alcaligenes faecalis* during feast and famine regimes. *Wat Res* 2000, *34*, 2080-2088.

[178] Miller, L. G., Oremland, R. S., Paulsen, S., Measurement of nitrous oxide reductase activity in aquatic sediments. *Appl Environ Microbiol* 1986, *51*, 18-24.

[179] Goretski, J., Zafiriou, O., Hollocher, T., Steady-state nitric oxide concentrations during denitrification. *J Biol Chem* 1990, *265*, 11535-11538.

[180] Hermansson, A., Lindgren, P.-E., Quantification of Ammonia-Oxidizing Bacteria in Arable Soil by Real-Time PCR. *Appl Environ Microbiol* 2001, *67*, 972-976.

[181] Claus, G., Kutzner, H. J., Denitrification of nitrate and nitric acid with methanol as carbon source. *Appl Environ Microbiol* 1985, *22*, 378-381.

[182] Masih, A. M. M., Albinali, K., DeMello, L., Price dynamics of natural gas and the regional methanol markets. *Energ Policy* 2010, *38*, 1372-1378.

[183] da Silva, G. P., Mack, M., Contiero, J., Glycerol: a promising and abundant carbon source for industrial microbiology. *Biotechnol Adv* 2009, *27*, 30-39.

[184] Bill, K. A., Bott, C. B., Murthy, S. N., Evaluation of alternative electron donors for denitrifying moving bed biofilm reactors (MBBRs). *Water Sci Technol* 2009, *60*, 2647-2657.

[185] Bodík, I., Blšťákováa, A., Sedláčeka, S., Hutňana, M., Biodiesel waste as source of organic carbon for municipal WWTP denitrification. *Bioresource Technol* 2009, *100*, 2452-2456.

[186] Hallin, S., Pell, M., Metabolic properties of denitrifying bacteria adapting to methanol and ethanol in activated sludge. *Water Res* 1998, *32*, 13-18.

[187] Sage, M., Daufin, G., Gésan-Guiziou, G., Denitrification potential and rates of complex carbon source from dairy effluents in activated sludge system. *Water Res* 2006, *40*, 2747-2755.

[188] Lu, H., Chandran, K., Factors promoting emissions of nitrous oxide and nitric oxide from denitrifying sequencing batch reactors operated with methanol and ethanol as electron donors. *Biotechnol Bioeng* 2010, *106*, 390-398.

[189] Aspegren, H., Nyberg, U., Andersson, B., Gotthardsson, S., la Cour Jansen, J., Post denitrification in a moving bed biofilm reactor process. *Water Sci Technol* 1998, *38*, 31-38.

[190] Labelle, M. A., Juteau, P., Jolicoeur, M., Villemur, R., *et al.*, Seawater denitrification in a closed mesocosm by a submerged moving bed biofilm reactor. *Water Res* 2005, *39*, 3409-3417.

[191] Ødegaard, H., Rusten, B., Westrum, T., A new moving bed biofilm reactor-applications and results. *Water Sci Technol* 1994, *29*, 157-165.

[192] Satoh, H., Yamakawa, T., Kindaichi, T., Ito, T., Okabe, S., Community structures and activities of nitrifying and denitrifying bacteria in industrial wastewater-treating biofilms. *Biotechnol Bioeng* 2006, *94*, 762-772.

[193] Schwartz, E., Analyzing microorganisms in environmental samples using stable isotope probing with $H_2{}^{18}O$. *Cold Spring Harb Protoc* 2009, *doi:10.1101/pdb.prot5341*.

[194] Lane, D. J., *16S/23S rRNA Sequencing*, Wiley, New York 1991.

[195] Ashelford, K. E., Chuzhanova, N. A., Fry, J. C., Jones, A. J., Weightman, A. J., New screening software shows that most recent large 16S rRNA gene clone libraries contain chimeras. *Appl Environ Microbiol* 2006, *72*, 5734-5741.

[196] Nadkarni, M. A., Martin, F. E., Jacques, N. A., Hunter, N., Determination of bacterial load by real-time PCR using a broad-range (universal) probe and primers set. *Microbiology* 2002, *148*, 257-266.

[197] Grabinska-Loniewska, A., Biocenosis diversity and denitrification efficiency. *Water Res* 1991, *25*, 1575-1582.

[198] Tago, Y., Yokota, A., *Comamonas badia* sp. nov., a floc-forming bacterium isolated from activated sludge. *J Gen Appl Microbiol* 2004, *50*, 243-248.

[199] Tabrez Khan, S., Hiraishi, A., *Diaphorobacter nitroreducens* gen. nov., sp. nov., a poly(3-hydroxybutyrate)-degrading denitrifying bacterium isolated from activated sludge. *J Gen Appl Microbiol* 2002, *48*, 299-308.

[200] Khardenavis, A., Kapley, A., Purohit, H., Simultaneous nitrification and denitrification by diverse *Diaphorobacter* sp. *Appl Microbiol Biotechnol* 2007, *77*, 403-409.

[201] Sawada, H., Kuykendall, L. D., Young, J. M., Changing concepts in the systematics of bacterial nitrogen-fixing legume symbionts. *J Gen Appl Microbiol* 2003, *49*, 155-179.

[202] Maszenan, A. M., Rees, G. N., *Tessaracoccus bendigoensis* gen. nov., sp. nov., a Gram-positive coccus occurring in regular packages or tetrads, isolated from activated sludge biomass. *Int J Syst Bacteriol* 1999, *49*, 459-468.

[203] Allegrucci, M., Sauer, K., Characterization of colony morphology variants isolated from *Streptococcus pneumoniae* biofilms. *J Bacteriol* 2007, *189*, 2030-2038.

[204] Allison, D. G., Gilbert, P., Lappin-Scott, H. M., Wilson, M., *Community Structure and Co-operation in Biofilm*, Cambridge University Press, Cambridge, England 2000.

[205] Kirisits, M. J., Prost, L., Starkey, M., Parsek, M. R., Characterization of colony morphology variants isolated from *Pseudomonas aeruginosa* biofilms. *Appl Environ Microbiol* 2005, *71*, 4809-4821.

[206] Davey, M. E., O'Toole, G. A., Microbial biofilms: from ecology to molecular genetics. *Micarobiol Mol Biol R* 2000, *64*, 847-867.

[207] Stewart, P. S., Franklin, M. J., Physiological heterogeneity in biofilms. *Nat Rev Micro* 2008, *6*, 199-210.

[208] Su, J. J., Kafkewitz, D., Toluene and xylene degradation by a denitrifying strain of *Xanthomonas maltophilia* with limited or no oxygen. *Chemosphere* 1996, *32*, 1843-1850.

[209] Lu, S., Ryu, S. H., Chung, B. S., Chung, Y. R., *et al.*, *Simplicispira limi* sp. nov., isolated from activated sludge. *Int J Syst Evol Microbiol* 2007, *57*, 31-34.

[210] Daniel, R. M., Limmer, A. W., Steele, K. W., Smith, I. M., Anaerobic growth, nitrate reduction and denitrification in 46 *Rhizobium* strains. *J Gen Microbiol* 1982, *128*, 1811-1815.

[211] Biebl, H., Menzel, K., Zeng, A. P., Deckwer, W. D., Microbial production of 1,3-propanediol. *Appl Microbiol and Biotechnol* 1999, *52*, 289-297.

[212] Miyata, A., Yoshida, T., Yamaguchi, K., Yokoyama, C., *et al.*, Molecular cloning and expression of the gene for serine hydroxymethyltransferase from an obligate methylotroph *Hyphomicrobium methylovorum* GM2. *Eur J Biochem* 1993, *212*, 745-750.

[213] Ichiki, H., Tanaka, Y., Mochizuki, K., Yoshimatsu, K., *et al.*, Purification, characterization, and genetic analysis of Cu-containing dissimilatory nitrite reductase from a denitrifying halophilic archaeon, *Haloarcula marismortui*. *J Bacteriol* 2001, *183*, 4149-4156.

[214] Völkl, P., Huber, R., Drobner, E., Rachel, R., *et al.*, *Pyrobaculum aerophilum* sp. nov., a novel nitrate-reducing hyperthermophilic archaeum. *Appl Environ Microbiol* 1993, *59*, 2918-2926.

[215] Hinojosa, J., Riffat, R., Fink, S., Murthy, S., *et al.*, *Water Environment Federation Technical Exhibition and Conference (WEFTEC)*, Water Environment Federation, Alexandria, VA, Chicago, IL 2008, pp. 274-288.

[216] Pérez, J., Picioreanu, C., van Loosdrecht, M. C. M., Modeling biofilm and floc diffusion processes based on analytical solution of reaction-diffusion equations. *Wat Res* 2005, *39*, 1311-1323.

[217] Boe-Hansen, R., Albrechtsen, H.-J., Arvin, E., Jørgensen, C., Bulk water phase and biofilm growth in drinking water at low nutrient conditions. *Water Res* 2002, *36*, 4477-4486.

[218] Chistoserdova, L., Kalyuzhnaya, M. G., Lidstrom, M. E., The expanding world of methylotrophic metabolism. *Annu Rev Microbiol* 2009, *63*, 477-499.

[219] McDonald, I. R., Bodrossy, L., Chen, Y., Murrell, J. C., Molecular ecology techniques for the study of aerobic methanotrophs. *Appl Environ Microbiol* 2008, *74*, 1305-1315.

[220] Austin, D., Larson, T. J., Nucleotide sequence of the *glpD* gene encoding aerobic sn-glycerol 3-phosphate dehydrogenase of *Escherichia coli* K-12. *J Bacteriol* 1991, *173*, 101-107.

[221] Forage, R. G., Lin, E. C., *dha* system mediating aerobic and anaerobic dissimilation of glycerol in *Klebsiella pneumoniae* NCIB 418. *J Bacteriol* 1982, *151*, 591-599.

[222] Tchobanoglous, G., Burton, F. L., Stensel, H. D., *Metcalf and Eddy Wastewater Engineering: Treatment and Reuse*, McGraw Hill, New York, NY 2003.

[223] Marchesi, J. R., Sato, T., Weightman, A. J., Martin, T. A., *et al.*, Design and evaluation of useful bacterium-specific PCR primers that amplify genes coding for bacterial 16S rRNA. *Appl Environ Microbiol* 1998, *64*, 795-799.

[224] Fesefeldt, A., Gliesche, C. G., Identification of *Hyphomicrobium* spp. using PCR-amplified fragments of the mxaF gene as a molecular marker. *Syst Appl Microbiol* 1997, *20*, 387-396.

[225] Daniel, R., Stuertz, K., Gottschalk, G., Biochemical and molecular characterization of the oxidative branch of glycerol utilization by *Citrobacter freundii*. *J Bacteriol* 1995, *177*, 4392-4401.

[226] Garrity, G. M., Brenner, D. J., Krieg, N. R., Staley, J. R., Springer - Verlag 2005, pp. 489-490.

[227] Kalyuzhnaya, M. G., 2010.

[228] Homann, T., Tag, C., Biebl, H., Deckwer, W.-D., Schink, B., Fermentation of glycerol to 1,3-propanediol by *Klebsiella* and *Citrobacter* strains. *Appl Microbiol Biotechnol* 1990, *33*, 121-126.

[229] Huang, H. K., Tseng, S. K., Nitrate reduction by *Citrobacter diversus* under aerobic environment. *Appl Microbiol Biotechnol* 2001, *55*, 90-94.

[230] Heylen, K., Lebbe, L., De Vos, P., *Acidovorax caeni* sp. nov., a denitrifying species with genetically diverse isolates from activated sludge. *Int J Syst Evol Microbiol* 2008, *58*, 73-77.

[231] Ma, Y. F., Zhang, Y., Zhang, J. Y., Chen, D. W., *et al.*, The complete genome of *Comamonas testosteroni* reveals its genetic adaptations to changing environments. *Appl Environ Microbiol* 2009, *75*, 6812-6819.

[232] Copeland, A., Lucas, S., Lapidus, A., Barry, K., *et al.*, Complete sequence of chromosome 1 of *Acidovorax* sp. JS42. Submitted to the EMBL/GenBank/DDBJ databases. 2006.

[233] Ruch, F. E., Lengeler, J., Lin, E. C. C., Regulation of glycerol catabolism in *Klebsiella aerogenes*. *J Bacteriol* 1974, *119*, 50-56.

[234] Schär, H.-P., Chemla, P., Ghisalba, O., Methanol dehydrogenase from *Hyphomicrobium* MS 223. *FEMS Microbiol Lett* 1985, *26*, 117-122.

[235] Santos, S. G. d., Varesche, M. B. A., Zaiat, M., Foresti, E., Comparison of mthanol, ethanol, and methane as electron donors for denitrification. *Environ Eng Sci* 2004, *21*, 313-320.

[236] Hagman, M., Nielsen, J. L., Nielsen, P. H., Jansen, J. l. C., Mixed carbon sources for nitrate reduction in activated sludge-identification of bacteria and process activity studies. *Wat Res* 2008, *42*, 1539-1546.

[237] Osaka, T., Shirotani, K., Yoshie, S., Tsuneda, S., Effects of carbon source on denitrification efficiency and microbial community structure in a saline wastewater treatment process. *Water Res* 2008, *42*, 3709-3718.

[238] Lu, H., Nuruzzaman, F., Ravindhar, J., Chandran, K., Alcohol dehydrogenase expression as a biomarker of denitrification activity in activated sludge using methanol and glycerol as electron donors. *Environ Microbiol.* 2011, *doi: 10.1111/j.1462-2920.2011.02568.x*.

[239] Kolkman, A., Olsthoorn, M. M. A., Heeremans, C. E. M., Heck, A. J. R., Slijper, M., Comparative proteome analysis of *Saccharomyces cerevisiae* grown in chemostat cultures limited for glucose or ethanol. *Mol Cell Proteomics* 2005, *4*, 1-11.

[240] Kalyuzhnaya, M. G., Beck, D. A., Suciu, D., Pozhitkov, A., *et al.*, Functioning in situ: gene expression in *Methylotenera mobilis* in its native environment as assessed through transcriptomics. *ISME J* 2010, *4*, 388-398.

[241] Hendrickson, E. L., Beck, D. A., Wang, T., Lidstrom, M. E., *et al.*, Expressed genome of *Methylobacillus flagellatus* as defined through comprehensive proteomics and new insights into methylotrophy. *J Bacteriol* 2010, *192*, 4859-4867.

[242] Kittichotirat, W., Good, N. M., Hall, R., Bringel, F., *et al.*, Genome sequence of *Methyloversatilis universalis* FAM5^T, a methylotrophic representative of the order Rhodocyclales. *J Bacteriol* 2011, JB.05331-05311.

[243] Ward, N., Larsen, O., Sakwa, J., Bruseth, L., *et al.*, Genomic insights into methanotrophy: the complete genome sequence of *Methylococcus capsulatus* (Bath). *PLoS Biol* 2004, *2*, e303.

[244] Bosch, G., Skovran, E., Xia, Q., Wang, T., *et al.*, Comprehensive proteomics of *Methylobacterium extorquens* AM1 metabolism under single carbon and nonmethylotrophic conditions. *Proteomics* 2008, *8*, 3494-3505.

[245] Laukel, M., Rossignol, M., Borderies, G., Volker, U., Vorholt, J. A., Comparison of the proteome of *Methylobacterium extorquens* AM1 grown under methylotrophic and nonmethylotrophic conditions. *Proteomics* 2004, *4*, 1247-1264.

[246] Heijnen, J. J., Van Dijken, J. P., In search of a thermodynamic description of biomass yields for the chemotrophic growth of microorganisms. *Biotechnol Bioeng* 1992, *39*, 833-858.

[247] Bradford, M. M., A rapid and sensitive method for the quantitation of microgram quantities of protein utilizing the principle of protein-dye binding. *Anal Biochem* 1976, *72*, 248-254.

[248] Kapp, E., Schütz, F., *Current Protocols in Protein Science*, John Wiley & Sons, Inc. 2001.

[249] Salway, J. G., Granner, D. K., *Metabolism at a Glance, Second Edition* Blackwell Publishing, London, England 2004.

[250] Schmidt, S., Christen, P., Kiefer, P., Vorholt, J. A., Functional investigation of methanol dehydrogenase-like protein XoxF in *Methylobacterium extorquens* AM1. *Microbiology* 2010, *156*, 2575-2586.

[251] Frimmer, U., Widdel, F., Oxidation of ethanol by methanogenic bacteria. *Arch Microbiol* 1989, *152*, 479-483.

[252] Chistoserdova, L., Vorholt, J. A., Thauer, R. K., Lidstrom, M. E., C1 transfer enzymes and coenzymes linking methylotrophic bacteria and methanogenic archaea. *Science* 1998, *281*, 99-102.

[253] Vorholt, J., Cofactor-dependent pathways of formaldehyde oxidation in methylotrophic bacteria. *Arch Microbiol* 2002, *178*, 239-249.

[254] Chistoserdova, L., Laukel, M., Portais, J. C., Vorholt, J. A., Lidstrom, M. E., Multiple formate dehydrogenase enzymes in the facultative methylotroph

Methylobacterium extorquens AM1 are dispensable for growth on methanol. *J Bacteriol* 2004, *186*, 22-28.

[255] Chistoserdova, L., Crowther, G. J., Vorholt, J. A., Skovran, E., *et al.*, Identification of a fourth formate dehydrogenase in *Methylobacterium extorquens* AM1 and confirmation of the essential role of formate oxidation in methylotrophy. *J Bacteriol* 2007, *189*, 9076-9081.

[256] Šmejkalová, H., Erb, T. J., Fuchs, G., Methanol assimilation in *Methylobacterium extorquens* AM1: demonstration of all enzymes and their regulation. *PLoS ONE* 2010, *5*, e13001.

[257] Mokhayeri, Y., Riffat, R., Murthy, S., Bailey, W., *et al.*, Balancing yield, kinetics and cost for three external carbon sources used for suspended growth post-denitrification. *Wat Sci Tech* 2009, *60*, 2485-2491.

[258] Chistoserdova, L., Modularity of methylotrophy, revisited. *Environ Microbiol* 2011, no-no.

[259] Kornberg, H. L., The role and control of the glyoxylate cycle in *Escherichia coli*. *Biochem J* 1966, *99*, 1-11.

[260] Hoffmann, T., Frankenberg, N., Marino, M., Jahn, D., Ammonification in *Bacillus subtilis* utilizing dissimilatory nitrite reductase is dependent on *resDE*. *J Bacteriol* 1998, *180*, 186-189.

[261] Tiedje, J. M., Sexstone, A. J., Myrold, D. D., Robinson, J. A., Denitrification: ecological niches, competition and survival. *Antonie van Leeuwenhoek* 1982, *48*, 569-583.

[262] Fazzolari, É., Nicolardot, B., Germon, J. C., Simultaneous effects of increasing levels of glucose and oxygen partial pressures on denitrification and dissimilatory nitrate reduction to ammonium in repacked soil cores. *Eur J Soil Biol* 1998, *34*, 47-52.

[263] Nijburg, J. W., Coolen, M. J. L., Gerards, S., Gunnewiek, P., Laanbroek, H. J., Effects of nitrate availability and the presence of glyceria maxima on the composition and activity of the dissimilatory nitrate-reducing bacterial community. *Appl Environ Microbiol* 1997, *63*, 931-937.

[264] Cali, B. M., Micca, J. L., Stewart, V., Genetic regulation of nitrate assimilation in *Klebsiella pneumoniae* M5al. *J Bacteriol* 1989, *171*, 2666-2672.

[265] Bender, R. A., Friedrich, B., Regulation of assimilatory nitrate reductase formation in *Klebsiella aerogenes* W70. *J Bacteriol* 1990, *172*, 7256-7259.

[266] 't Riet, J. v., Stouthamer, A. H., Planta, R. J., Regulation of nitrate assimilation and nitrate respiration in *Aerobacter aerogenes*. *J Bacteriol* 1968, *96*, 1455-1464.

[267] Stewart, V., Bledsoe, P. J., Chen, L. L., Cai, A., Catabolite repression control of *napF* (periplasmic nitrate reductase) operon expression in *Escherichia coli* K-12. *J Bacteriol* 2009, *191*, 996-1005.

[268] Richardson, D. J., Ferguson, S. J., The influence of carbon substrate on the activity of the periplasmic nitrate reductase in aerobically grown *Thiosphaera pantotropha*. *Arch Microbiol* 1992, *157*, 535-537.

[269] Anderson, A. J., Dawes, E. A., Occurrence, metabolism, metabolic role, and industrial uses of bacterial polyhydroxyalkanoates. *Microbiol Rev* 1990, *54*, 450-472.

[270] Lee, S. Y., Bacterial polyhydroxyalkanoates. *Biotechnol Bioeng* 1996, *49*, 1-14.

[271] Follner, C. G., Madkour, M., Mayer, F., Babel, W., Steinbuchel, A., Analysis of the PHA granule-associated proteins GA20 and GA11 in *Methylobacterium extorquens* and *Methylobacterium rhodesianum*. *J Basic Microbiol* 1997, *37*, 11-21.

[272] de Almeida, A., Nikel, P. I., Giordano, A. M., Pettinari, M. J., Effects of granule-associated protein *phaP* on glycerol-dependent growth and polymer production in poly(3-Hydroxybutyrate)-producing *Escherichia coli*. *Appl Environ Microbiol* 2007, *73*, 7912-7916.

[273] de Almeida, A., Catone, M. V., Rhodius, V. A., Gross, C. A., Pettinari, M. J., PhaP, a poly(3-hydroxybutyrate) granule-associated protein, has an unexpected stress reducing effect in Escherichia coli. *Appl. Environ. Microbiol.* 2011, AEM.05469-05411.

[274] Grabinska-Loniewska, A., Biocenosis diversity and denitrification efficiency. *Wat Res* 1991, *25*, 1575-1582.

APPENDIX

A.I Supplementary information

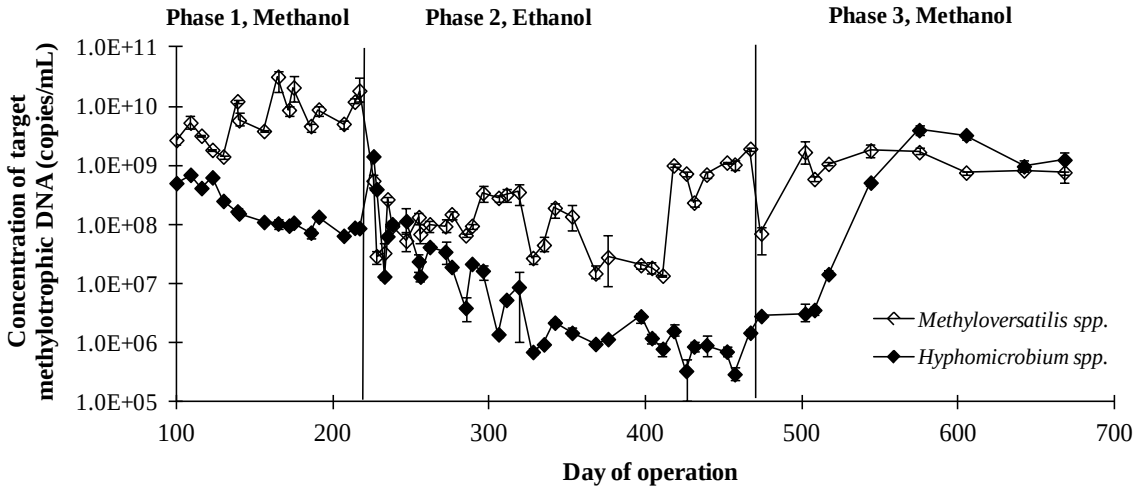

Figure S-1: Relative abundance of *Methyloversatilis* spp. and *Hyphomicrobium* spp. related methylotrophic bacteria in the SBR during phase 1 (methanol feeding); phase 2 (ethanol feeding) and phase 3 (methanol feeding) of denitrifying SBR operation

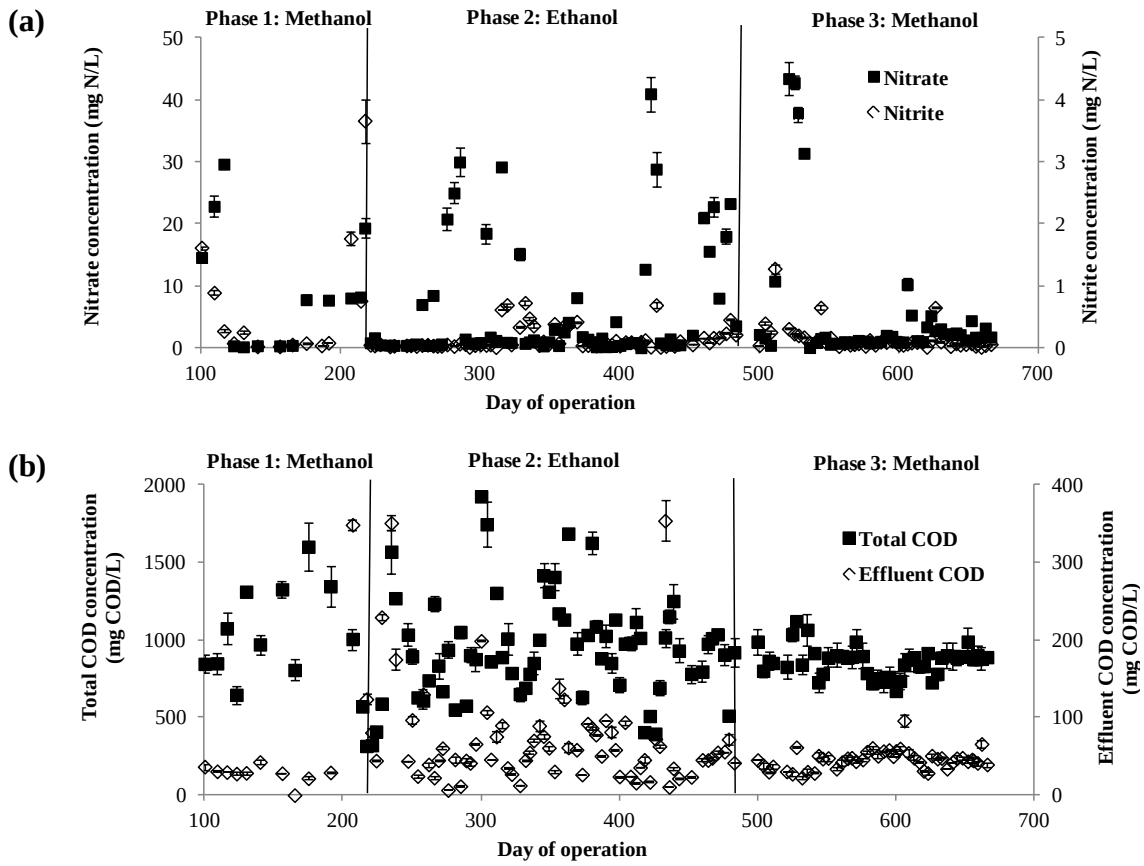

Figure S-2. SBR performance during phase 1 (methanol); phase 2 (ethanol) and phase 3 (methanol): (a) nitrate and nitrite; (b) total COD and effluent COD concentrations, measured in duplicate.

Extant batch denitrification assays

Extant batch denitrification assays were initiated with 500 mL suspended biomass (or 10 carriers for the biofilm with approximately equal amount of 0.5 g COD total biomass) from the SB-IFAS reactor. Suspended biomass was centrifuged and washed before resuspension in 500 mL fresh feed medium without nitrate, as described in *Materials and Methods*. Biofilm biomass was suspended in the same medium without prewashing. N_2 was introduced to the vessel for 10 min to strip out the air in the medium. The batch test was performed under anoxic conditions afterward by covering the surface of the mixed liquor. The initial biomass concentration during the batch assays was approximately 1 g O_2 eq /L. Sodium nitrate and glycerol were added at t = 0 and t = 21 min, respectively, to achieve an initial concentration of 442 mg nitrate / L and 205 mg glycerol /L. Nitrate and nitrite concentrations were measured at t = 0, 11, 21, 23, 33, 43, 58, 88, 118, 148, 178 min. Linear regression was performed on nitrate depletion data after the first 21 min endogenous decay phase. The slope thus obtained was divided by the initial biomass concentration to get the specific denitrification rates (expressed as mg nitrate/ g O_2 eq / h). Extant batch denitrification assays and nitrate concentration measurements were not replicated due to the analytical effort and sampling involved. Biomass concentrations were always measured in duplicate.

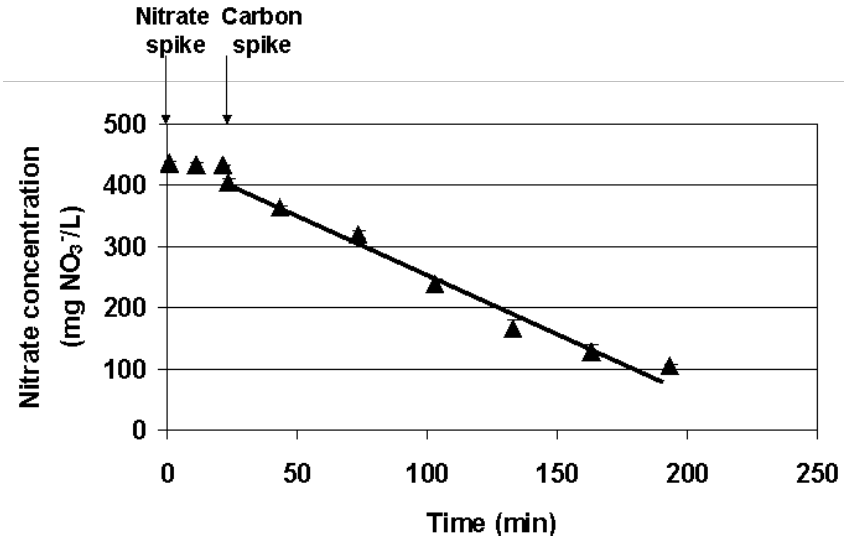

Figure S-3: A representative external batch denitrification profile for nitrate reduction

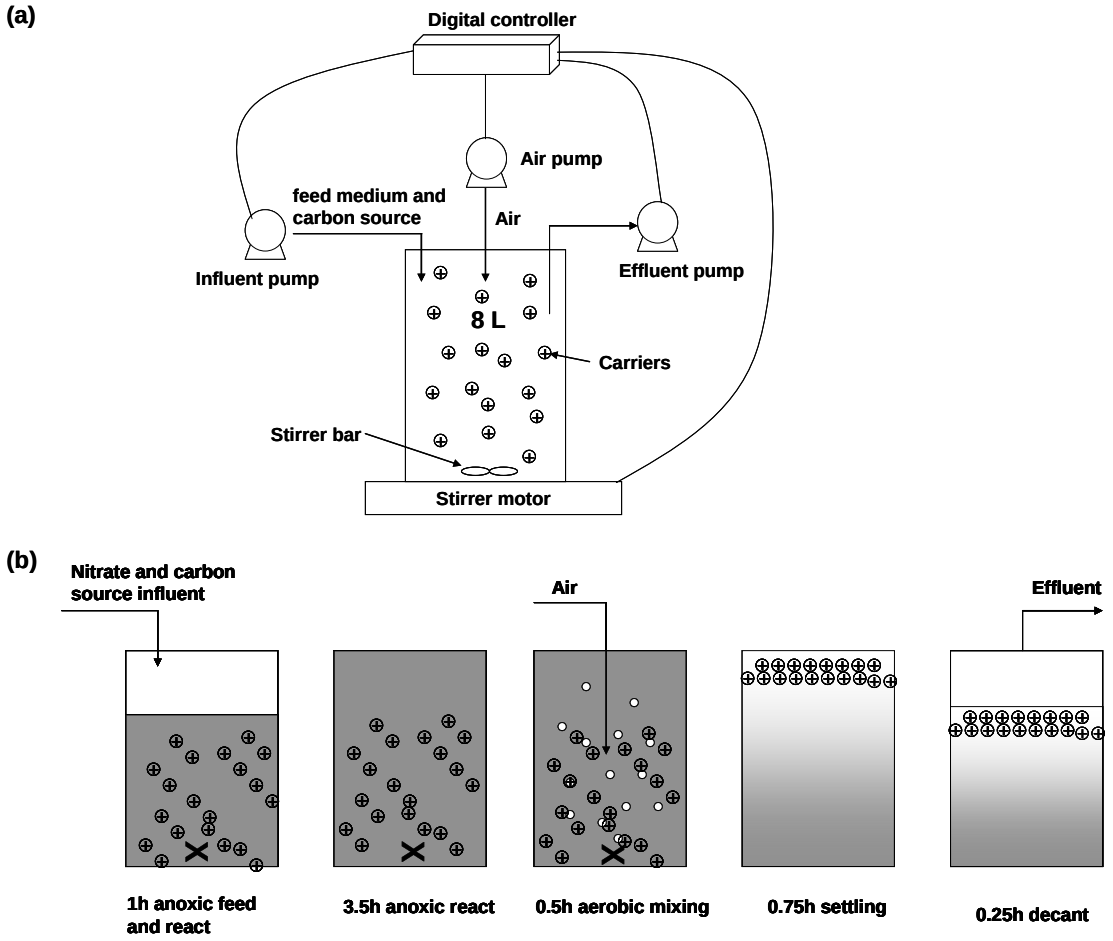

Figure S-4: Scheme of the SB-IFAS reactor (a) and the sequencing batch reactor cycles employed (b).

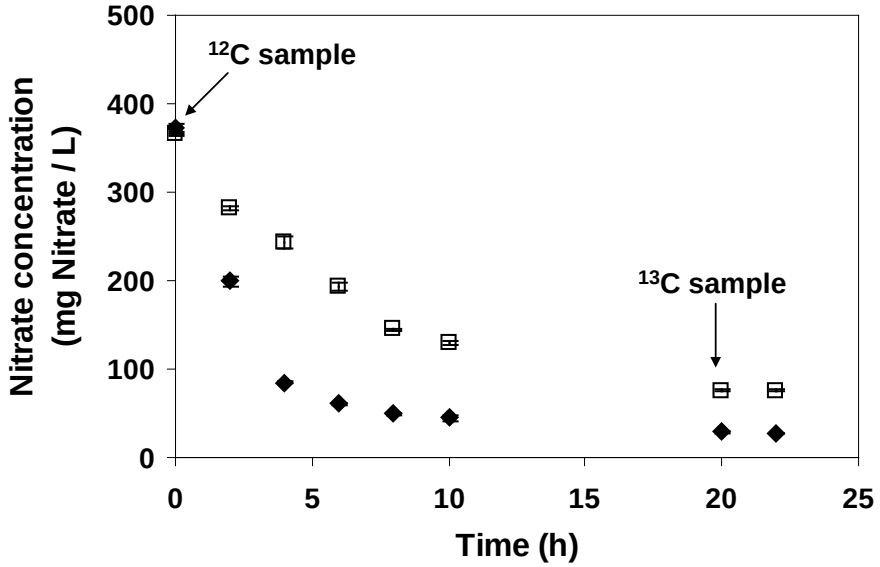

Figure S-5: Nitrate depletion curve for SIP experiments with suspended (◆) and biofilm (▫) biomass. Concentrations were measured in duplicate.

Quality check of density gradient separation of ^{12}C and ^{13}C DNA fractions

DNA fractions were separated in a cesium chloride gradient via ultracentrifugation. Three recovered DNA fractions (light, heavy, and a fraction in the middle) from the ^{13}C labeled suspended (S13) and ^{13}C labeled attached (A13) samples were quantified using real-time polymerase chain reaction (qPCR) using eubacterial 16S rRNA gene primers as described in *Materials and Methods* of Chapter 4. Based on qPCR results, the DNA concentrations of the light and heavy fractions were at least one order of magnitude higher than the fraction in the middle, indicating that the 'light'and 'heavy' fractions were adequately separated after 70 hours of ultracentrifugation (Figure S-6).

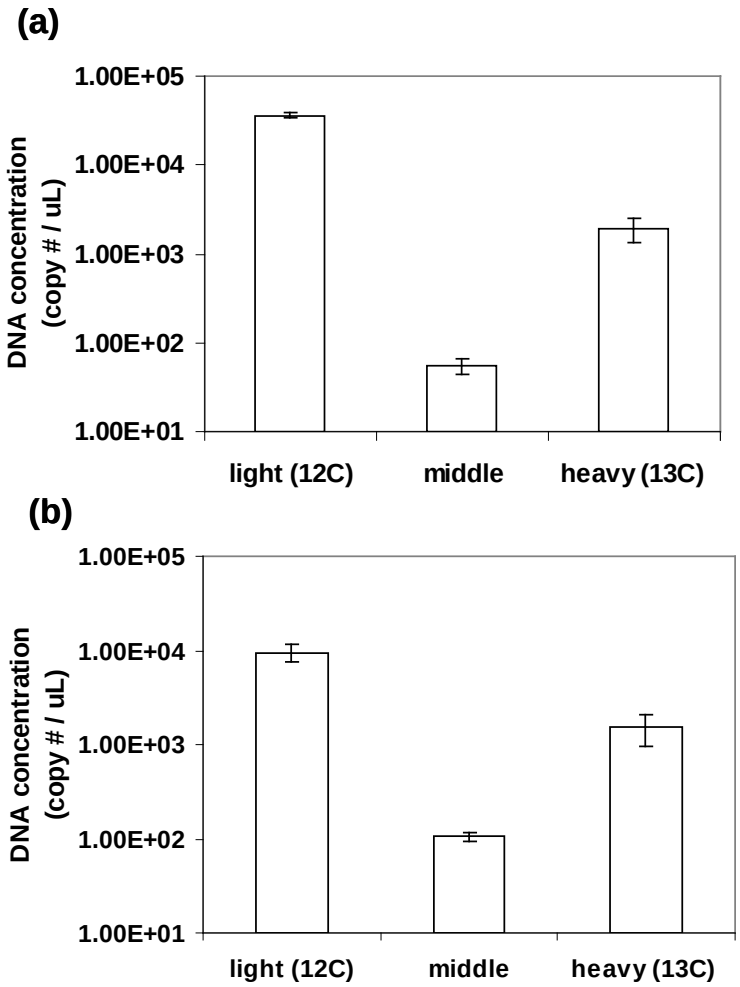

Figure S-6: Concentration of three DNA fractions recovered from (a) S13 and (b) A13 sample. Error bars indicate one standard deviation of duplicate qPCR assays

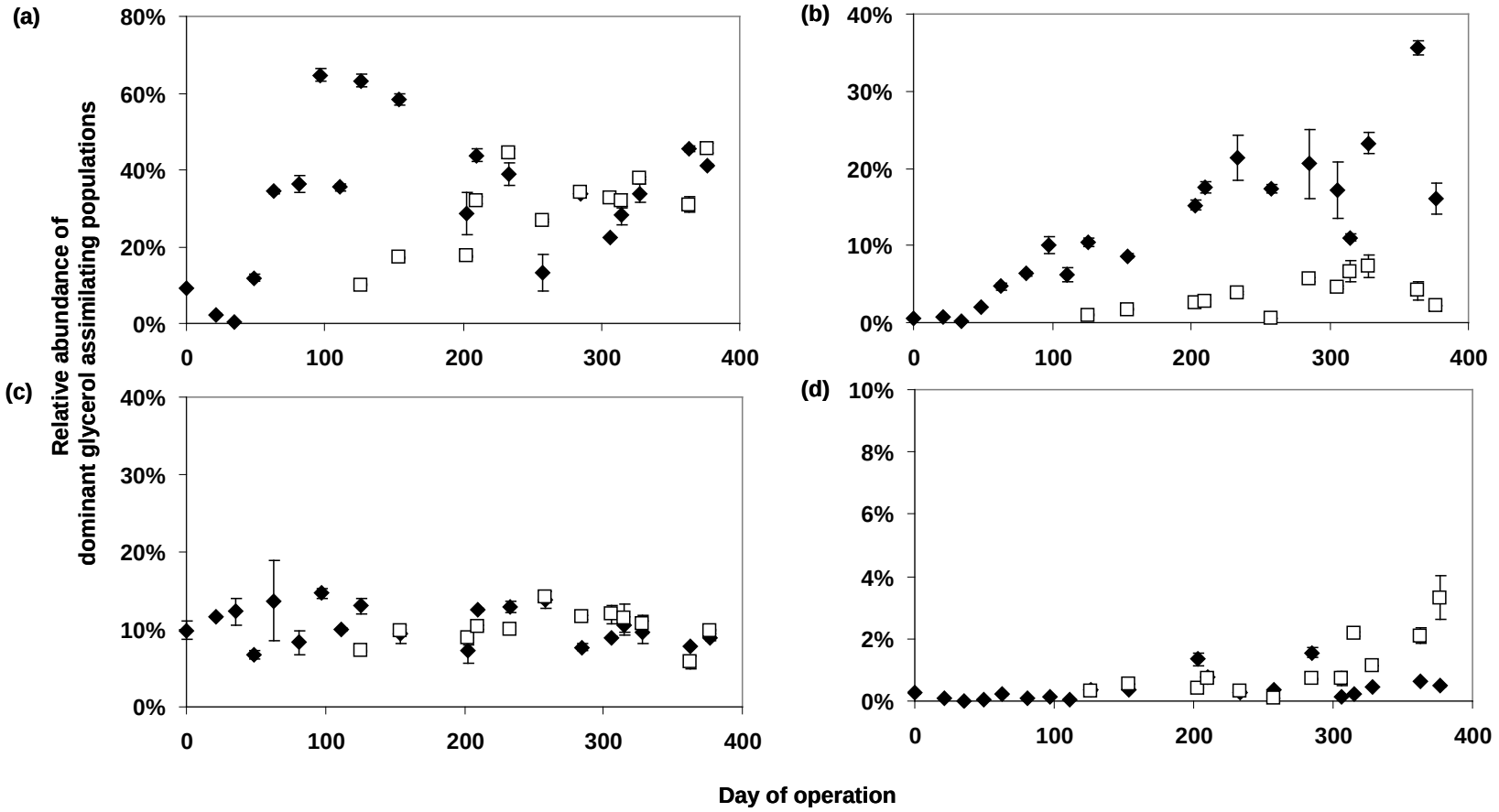

Figure S-7: Relative abundance of the four dominant glycerol assimilating populations across a year in the suspended (◆) and biofilm (□) phase. (a) *Comamonas* spp. (b) *Diaphorobacter* spp. (c) *Tessaracoccus* spp. (d) *Bradyrhizobium* spp. Error bars indicate one standard deviation of qPCR assays.

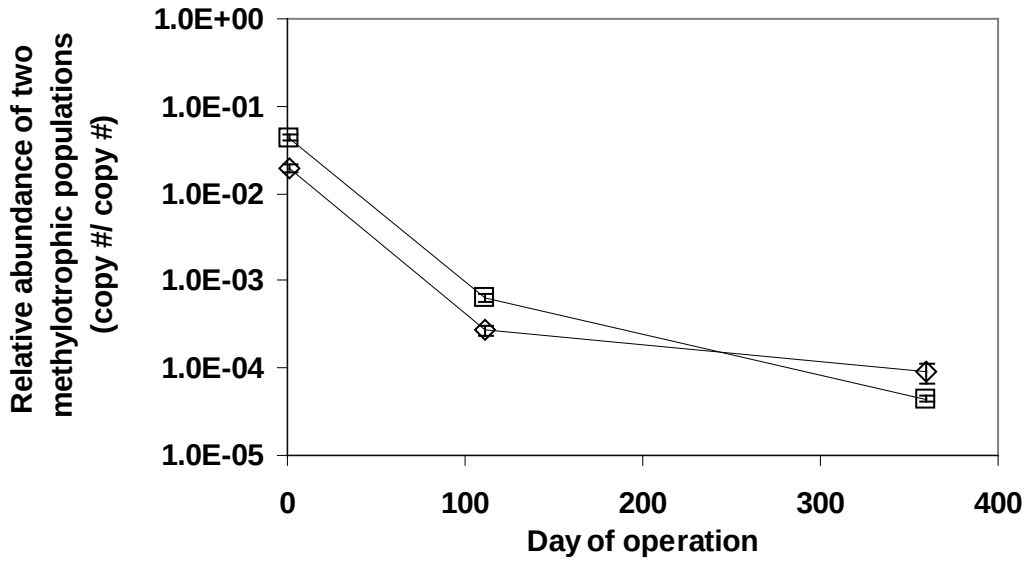

Figure S-8: 16S rRNA gene copy numbers of *Hyphomicrobium* spp. (⊟) and *Methyloversatilis* spp. (◇) related populations normalized to eubacterial 16S rRNA copy numbers in the suspended phase of the SB-IFAS reactor. Error bars indicate one standard deviation of triplicate qPCR assays.

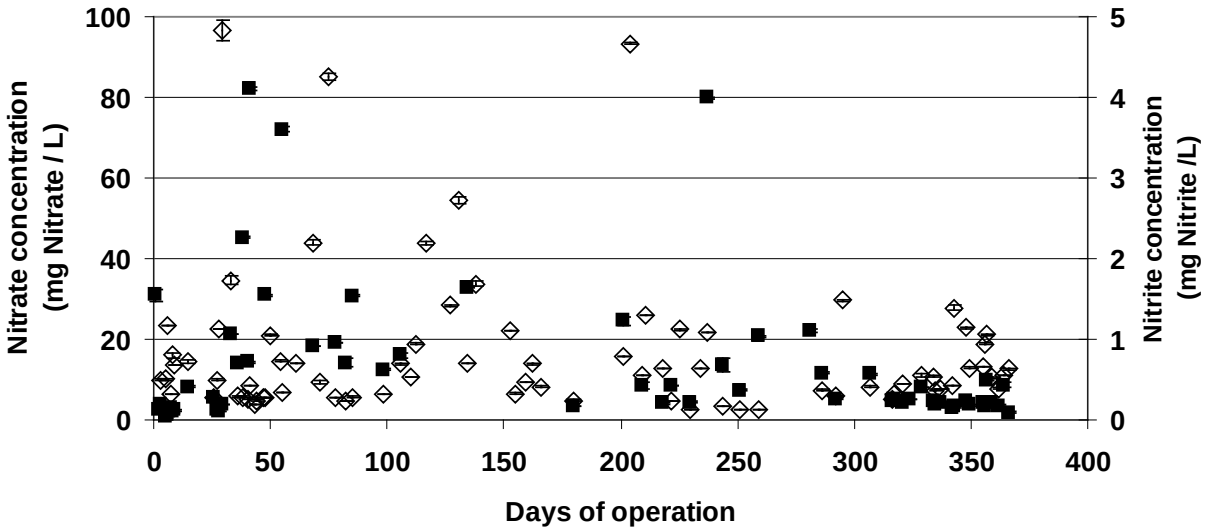

Figure S-9: Effluent concentrations of nitrate (◇) and nitrite (■) from the SB-IFAS reactor during this study, measured in duplicate.

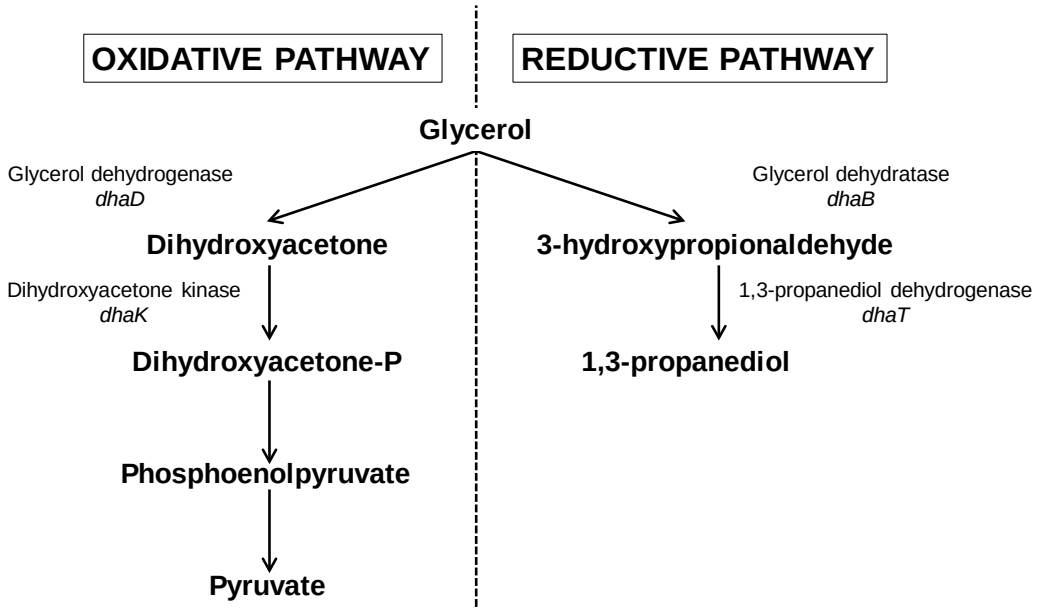

Figure S-10: Metabolism of glycerol under oxidative and reductive conditions (adapted from [183])

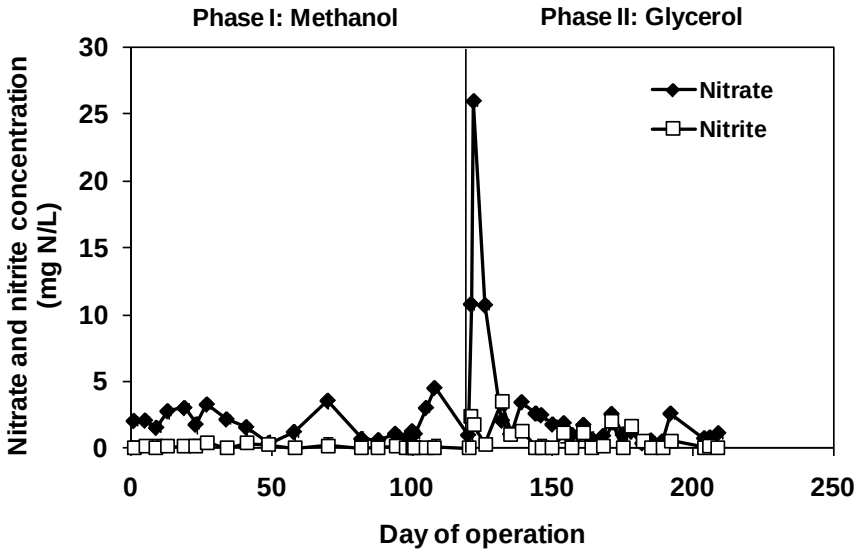

Figure S-11: Effluent concentrations of nitrate (◆) and nitrite (□) from the SBR, measured in duplicate

$$\begin{aligned}&\text{Weighted biomarker concentrations (species A, functional gene I)}\\&=\text{Fraction of species A in the community} \times \text{functional gene I transcription level}\\&=\frac{\text{16S rRNA gene of species A}}{\text{16S rRNA gene of eubacteria}} \times \frac{\text{Functional gene I mRNA in species A}}{\text{16S rRNA of species A}}\end{aligned} \qquad \text{(Equation S-1)}$$

the units for all concentrations are copies/copies

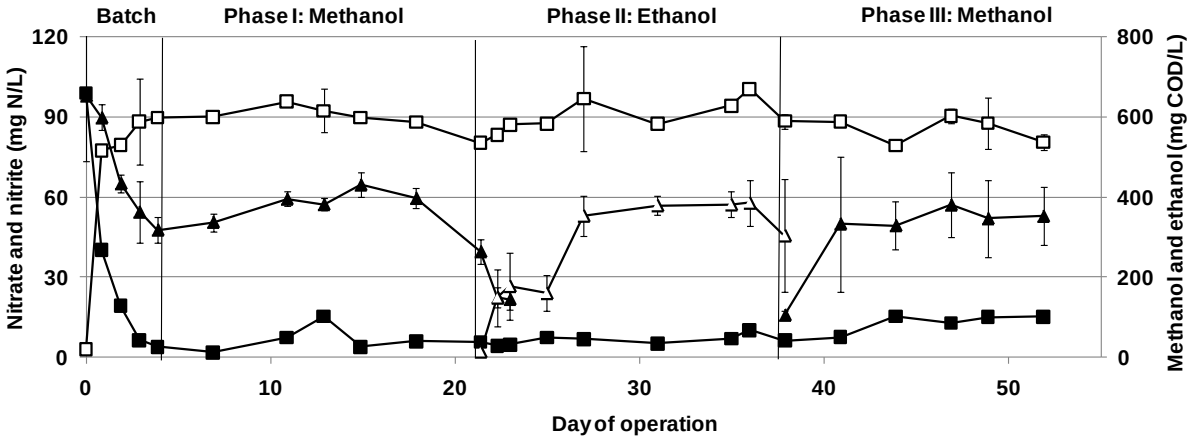

Figure S-12: A representative profile of chemostat performance measured in duplicate for nitrate ( ) and nitrite ( ),quintuplicate for methanol ( ) and ethanol ( ).

A.II Protocols for molecular analysis

A.II.1 Stable isotope probing

1. Weigh out 16 centrifuge tubes (1 mL) per sample (minimum 4 decimal places).
2. Preparation of CsCl solution. Desired density ~ 1.76 g/mL.
   a) This implies that CsCl is 59% by weight in the solution ➔ in 40 mL solution of TE, x/(x+40) = 0.59 ➔ x=57.5610g.
   b) Record the actual weight of measured CsCl and dissolve in corresponding 1X TE buffer.
3. Refraction measurements
   a) Adjust nd-TC (refraction index) reading by adding 1x TE buffer.
   b) Readings should be from ~ 1.50-1.55 and equation used is:
      density = $10.269x^2 - 17.52x + 6.08$, where x is the nD-TC reading
4. Preparation for spinning
   a) Materials needed: heat sink and heat sealer cap; tweezers for taking off heat-sealer cap; centrifuge tubes (Beckman ½ x 2in 13 x 51 mm, Catlog: 342412); multiple 1mL syringes; 10 mL tubes for mixing sample and CsCl; 10 mL glass pipette; 1mL pipette
   b) Mix 6mL CsCl solution with 0.25 mL sample. Vortex for a short time, and transfer to Beckman centrifuge tubes
   c) Heat-seal centrifuge tubes
   d) Weigh all centrifuge tubes and record the weight
5. Ultracentrifugation-Beckman
   a) Materials needed: rotor (Beckman vti65.2); torque wrench; rotor caps

b) Balance the rotor accordingly

c) Use torque wrench to screw in the caps

d) Put the rotor into centrifuge after securely screwing in the caps.

e) Set specs on centrifuge: Temp = 20 ºC; Soft spin = No; RPM = 55000; Hour = 20-24; Brake = Off at 500 RPM; Hold = On

f) Start running centrifugation and write down current revolutions as displayed on the centrifuge.

6. Collect fractions

a) Write down the duration of spin and final amount of revolutions after 20-24 hours.

b) Loosen each of the caps in the rotor with torque wrench.

c) Try to move the centrifuge tubes as little as possible so as not to disturb the gradient.

d) Sampling contraption

- Clean contraption by putting ethanol then DI water through the needle. Do so between each sample.

- Poke two holes in centrifuge tube with heated needles (22 gauge for air, 16 gauge for uptake); heat these needles by Bunsen burner.

- Gently lower attached needle into the needle the 16G hole by bringing it to that level then using the top screws to push it in.

- Once it is in, adjust the screws with balance meter to make sure apparatus is level

- Attach a 1mL syringe to top and withdraw first sample (may be >300 uL)

- Turn 2 full revolution for next sample and continue until all 16 fractions are withdrawn (it may take 3 or 4 turns to remove the bottom fraction).

7. Post-spin processing.
    a) Weigh each tube again (16 fractions/tubes per sample)
    b) Measure refraction index in each tube using ~70 uL for the refractometer.
    c) Plot density vs. cumulative volume after obtaining the volume (mass/density) of each sample from data. Note the R^2 values of these plots.
8. DNA precipitation by ethanol
    a) Transfer 0.125 mL sample from each fraction into clean 1.5 mL tubes.
    b) Add 0.375 mL DI to each of the 0.125 mL fractions. This is to dilute.
    a) Add 1mL 100% ethanol to the above fractions
    b) Leave all fractions overnight at 4 ºC
    c) Next day, centrifuge all tubes for 15-20 mins at 16,000 rpm.
    d) After centrifuging, dispose of supernatant and add 70 % ethanol.
    e) Centrifuge all tubes for 5 mins at 16,000 rpm
    f) Dispose of supernatant and let the rest of the liquid evaporate
    g) When all of the remaining liquid evaporated, re-suspend DNA in 50 uL DI
    h) Precipitated DNA samples are ready for downstream analysis (PCR).

A.II.2 DNA Extraction

1. Harvest cells
    a) Harvest 50 uL mixture from 5 mL frozen sample (centrifuged and stored at -80°C) in a 1.5 mL micro-centrifuge tube
    b) Centrifuge for 10 min at 7500 rpm and discard supernatant

2. Make enzymatic lysis buffer (ELB)
    a) 20mM Tris-Cl, pH =8.0; 2mM sodium EDTA, pH=8.0; 1.2% Triton X-100.
    b) Vortex and filter the mixture in the hood and fill into micro-centrifuge tubes.
    c) Every time, add fresh lysozyme (200 mg/L, stored at -20°C) to the filtered ELB solution (final concentration of 20 mg/L).
3. Resuspend bacterial pellets in 180 uL ELB.
4. Incubate for 1h at 37 ºC
5. Add 25 uL proteinase K and 200 uL buffer AL. Mix by vortexing.
6. incubate at 56 ºC for 1h
7. Add 200 uL pure ethanol (filtered) and mix thoroughly by vortexing.
8. Pipet all the mixture into the DNeasy Mini spin column placed in a 2 mL collection tube. Centrifuge at 8000 rpm for 1 min.
9. Place the DNeasy mini spin column in a new 2 mL collection tube and add 500 uL buffer AW1. Centrifuge for 1min at 8000 rpm. Discard flow-through and collection tube.
10. Place the DNeasy mini spin column in a new 2 mL collection tube and add 500 uL buffer AW2. Centrifuge for 4min at 132000 rpm (max rate). Discard flow-through and collection tube.
11. Place the DNeasy Mini spin column in a clean 1.5mL micro-centrifuge tube and pipette 100 uL buffer AE to the membrane.
12. Incubate at room temperature for 1min and centrifuge for 1min at 8000 rpm.
13. Store extracted DNA samples at -80°C.

A.II.3 Cloning

1. Purify PCR products by acetate precipitation (for cloning, optimal)
    a) For 20uL PCR, add 2uL sodium acetate (#M) to each well (1.5 ml tube)
    b) Add 50uL 100% EtOH (stored at -20C) to each well
    c) Incubate at -20C for 20 min
    d) Spin all tubes at max speed for 30 min (4C)
    e) Pipet out liquid (should see white pellet)
    f) Add 70ulL 70% EtOH (stored at -20C) to each tube
    g) Spin all tubes at max speed for 15 min (4C)
    h) Pipet out all liquid
    i) Dry the pellet for a few minutes in air resuspend in Buffer EB (8uL)
2. Clone the PCR products with TOPO TA 4.0 cloning kit
    a) Mix PCR products with salt solution and the TOPO vector. PCR products = 2uL; salt solution = 0.5uL; TOPO vector = 0.5uL
    b) Incubate at RT for 5~30 min
    c) Take 2 uL from the PCR tube and add 25 uL *E. coli* competent cells ()
    d) Mix gently (always keep *E. coli* cells on the ice and don't shake too much) and incubate cells on the ice for 5~30min
    e) Heat shock at 42 ºC for 30 sec using water bath (no shaking)
    f) Immediately transfer the tube onto ice for 5~30 min
    g) Add 125uL SOC medium
    h) Incubate at 37 ºC for 1h with horizontal shaking
    i) Spread 50uL (duplicate 100ml) to LB plate (contains amptcillin 50ug/ml

j) Incubate overnight at 37 ºC (Don't exceed 24h)

k) Pick 5 white clones and transfer to LBA tube (1.5ml medium)

l) Incubate overnight at 37 ºC

3. Plasmid Preparation

a) Transfer 1.5 ml culture to 1.5 ml centrifuge tube and centrifuge 1mtn cut max

b) Decant supernatant and Resuspend in 250 uL Buffer R3 (stored at 4 ºC)

c) Add 250 uL Buffer L7 and mix by inverting

d) Add 350 ml Buffer N4 and mix by inverting.

e) Centrifuge at 16,000 rpm for 10min 14 ºC

f) Transfer all supernatant to Qiagen Spin Column and add the wash tube

g) Centrifuge at 16,000 rpm for 1min. Discard flow through and keep the wash tube

h) Add 0.7 ml Buffer W9 to the column and centrifuge at max for 1min

i) Discard flow through and centrifuge again to remove the residual liquid

j) Put the column into a new 1.5 ml centrifuge tube (labeled) and add 50 uL Buffer TE to the center of the column

k) Elute 1 min at room temperature and centrifuge 1 min at 16,000 rpm

A.II.4 RNA extraction

1. Prepare TE buffer (30mM Tris-Cl, 1mM EDTA, pH=8) by adding 0.6mL 1M Tris-Cl stock, 1mL 20mM Na_2-EDTA to DI water. Final vol: 20mL, and filter the solution.
2. Prepare the following mixture (total vol=220uL for each sample): TE buffer=185 uL; Lysozyme (200mg/mL)=15 uL and proteinase K=20uL
3. Add the mixture to the pellet (1mL sample, centrifuged and stored at -80^{o}C), resuspend the pellet by pipetting up and down several times

4. Mix by vortexing 10s, and incubate at room temperature (15-25^{o}C) for 15min. Vortex 5-6 times during the incubation.
5. Add 700uL buffer RLT and vortex vigorously. If particulate material is visible, use only the supernatant after short centrifugation.
6. Add 500uL 100% ethanol. Mix by pipetting.
7. Transfer up to 700uL lysate to an RNeasy Mini Spin column.
8. Centrifuge at max speed for 15s. Discard the flow-through and reuse the collection tube. Repeat step 7 if lysate is more than 700uL.
9. Add 350uL buffer RW1 to the spin column and centrifuge for 15s at max to wash the spin column membrane. Discard flow-through and reuse the collection tube in step 11.
10. Prepare DNase incubation mix (100 uL) = 10 uL Promega RQ1 DNase + 90uL RQ1 buffer. Mix gently and slowly spin down.
11. Add the DNase incubation mix directly to the RNeasy spin column membrane, and incubate at room temperature (20-30 ^{o}C) for 15min.
12. Add 350uL buffer RW1 to the RNeasy spin column, wait for 5min, and then centrifuge for 15s at max. Discard the flow-through and collection tube.
13. Place the RNease Mini spin column in a new 2mL collection tube and add 500uL buffer RPE to it.
14. Centrifuge at max speed for 15s. Discard the flow-through and reuse the collection tube.
15. Add 500uL buffer RPE to the spin column and centrifuge for 3min at max speed to wash the column membrane.

16. Place the spin column in a 1.5mL RNase-free tube (provided) and add 50uL of RNase-free water directly to the spin column membrane.
17. Centrifuge for 1min at max speed to elute the RNA.
18. Store extracted RNA samples at -80°C.

A.II.5 Reverse transcription

1. Mix the following reagents with RNA template in 96-well plates or PCR tubes (14uL in each well): 2uL DNA wipeout buffer (7X); 11uL DNase/RNase free water and 1uL RNA template.
2. Incubate in the water bath at 42 °C for 2 min
3. Add the following reverse transcription reagents to PCR tubes, in each well: 4uL Quanti-script RT buffer (5X); 1uL RT primer mix and 1uL Quanti-script transcriptase.
4. Put all tubes into iQ5 and start the RT program: 20min at 42 °C and 3min at 95 °C.
5. Store all cDNA samples at -80°C.

A.II.6 Real-time PCR

1. Decide final concentration of template and primers and calculate the amount of supermix, primers and water to add.
2. Make the aliquot:
    a) Pipeting safety factor is +1/20 samples (i.e. for 40 samples, safety number= 42); standard (7 series*2); negative control (2), positive control (2) and samples (triplicate)
    b) Mix forward and reverse primers, water and supermix.
    c) Add 24uL aliquot to each well (96-well plate)

3. Add 1uL DNA template to each well
4. Cover the plate with the plastic film and place it into iQ5 machine.
5. Start running the amplification program (usually > 35 cycles with melting curve analysis) and collect data after the qPCR is completed.

A.II.7 Gel electrophoresis

1. Enzyme Digestion (for plasmids, optimal)
    a) Mix 3uL H2O + 0.5uL EcoRI + 0.5ul EcoRI buffer + 1ul plasmid extracted
    b) Incubate tubes at 37 ºC for 1 h
2. Prepare the 1% agarose gel solution (3g agarose powder + 300 ml 0.5X TBE buffer, heat to dissolve)
3. Mix 25 ml gel solution with 1.25 ul ethedium bromide.
4. Poor the gel solution into the electrophoresis chamber (combs placed)
5. Wait for the gel to cool down and add 100 mL 0.5X TBE buffer in the gel box
6. Load samples: add 5 uL in each well
7. Power On: 75 V for 30-40 min

LIST OF PUBLICATIONS

Core dissertation publications (peer reviewed journal articles and conference proceedings):

1 **Huijie Lu**, Marina Kalyuzhnaya, Kartik Chandran. 2011. Comparative proteomic and transcriptional analysis of *Methyloversatilis universalis* FAM5 grown on methanol and ethanol under anoxic conditions. (In preparation)

2 **Huijie Lu**, Farhan Nuruzzaman, Kartik Chandran. 2011. Alcohol dehydrogenase expression as a biomarker of denitrification activity in activated sludge using methanol and glycerol as electron donors. *Environmental Microbiology* doi:10.1111/j.1462-2920.2011.02568.x

3 **Huijie Lu**, Kartik Chandran. 2010. Diagnosis and quantification of glycerol assimilating denitrifying bacteria in a moving bed biofilm reactor via ^{13}C DNA stable-isotope probing. *Environmental Science and Technology* 44 (23): 8943–8949.

4 **Huijie Lu**, Kartik Chandran. 2010. Factors promoting emissions of nitrous oxide and nitric oxide from denitrifying sequencing batch reactors operated with methanol and ethanol as electron donors. *Biotechnology and Bioengineering* 106(3):390-398.

5 Vladmir Baytshtok, **Huijie Lu**, Hongkeun Park, Sungpyo Kim, Ran Y, Kartik Chandran. 2009. Impact of varying electron donors on the molecular microbial ecology and biokinetics of methylotrophic denitrifying bacteria. *Biotechnology and Bioengineering* 102(6):1527-36.

6 **Huijie Lu**, Farhan Nuruzzaman, Janani Ravindhar, Kartik Chandran. Gene expression biomarkers of denitrification activity using methanol and glycerol as electron donors. Proceeding of Water Environment Federation's Annual Technical Exhibition and Conference. Los Angeles, CA, 2011

7 **Huijie Lu**, Mathew Sabu, Ruby Monichan, Kartik Chandran. Niche differentiation between biofilm and suspended microbial communities assimilating glycerol in a denitrifying moving bed biofilm reactor. Proceedings of Biofilm Reactor Technology Conference. Portland, OR, 2010

8 Vladimir Baytshtok, **Huijie Lu**, Hongkeun Park, Ran Yu, Sungpyo Kim, Kartik Chandran. Elucidating the structure and function of heterotrophic denitrification on different organic electron donors. Proceedings of Specialized Conference on Microbial Population and Dynamics in Biological Wastewater Treatment. Aalborg, Denmark, 2009.

Coauthor publications (peer reviewed journal articles and conference proceedings):

1 Ran Yu, **Huijie Lu**, Mark C. M. van Loosdrecht, Kartik Chandran. Proteomics of nitric oxide (NO) and nitrous oxide (N_2O) production by *Nitrosomonas europaea* 19718. *Environmental Microbiology*. Submitted, under review

2 Daliang Ning, Hui Wang, Chang ding, **Huijie Lu**. 2010. Novel evidence of cytochrome P450-catalyzed oxidation of phenanthrene in *Phanerochaete chrysosporium* under ligninolytic conditions. *Biodegradation* 21(6):889-901

3 Ran Yu, Janani Ravindhar, **Huijie Lu** and Kartik Chandran. Unique directionality and metabolic modeling of nitrous oxide and nitric oxide emissions from nitrification. Proceedings of Water Environment Federation's Annual Technical Exhibition and Conference. New Orleans, LA, 2010